Journal of Structural Geology 86 (2016) 95–152

Contents lists available at ScienceDirect

Journal of Structural Geology

journal homepage: www.elsevier.com/locate/jsg

Review article

# Clay smear: Review of mechanisms and applications

Peter J. Vrolijk [a, *], Janos L. Urai [b], Michael Kettermann [b]

[a] ExxonMobil Upstream Research Company, S1.2A.478, 22777 Springwoods Village Parkway, Spring, TX 77389, USA
[b] Structural Geology, Tectonics and Geomechanics, Energy and Mineral Resources Group, RWTH Aachen University, Lochnerstrasse 4-20, D-52056 Aachen, Germany

ARTICLE INFO

*Article history:*
Received 31 March 2015
Received in revised form
21 September 2015
Accepted 28 September 2015
Available online 3 November 2015

*Keywords:*
Clay smear
Fault process
Sedimentary rocks
Experiments
Fluid flow

ABSTRACT

Clay smear is a collection of fault processes and resulting fault structures that form when normal faults deform layered sedimentary sections. These elusive structures have attracted deep interest from researchers interested in subsurface fluid flow, particularly in the oil and gas industry. In the four decades since the association between clay-smear structures and oil and gas accumulations was introduced, there has been extensive research into the fault processes that create clay smear and the resulting effects of that clay smear on fluid flow. We undertake a critical review of the literature associated with outcrop studies, laboratory and numerical modeling, and subsurface field studies of clay smear and propose a comprehensive summary that encompasses all of these elements. Important fault processes that contribute to clay smear are defined in the context of the ratio of rock strength and *in situ* effective stresses, the geometric evolution of fault systems, and the composition of the faulted section. We find that although there has been progress in all avenues pursued, progress has been uneven, and the processes that disrupt clay smears are mostly overlooked. We highlight those research areas that we think will yield the greatest benefit and suggest that taking these emerging results within a more process-based framework presented here will lead to a new generation of clay smear models.
© 2015 ExxonMobil Upstream Research Company. Published by Elsevier Ltd. This is an open access article under the CC BY license (http://creativecommons.org/licenses/by/4.0/).

**Contents**



* Corresponding author.
*E-mail addresses:* peter.vrolijk@exxonmobil.com (P.J. Vrolijk), j.urai@emr.rwth-aachen.de (J.L. Urai), michael.kettermann@emr.rwth-aachen.de (M. Kettermann).

http://dx.doi.org/10.1016/j.jsg.2015.09.006
0191-8141/© 2015 ExxonMobil Upstream Research Company. Published by Elsevier Ltd. This is an open access article under the CC BY license (http://creativecommons.org/licenses/by/4.0/).

## 1. Introduction

Clay smear is among the family of structures that deflect fluid flow in sedimentary basins. Clay smear processes were originally conceived for (Smith, 1966; Weber et al., 1978) and continue to be applied to problems of cross-fault flow when porous and permeable rocks, specifically sandstones and shales, are cut by normal faults. Within this conceptual framework a series of stacked sandstone and clay-rich shale beds are offset with a normal displacement, and during that offset clays from shale beds may become entrained within the fault zone and redistributed along its length between the footwall and hanging wall beds (Fig. 1). While this general description is accurate, it is too imprecise to be of much practical use. Our goals in this paper are to critically review and summarize the state of knowledge for the fault processes that occur within the ellipse in Fig. 1, to evaluate how these processes affect cross-fault flow and whether current models of these processes adequately perform their task, and to speculate on how the next level of understanding into these problems might be achieved. Although much of this literature is based on quantitative analysis, the breadth of this review requires us to approach the subject in a qualitative manner informed by the quantitative background.

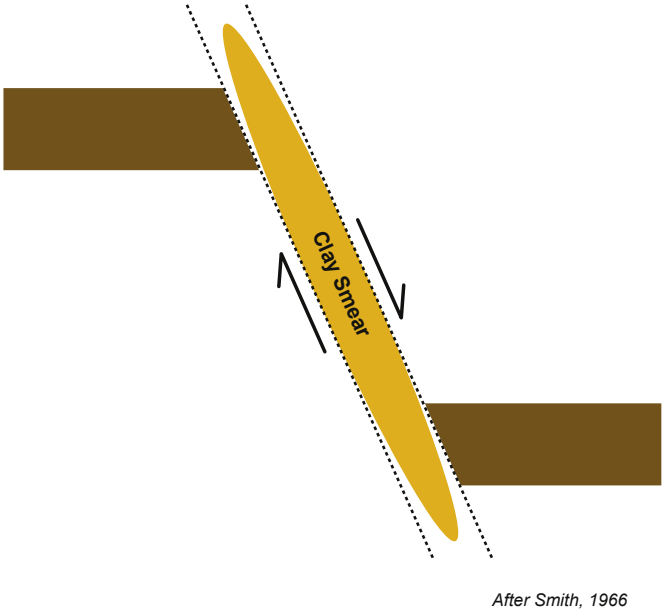


**Fig. 1.** Most general definition of clay smear as conceptualized by Smith (1966) in which a fault zone (shear zone) contains clay derived from a faulted and offset shale bed. Many processes occur within yellow 'Clay Smear' ellipse, and a primary goal of review is to provide process framework that leads to more successful predictive models. Note that for an infinitely thin fault zone, there is no clay smear.

The central theme in this analysis is the geometry of all the components that comprise a fault zone, including:

- The geometry of the fault zone margins
- The heterogeneously deformed high shear-strain intervals within the fault zone that accommodate the vast majority of the fault displacement
- The distribution and occurrence of less deformed components within the fault zone, including fault relays and lenses
- The geometry and folding of beds bounding the fault in the footwall and hanging wall

It is this geometric arrangement that exerts the primary influence on cross-fault flow given the permeability of each component, just as the distribution, geometry, and properties of sandstones within fluvial channels is a primary concern of sedimentologists and stratigraphers when evaluating sub-surface flow. A fault zone must have finite thickness for clay smear to exist (Fig. 1); a fault surface, (i.e. an infinitely thin fault zone), contains no clay smear. Moreover, this geometric pattern is the product of the deformation caused by faulting the stratigraphic section. In theory, a forward model of the fault history based on geomechanical principles could yield the same geometric products. Although there have been attempts to relate clay smear to other flow problems, like flow along the fault zone (e.g., Caine and Minor, 2009), our discussion is restricted to summarizing clay smear processes and their effect on cross-fault flow.

Research into clay smear includes both basic and applied components. Basic research explores the initiation and evolution of normal faults, including localization phenomena, in clastic sedimentary rocks (Mandl, 1988) while the applied research approach focuses on the effects of normal faults on subsurface fluid flow. We begin this review with the field outcrop, laboratory experimental and numerical studies (Fig. 2) at the basic research end of the spectrum and then address applications of clay smear concepts in subsurface flow environments. While some might view basic and applied research areas as separate endeavors, we find tremendous benefit in considering them together. Indeed, we think the research community likely stands at a point where both ends of the research spectrum could improve with a new level of integration, how more process-based fault models will yield better cross-fault flow predictive models and how better subsurface flow studies will be more

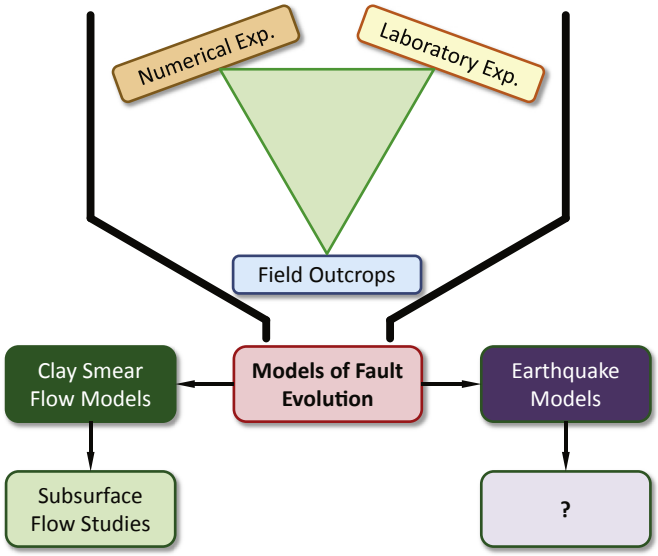


**Fig. 2.** Clay smear process framework developed through studies of field outcrops, analytical & numerical experiments, and laboratory experiments, all of which contribute to models of fault evolution, which are in turn used to develop subsurface flow models. Clay smear flow models used to predict cross-fault flow and thus tested by subsurface flow studies. Less well developed is how models of fault evolution lead to earthquake prediction models, and data to test those models are beyond the scope of this work.

effective at testing improved predictive flow models.

### 1.1. Readers' guide

This is a comprehensive review of decades of research in many different technical areas that may go beyond the needs of some readers while others may require the detail provided in order to accept our conclusions. We chose this approach because we felt a comprehensive, critical evaluation of the literature is lacking. To accommodate the needs of different types of readers, we offer the following suggestions.

*Curious reader*: for readers who wish to learn something about this general area, we recommend Sections 1, 2, 3.4, and 4 and the following figures in addition to those cited in these sections (Figs. 4, 21, 22, 27, 28, and 29).

*Involved reader*: those readers interested in learning something about the discipline components reviewed (e.g., experimentalists seeking to find a summary of laboratory experiments in this topic area) are directed to the following additional sections that summarize each component section (Sections 3.1.4, 3.2.4, and 3.3.8).

*Expert reader*: the entire critical review is intended for the most enthusiastic readers. However, there is the opportunity to select one or more topical area for consideration.

The summary discussion sections in this paper that are recommended to the casual and involved readers reflect the opinions of the authors to express a comprehensive opinion based on the works of many authors. Although these sections are written with few citations to improve readability, we give proper citation credit to those authors in the more detailed review of the individual papers, and those readers should seek proper author attribution in the more complete discussion sections.

### 1.2. Clay smear definition

Clay smear is a term that was never precisely defined and so has meant different things to different people over time. We struggled with existing definitions to account for structurally coherent but folded lenses of shale like those described by Berg and Avery (1995) in light of the general perception of clay smear as a mono-lithologic, attenuated interval of high shear strain without any contribution of lithologic mixing. Focusing on process models of clay smear development, we found the most general and inclusive definition to be most useful (Table 1). Some will favor a more restricted definition, but we think that perspective hinders an understanding of process. The basis for our definition should be apparent in this review, and we return to this definition in the Discussion section.

A Table of Nomenclature (Table 1) is included because this review touches on many disparate disciplines, some of which may be unfamiliar to some readers. A more complete Nomenclature summary is compiled in Supplementary materials.

**Table 1**
Table of nomenclature.

| Term | Definition | Reference |
|---|---|---|
| Abrasion | mechanical wearing, grinding, scraping, or rubbing away (or down) of rock surfaces by friction and; expansion of geomorphic definition to fault processes includes continuous migration of fault zone boundaries into footwall and/or hanging wall with increasing fault offset. | Mod 1 |
| Apparent cohesion | resistance of particles to being pulled apart, due to the surface tension of the moisture film surrounding each particle | 2 |
| Boudinage | structure common in strongly deformed sedimentary and metamorphic rocks, in which an original continuous competent layer or bed between two less competent layers has been stretched, thinned and broken at regular intervals into bodies resembling boudins or sausages, elongated parallel to the fold axes. | 1 |
| Capillary leak | Condition for which the buoyant pressure at the top of an oil or gas column overcomes the capillary pressure, leading to a condition of oil and gas migration (Ant: Capillary seal; Cf: displacement pressure in AGI Glossary). | Mod 1 |
| Capillary seal | A seal for which the impediment to oil and gas flow is created by capillary forces (Cf: seal). | Mod 1 |
| Clay gouge | A clayey deposit in a fault zone; fault gouge | 1 |
| Clay injection | The forcing, under abnormal pressure, of sedimentary material (downward, upward, or laterally) into a pre-existing deposit or rock, either along some plane of weakness or into a crack or fissure (Cf. Sand injection; AGI Glossary). | 1 |
| Clay smear | Clay smear forms in normal faults that deform layered sedimentary sequences, typically clastic sequences, and is a type of clay gouge that develops by mechanical processes alone. Clay smear includes the entire fault zone from the most highly deformed clay to stratigraphically coherent fault lenses of shale, thus resulting in a lithologically and structurally heterogeneous fault zone, and typically becomes important once beds are completely offset from themselves. Although clay smear encompasses many fault processes and structures, its main utility is in applications to cross-fault flow problems. | New |
| Clay smear potential (CSP) | One of a series of definitions of the amount of clay smear in a fault zone derived from the normal offset of a sandstone/shale sequence. CSP is the ratio of the square of a shale bed thickness divided by the fault throw for that bed. | New |
| Clay smear termination | (1) Umbrella term for processes that cause clay smear to become discontinuous. (2) The discontinuity of clay smear; hole in clay smear. | New |
| Contractional relay | Synonymous for a contractional jog or overstep that connects two sub-parallel but non-collinear portions of a fault zone and causes local contraction in the wall-rocks as they are displaced | Mod 3 |

(*continued on next page*)

**Table 1** (*continued*)

| Term | Definition | Reference |
|---|---|---|
| Dilatancy | Increase in bulk volume during deformation, caused by a change from close-packed structure to open-packed structure, accompanied by an increase in pore volume. The latter is accompanied by rotation of grains, microfracturing, and grain boundary slippage; an increase (positive dilation) or a decrease (negative dilation) in volume | 1, 2 |
| Drained deformation conditions | A deformation slow enough to allow fluid pressures in the deformed rock or soil body to remain hydrostatic. | New |
| Fault juxtaposition diagram | A diagram used to predict the juxtapositions of hanging wall and footwall lithologies for a given fault geometry and displacement (Knipe, 1997). It can be used to estimate the sealing potential of a fault (Peacock et al., 2000; Cf: Stratigraphic separation diagram; AGI Glossary). | 1, 2 |
| Fault lens | A rock body, deformed or undeformed, that is bordered by two fault strands that link above and below the rock body. | New |
| Fault-bounded trap | Trap for oil or gas formed by fault juxtaposition of an impermeable bed (e.g., shale) against the reservoir body, or a reservoir that is bounded by a sealing fault. | New |
| Geocellular reservoir simulation model | A numerical model, often a finite difference model, composed of many grid nodes that contain volumetric information (e.g., porosity and fluid saturations) and connections between neighboring grid nodes that represent flow properties (e.g., permeability or transmissivity). Model is used to calculate flow behavior for defined fluid distribution boundary conditions (e.g., pressure and saturation in a multi-phase model based on an *a priori* definition of flow properties derived from a 3D geologic description of lithotypes and their associated properties. | New |
| Kinematically preferred | Movements that result in *Kinematic coherence* (defined as the existence of synchronous slip rates and slip distributions that are arranged such that geometric coherence is maintained; AGI Glossary). | Mod 1 |
| Mechanical clay injection potential (MCIP): | This criterion predicts the tendency of lateral clay injection into a pull-apart structure in the fault. $MCIP = \frac{\sigma'_1(1-\sin\phi)}{(1-\cos\phi)C}$, $\sigma'_1$: maximum principle effective stress, $\varphi$: internal friction angle (degrees), C: cohesion. | 4 |
| Normally consolidated | Consolidation of sedimentary material in equilibrium with overburden pressure | 1 |
| Phyllosilicate framework fault rock | Fault rock developed from the deformation of impure sandstones with phyllosilicate concentrations. The mixture of phyllosilicates and framework silicates generates fault rocks where the porosity and permeability are controlled by the creation of anastomosing networks of microsmears around framework fragments or clasts. The seals arise from the deformation of detrital diagenetic phyllosilicates located between detrital framework grains, or from the deformation of phyllosilicate laminations | 5 |
| Polar continua | a type of continuum mechanics (alternately referred to as micropolar continua or Cosserat continua) in which each material point is assigned a microstructure that is equivalent to a rigidly rotating microbody, yielding six degrees of freedom that are divided between translation and microrotation (Cf: textbooks by Gerard A. Maugin). | New |
| Probabilistic shale smear factor (PSSF): | One of a series of definitions of the amount of clay smear in a fault zone derived from the normal offset of a sandstone/shale sequence. SFF is the ratio of fault throw for an individual shale bed to its thickness. | New |
| Relative permeability | In multiphase flow in porous media, the relative permeability of a phase is a dimensionless measure of the effective permeability of that phase. It is the ratio of the effective permeability of that phase to the absolute permeability. It can be viewed as an adaptation of Darcy's law to multiphase flow | 6 |
| Releasing bend/releasing step | A spatial variation in the orientation of a fault-plane that causes local extension in the wall-rocks as they are displaced around the bend | 3 |
| Sand injection | (a) The forcing, under abnormal pressure, of sedimentary material (downward, upward, or laterally) into a pre-existing deposit or rock, either along some plane of weakness or into a crack or fissure; e.g. the transformation of wet sands and silts to a fluid state and their emplacement in adjacent sediments, producing structures such as sandstone dikes or sand volcanoes. See also: intrusion [sed]. (b) A sedimentary structure or rock formed by injection. | 1 |
| Seal capacity | the amount of oil or gas that collects when its upward migration is impeded, often expressed as a buoyant pressure derived from the height of oil or gas collected and its corresponding density. | New |
| Shale gouge ratio (SGR) | One of a series of definitions of the amount of clay smear in a fault zone derived from the normal offset of a sandstone/shale sequence. SGR is the ratio of the sum of all shale intervals times their thickness divided by the fault throw. | New |
| Shale Smear Factor (SFF) | One of a series of definitions of the amount of clay smear in a fault zone derived from the normal offset of a sandstone/shale sequence. SFF is the ratio of fault throw for an individual shale bed to its thickness. | New |
| Source bed cut-offs | lines in the hanging wall and footwall marking the boundary between a fault surface and a planar marker (bed, dyke, etc.; Peacock et al., 2000); the line defined at a source bed that contributes clay into the fault zone | 3 |
| Squeezing block | A rock body above a layer of ductile clay in the footwall of a developing fault that is bound by two synthetic faults. The specific fault pattern allows a downward movement of the squeezing block which causes a thinning of the ductile clay and results in an injection of the clay into the fault | 4 |
| Transmissibility multipliers | Term used in finite difference calculations of subsurface oil and gas flow to reflect various degrees of flow impedance across faults (i.e. factor applied to transmissibility defined between nodes on either side of a fault). | Mod 7 |

References: New – definition created by authors; Mod # – definition modified from reference cited (below); # – definition used from reference cited.
1. AGI Glossary of Geology.
2. http://www.mindat.org/glossary/apparent_cohesion.
3. Peacock et al. (2000).
4. van der Zee et al. (2003).
5. Knipe (1997).
6. https://en.wikipedia.org/wiki/Relative_permeability.
7. Manzocchi et al. (1999).

## 2. Clay smear – a process to address a problem

Clay smear emerged as a geologic concept within Shell in the 1970's (F. Lehner, pers. comm. to J.L. Urai, 1997). The concept originally arose from field observations combined with laboratory experiments and a supporting analytical model (Lehner and Pilaar, 1997) with the intent of accounting for trapped gas and oil columns in faulted anticlines. Clay smear processes helped fill in the enigmatic fault zones that Smith (1966) identified as potential seal elements with Weber et al. (1978) the first published reference to this work.

Although Smith (1966) recognized the importance of defining reservoir juxtaposition geometries, it is important to reflect that the subsurface data available for this analysis was restricted to 2D seismic data with limited geophone offsets (with respect to modern data), primitive seismic processing capabilities, but continuous well log information. Because well data were some of the most definitive subsurface data, it is natural to develop an analytical method

around them (i.e. fault offset of a stratigraphic section defined by a well). We think that this early decision to apply clay smear to gas and oil accumulations in faulted traps was an essential reason for the development of this area of science in the subsequent decades.

### 2.1. Clay smear as a capillary seal

Smith (1966) recognized that the properties of a fault zone had the potential to affect oil and gas trapping and subsequent oil and gas production across faults. Weber et al. (1978), however, limited their discussion only to the capillary seal problem. Smith (1980) described how a fault gouge acting as a capillary seal was one of four scenarios encountered in the subsurface that either juxtapose sandstones of the same or different ages and result in a capillary seal or leak (Smith, 1980). The identification of these four potential conditions has remained unchanged since.

Speksnijder (1987) referred to the application of a newly developed computer program for the calculation of clay smear effects in a producing field study, and Bouvier et al. (1989) for the first time used the term Clay Smear Potential (CSP) in a publication. Both of these publications refer to a personal communication from Lehner and Pilaar (1974), thus we attribute the genesis of this idea to Lehner and Pilaar (1974). Fulljames et al. (1997) published the algebraic form of the CSP expression for the first time and described how the observations, analysis, and inferences of Lehner and Pilaar (1997) could be applied to fault trap evaluations as well as cross-fault fault flow properties (including clay smear) for oil and gas production. This limited but nevertheless influential body of literature then formed the basis for all subsequent work on clay smear.

### 2.2. Alternative clay smear definitions

While the algorithmic description of the concepts described initially by Weber et al. (1978) waited 20 years for the publication of Fulljames et al. (1997), others developed alternative approaches for describing the clay smear process. Based on outcrop observations in Lancashire quarries, Lindsay et al. (1993) derived a dimensionless length parameter, the Shale Smear Factor (SSF). This parameter produces a value that like CSP is larger for greater offset from the source bed (Fig. 3). Perhaps an important realization is that both of these original clay smear definitions, CSP and SSF, were derived based on outcrop observations in fluvial-deltaic sequences with coal interbeds. One may ask: are the fault processes developed in these rock types the same for deformation of sandstones and shales deposited in other environments?

Yielding et al. (1997) reviewed CSP and SSF parameters and introduced two additional empirical equations for describing clay smear in faults (Fig. 3): the Smear Factor and the Shale Gouge Ratio (SGR). The smear factor was defined in such a way as to provide a continuum between CSP and SSF by introducing two exponents into the expression ($m$ and $n$). The exponent $m$ operates on the shale bed thickness in the numerator of the expression, and the $n$-exponent on the distance (throw) value in the denominator. In principle these exponents could be used to lengthen or shorten the effectiveness of a clay smear from any particular shale source bed. In contrast, the Shale Gouge Ratio (SGR) allows consideration of clay that may exist and be introduced into the fault from shale stringers and thin beds, intervals which might only generate an intermediate $V_{shale}$ (shale volume) value from a gamma-ray well-log that interrogates a volume of rock, allowing a more nuanced view of the stratigraphic section.

In the last decade, however, some publications have appeared with refined algorithms that further attempt to define parameters in the context of the cross-fault flow problem, by incorporating a probabilistic element to show where clay smears may be breached. Childs et al. (2007) defined a Simple Shear Zone (SZ) method that allowed them to calculate a thickness-weighted harmonic average of the faulted and offset lithologies (akin to a vertical permeability through a stratigraphic section) and a Probabilistic Shale Smear Factor (PSSF) in which holes in the clay smear are considered to exist anywhere along the fault surface (a more complete discussion of this approach comes later). Yielding (2012) further developed this theme by describing a work-process implementation of the PSSF method in the context of SGR modeling.

We think that the current variety of clay smear algorithms is significant in that they implicitly acknowledge a limitation in the existing clay smear model approaches. All models are variations on two geologic parameters: shale bed thickness and normal fault throw. None have any basis in the mechanics of faulting except for CSP, for which the ratio is associated with a general process model and includes the viscosity of the clay (Weber et al., 1978). All models simply state that the more shale in the faulted section, the more clay will be found in a fault zone and have no capacity to account for the rich variety of structures observed in natural faults.

We review the outcrop, laboratory and numerical, and subsurface field studies in this context (Fig. 2), and then combine these evaluations into a summary of the state of knowledge of each of these steps in the clay smear process. We then critically examine the application of this knowledge to problems of sub-surface fluid flow to evaluate its adequacy. Finally, we propose a framework for incorporating a mechanics-based fault process model into the existing geometric models of clay smear development, evolution, and continuity.

## 3. Three decades of research – evolution of the clay smear concept

### 3.1. Outcrop studies

Investigations of outcrop examples of normal faults with clay smear are an essential component of any attempt to uncover the processes that create and modify clay smear. Weber et al. (1978) and Lehner and Pilaar (1997) made analyses of normal faults in the Frechen lignite mines an integral part of their early understanding. Since then other authors have approached this problem in different geologic settings, with different observational frameworks, and with different objectives in mind. We think these differences are significant. To consolidate insights across these differences, we constructed an interpretation framework that places observations into three stages of the fault problem that we think are essential for the development and preservation of clay smear, distinguishing processes that:

1. Incorporate shale and mudstone into a fault zone
2. Deform and modify those clay-rich materials in a fault zone
3. Disrupt and terminate a clay smear, ultimately resulting in holes in the clay smear

Although we seek to gain insight about fault process from outcrop studies, that insight comes as an interpretation of the fault products that are observed. In this section we focus on synthesizing the spectrum of fault structures observed in nature and use the final discussion section to relate the fault processes that are explored in laboratory and numerical experiments to the fault products that are observed.

We consider the history of outcrop studies in three stages: (1) an early stage in which the general framework of the problem was outlined and many important issues were identified; (2) an

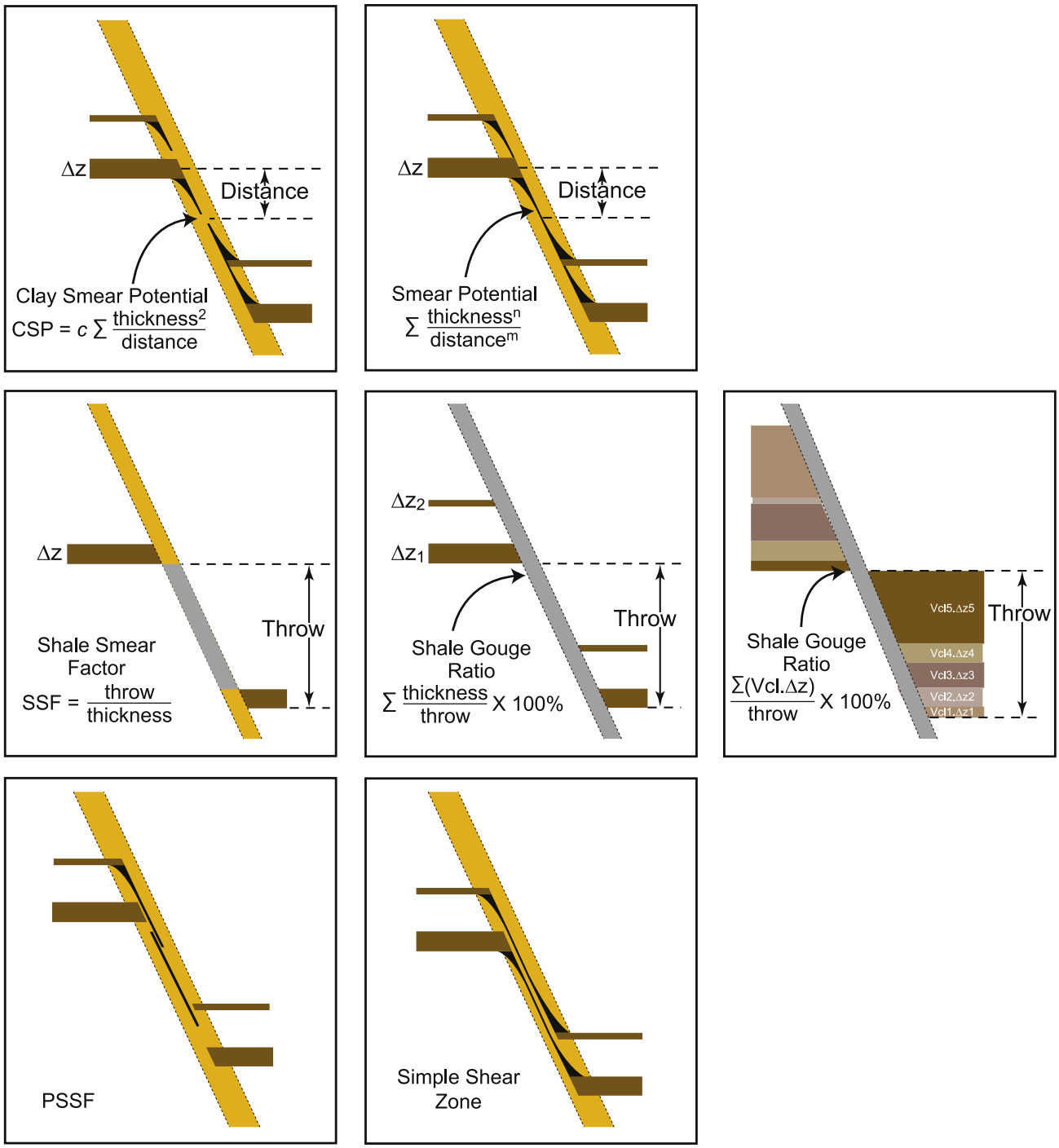


**Fig. 3.** Summary of various algorithmic approaches to modeling effects of clay smear. Top row: Clay Smear Potential (left) and Smear Potential (right) in which exponents for thickness and offset distance variables are adjustable values (*n* and *m* are set to 2 and 1, respectively, for CSP); for CSP, c is a calibration constant intended to account for rheological and stress-dependency effects. Middle row: Shale Smear Factor (left) and two variations of Shale Gouge Ratio in middle and right-hand figures. In basic SGR (middle) stratigraphic section discretized into binary shale and sandstone lithologies and thickness represents only shale component of section. In right-hand SGR case, $V_{shale}$ treated as continuous variable allowing sandstone with interpreted clay component contributing to modeled clay smear. Bottom row: Probabilistic Shale Smear Factor (left) reflects attempt to increase chance of holes forming with increasing SSF value, and Simple Shear Zone (right) represents end-member fault behavior where all lithologies become proportionately attenuated in fault zone according to original stratigraphic thicknesses. See text for further discussion and references for different algorithms. Figure modified from Yielding et al. (1997) and Childs et al. (2007).

intermediate stage where the problem was considered in different geologic environments; and (3) a modern stage characterized by work that refines and supplements understanding gained previously. We review this literature considering how it has helped advance understanding of the kinematic geometries and evolution of fault zones associated with clay smear, the extent to which general material property deductions influence clay smear, and the resulting relative importance of various fault processes (Fig. 2).

*3.1.1. Initial definition of process landscape*

Although Weber et al. (1978) referred to the Frechen outcrop observations in their original work, the full results of that work first appeared 20 years later in Lehner and Pilaar (1997). They describe normal faults of the lower Rhine Embayment, deforming Tertiary deltaic deposits in a sandstone-dominated depositional system (3× as much sandstone as shale) and made observations that subsequent authors have returned to while other observations have remained unconsidered.

The key observations made by Lehner and Pilaar (1997) include (Fig. 4):

- A layered fault structure arising from the variable incorporation of offset beds, including the amalgamation of individual clay smears derived from multiple mudstone beds into a composite clay smear (Fig. 5)
- The development of secondary shears that were interpreted as Riedel shears, primarily in the hanging wall and footwall but in some instances defining a strong fabric within the clay smear (Fig. 5)
- The development of folds in the hanging wall and footwall (Fig. 6)
- Structural thinning of mudstone beds in the hanging wall and footwall, sometimes associated with Riedel shears

On the basis of these observations, Lehner and Pilaar (1997) describe a fault zone as a layered shear zone comprising multiple slip surfaces that developed in both space and time. The resulting shear zone varies in thickness depending on the lithologic composition of the faulted interval. Fault segments that overlap often do so in a pull-apart geometry (Fig. 7) creating extensional fault overlaps into which hanging wall and footwall materials may flow (Table 2).

Recognizing the volume problem created when the volume of shale in the fault zone is less than the volume of clay smears that extend over 70 m vertically and 400 m laterally, Lehner and Pilaar (1997) describe a process of clay injection from thinning shale beds adjacent the fault into the pull-apart structures within the fault. They rely upon an interpretation framework of Riedel shears (D-, R-, and R'-shears) that both assist the thinning of shale beds and then modify the clay smear within the fault zones, including the

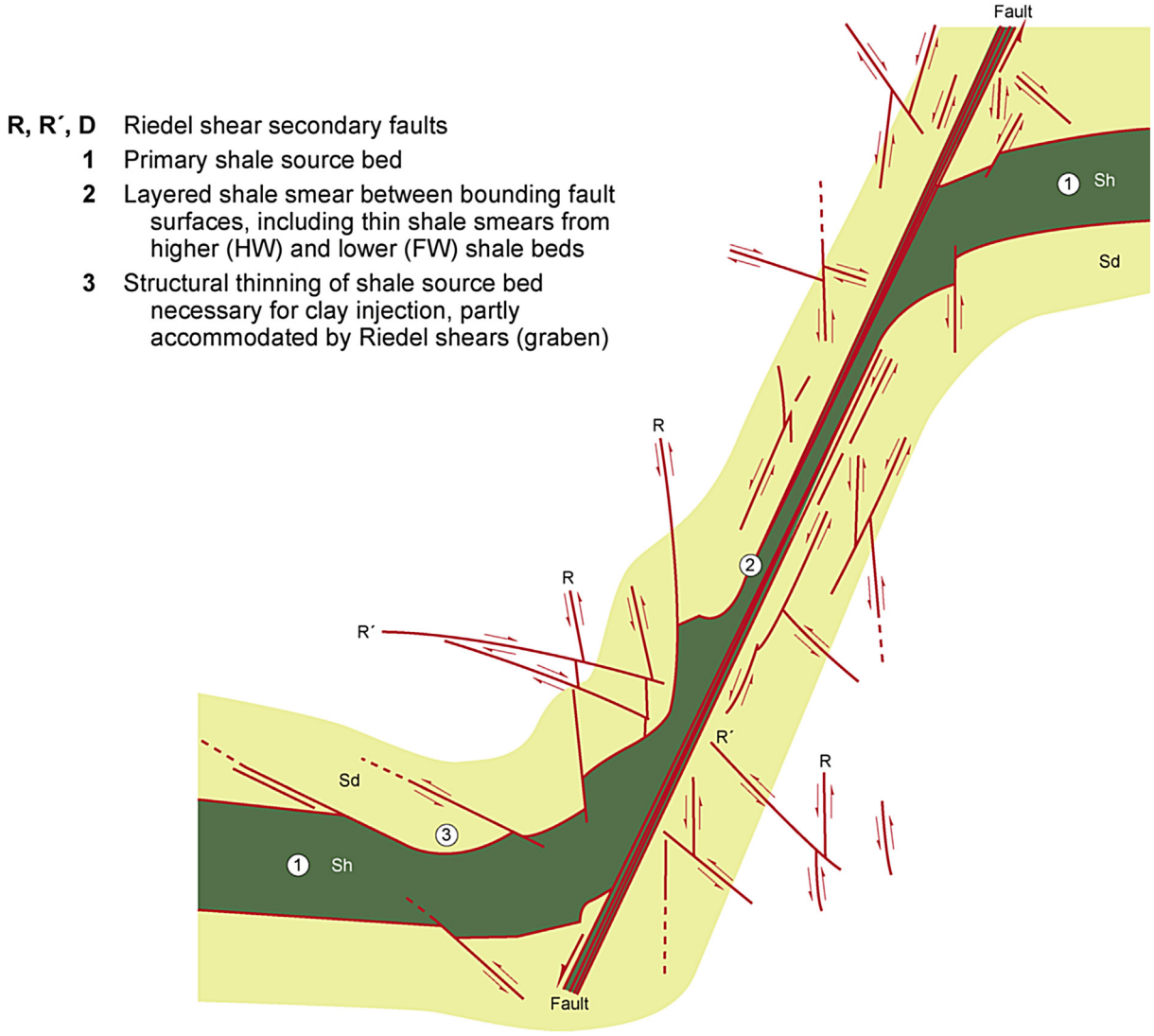


**Fig. 4.** Summary of fault zone elements developed in the Hambach mines, modified after Lehner and Pilaar (1997), including a layered fault zone structure comprising clay smears from multiple source beds; secondary shears interpreted as Riedel R-, R'-, and D-shears; hanging wall and footwall folds; and structural thinning of clay source bed, particularly in hanging wall. Note that figure is intended to be dimensionless, but drawing made from outcrops that are typically meters to 10's of meters in scale. Figure reprinted from Lehner and Pilaar (1997) with permission from Elsevier.

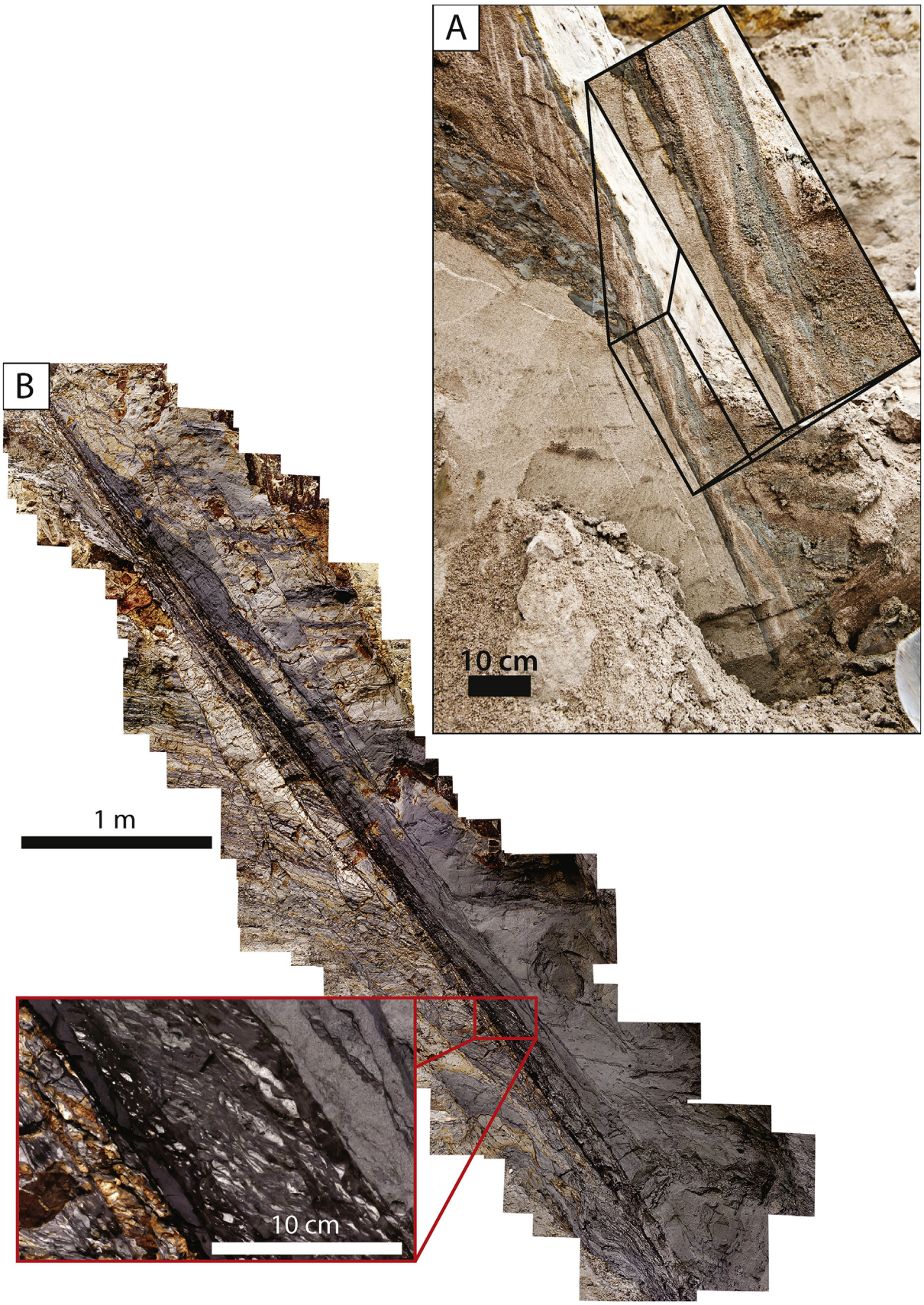


**Fig. 5.** Layered fault gouges from normal faults in (A) Hambach mines, and (B) Miri outcrops (after van der Zee and Urai, 2005). Hambach mine outcrop (A) maintains continuous sand layer between clay smears derived from different mudstone beds whereas sand becomes boudinaged into small phacoids in amalgamated matrix of clay smears in Miri outcrop (B). Fault offset in Hambach is several meters, while in Miri fault offset is 10's of meters.

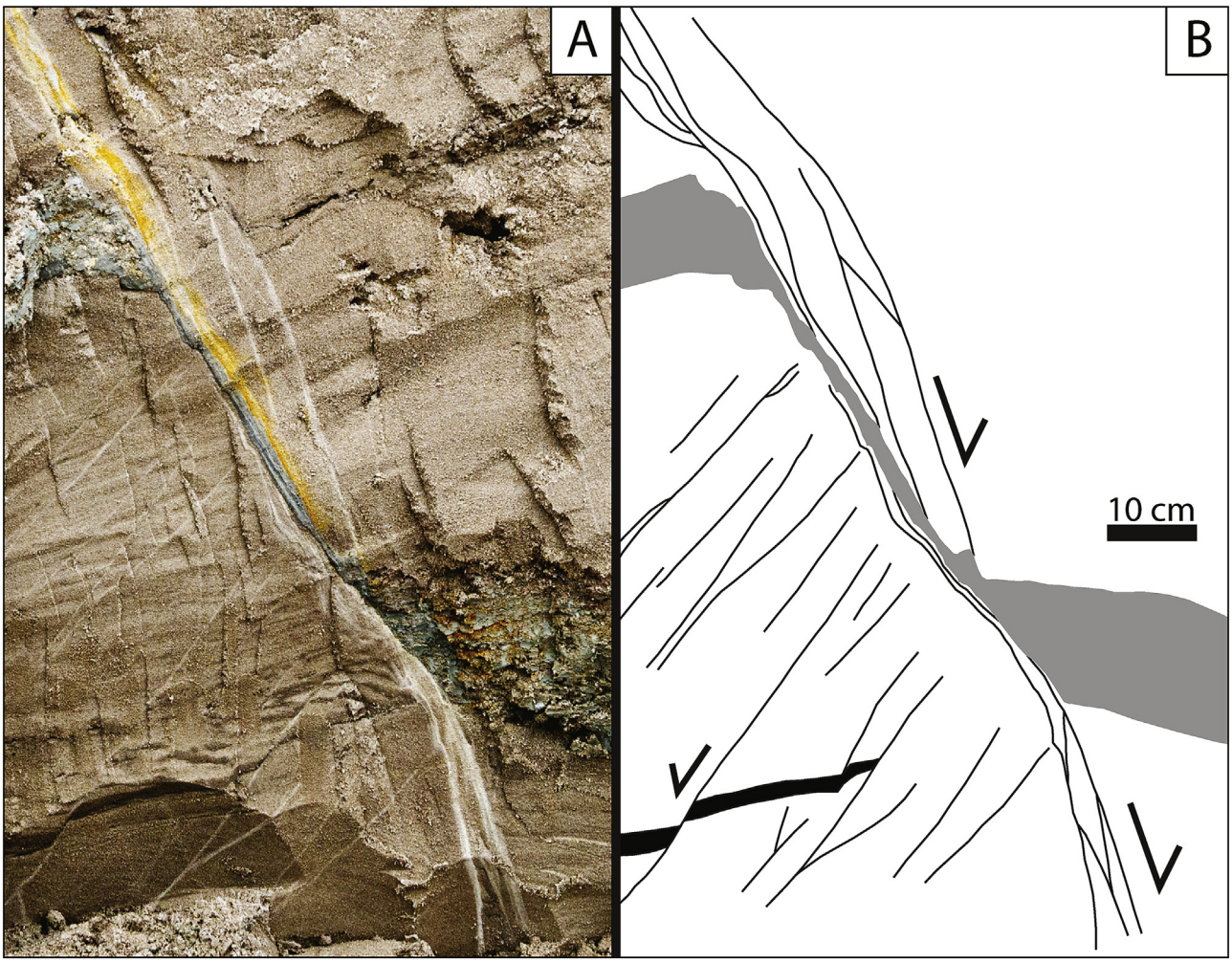


**Fig. 6.** Full displacement of clay bed in Hambach mine, Germany. Note fault refraction at base of outcrop which may contribute to folding of clay bed (different orientation of clay bed in HW versus FW). Light bands in sandstone are deformation bands (secondary faults) that help accommodate overall fault strain. Asperity at fault bend at bottom of outcrop contributes to abrasion of HW clay bed, resulting in incorporation of more clay into fault.

development of a sigmoidal shear pattern observed within the clay smear.

Lehner and Pilaar (1997) observed clay smear developed in every quarry location investigated, leading them to the deduction of clay smear processes that maintain the highest degree of continuity for small to modest offsets from the clay source bed. They offer no observations about how discontinuities in clay smears develop.

Lindsay et al. (1993) offer a complementary viewpoint based on observations from Pennsylvanian fluvial-deltaic sandstones, shales, and coals that are interpreted to have been deformed once all the units were lithified by burial to approximately 2 km. Lindsay et al. (1993) recognize three processes by which clay is incorporated into a fault zone:

1. Abrasion: shale beds faulted past sandstone beds are abraded by the sandstone roughness into a veneer. This appears to occur at scales ranging from the grain-scale to small fractured fragments. The products of the abrasion process include polished and slickensided fault surfaces expressed as veneers in cross-section.
2. Shear: the creation of a simple shear zone includes all of the rocks within the shear zone boundaries; no conditions are defined for the establishment of the shear zone, although drag folding of adjacent beds is described. Shear is interpreted to be responsible for the attenuation of clay smears observed with increasing distance from source beds.
3. Injection: although injection is identified as a process to help create thick clay smears, the corresponding evidence of a thinned hanging wall shale bed is difficult to discern in the field data presented.

In addition to these prominent features, Lindsay et al. (1993) recognized the importance of secondary fault development (i.e. fault relays) for shear zone evolution and understood how this history could affect clay smear processes.

Burhannudinnur and Morley (1997) identified cataclastic sand fragments within a clay smear, which led them to interpret grain-scale mixing of sand and clay. Although Burhannudinnur and Morley (1997) focused more on the geometry of fault networks to assist in seismic interpretation, they nevertheless describe folding of sandstone and shale beds adjacent to fault zones.

Based on these three initial studies, the foundation for clay smear processes was defined for normal faults in sandstone-dominated fluvial-deltaic deposits subjected to varying degrees of lithification.

### 3.1.2. *Broadening clay smear into additional environments*

Clay smear developed on the km-scale Moab Fault (Foxford

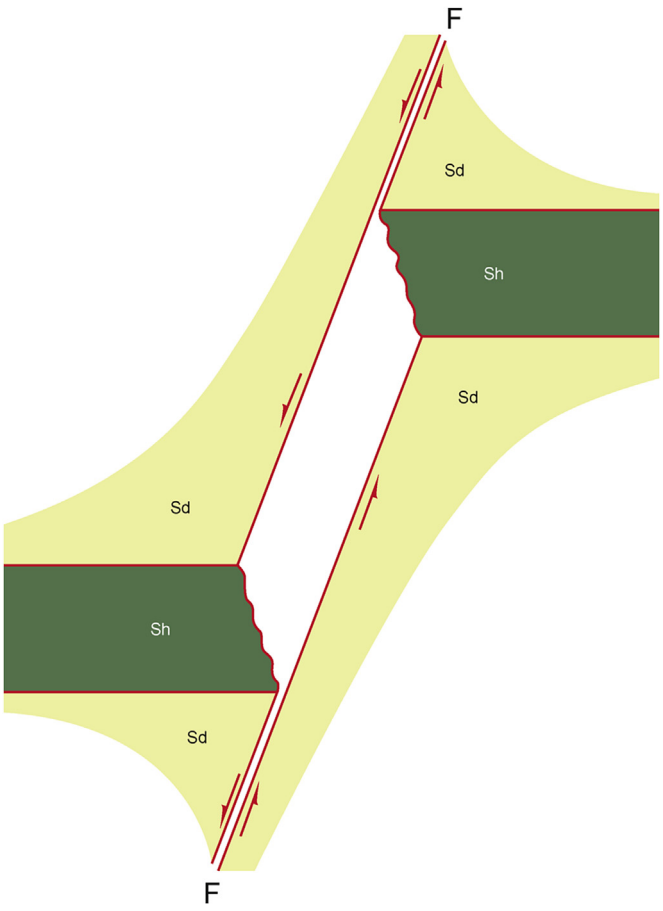


**Fig. 7.** Schematic of 'pull-apart' geometry of overlapping fault segments developed in releasing step geometry, after Lehner and Pilaar (1997), in which dilatant volume created by this fault geometry is necessary component of clay-injection process. Note that figure that figure is intended to be dimensionless, but drawing made from outcrops that are typically meters in scale. Figure reprinted from Lehner and Pilaar (1997) with permission from Elsevier.

et al., 1998) offers a new scale of observation for mudstones and shales deposited in a continental flood-plain to lacustrine environment. Because fault throws far exceed vertical outcrop dimensions, Foxford et al. (1998) offer no observations about processes that incorporate shales into a fault other than to deduce that the resulting fault zone observations are consistent with tip-line and asperity bifurcation processes occurring during fault propagation. These same processes are responsible for the creation of fault lenses and an overall layered fault zone structure.

In an important insight, Foxford et al. (1998) state that: 'the number of shaley gouge layers in a fault zone increases with the number of slip zones,' and they describe fault zones that consist of 2–9 slip zones; this is a further elucidation of the layered fault gouge structure. Subsequent work has failed to pursue this insight even though it contradicts the basic premise of all shale gouge calculations, which rely on stratigraphic details of the abundance and thickness of the faulted section while Foxford's statement relates clay smears to the fault zone structure. Moreover, Foxford et al. (1998) are the first to address Yielding et al.'s (1997) claim that SGR is a value testable by field observations. They construct a triangle-diagram with binned values of SGR for various sandstone juxtapositions and compare those values to outcrop observations about the presence or absence of shaley gouge (the more general gouge description is appropriate given the evidence for clay recrystallization processes revealed by fault dating studies by Pevear et al., 1997; Solum et al., 2005). Foxford et al. (1998) conclude that the 'thickness of the shaley gouge is variable even when juxtaposition and throw are essentially constant,' and no shale gouge is observed when the faulted section contains <20 % shale. They view methods like SGR as a means to account for a multitude of internal slip surfaces that develop in fault zones, creating a: 'layered or anastomosing internal structure' (Foxford et al., 1998).

The first report of clay smear in faults of the Albuquerque Basin (Rio Grande Rift) presented by Heynekamp et al. (1999) describes gravel, sand, and clay incorporated into fault zones from unlithified fluvial system deposits. A motivation for this work was to evaluate fault processes that impact groundwater flow in this area, and thus

**Table 2**
Rating summary of outcrop observations: clay smear structures.

| Stage | Fault zone structure | Observational quality | Comments |
|---|---|---|---|
| Shale incorporation into fault zone | Structural thinning of HW/FW beds | ★★★☆☆ | Necessary observation for clay injection process |
| | Fault lens & relay | ★★★☆☆ | For fault relays that cause additional shale to become incorporated into fault zone |
| | HW/FW folds | ★★☆☆☆ | May reflect migration of shear zone boundaries over time |
| | Fault-propagation fractures & breccias | ★★☆☆☆ | Fractures that develop at a propagating fault tip, perhaps via bending of a stiff bed |
| | Sand/clay mixing @ shear zone border | ★☆☆☆☆ | Grain-scale observations made at clay–sand interfaces |
| Clay smear evolution in fault zone | Layered fault gouge | ★★☆☆☆ | Preserves offset stratigraphic order, albeit missing some intervals |
| | Boudins | ★★☆☆☆ | Typically sand lenses encased in clay smear; may be traced back to source sand bed |
| | Fault lens & relays | ★★★☆☆ | Fault lenses occur within shear zone where bedding may be undeformed or rotating and shearing into gouge |
| | Fault segmentation | ★★☆☆☆ | Recognized as multiple slip surfaces developed within the overall shear zone |
| | Localized vs. distributed shear strain | ★★★☆☆ | Shear strain concentrated on 1–2 clay smears with less deformed materials between them |
| Clay smear termination | Riedels and other secondary faults | ★☆☆☆☆ | Most effective when developed at high angles to shear zone |
| | Gouge holes | ★☆☆☆☆ | Patch of sand–sand juxtaposition across fault zone |
| | Gouge thinning | ★☆☆☆☆ | Progressive thinning of a clay smear with increasing distance from source bed; taper geometry expressed in CSP definition |

Note: Star rating reflects score (red stars) out of maximum potential score (blue stars).

the fault classification scheme developed by Caine et al. (1996) to consider fluid flow problems was adopted. In this framework, modified to some degree for this unconsolidated sedimentary environment, the fault core is associated with a clay smear and is surrounded by a mixed zone that presumably defines the volume of rock deformed by folding, fault relays, and other secondary faults on either side of the fault core. The damage zone appears to have less hydrologic significance (i.e. improved cross-stratal permeability along the fault dip) in this setting than in the original classification (Caine et al., 1996).

Although the magnitude of fault throws relative to outcrop heights limits observations about how mudstones are incorporated into a fault zone, the observation of paired slip zones bounding the fault core further supports the idea of fault structure as an important element of clay smear processes. More observations for how the fault system evolves include:

- Grain-scale mixing of sand and clay
- Macroscopic mixing of fault lenses in the mixed zone described as 'rootless pods of intact bedding' (Heynekamp et al., 1999)
- Fault thickness, including mixed zone thickness, is influenced by fault geometry
- Greater offset of clay-rich units from source beds than coarser units in the fault zone, resulting in a fault that contains more clay than the adjacent beds

Much of the fault evolution appears to occur in the mixed zone that ranges from undeformed beds where sedimentary structures are preserved to foliated, tectonically mixed materials. This mixing is interpreted to be accomplished by 'attenuation of beds, shear along minor faults and foliation, and mixing from meter-scale blocks to the grain scale' (Heynekamp et al., 1999). Because the fault core/damage zone nomenclature lends itself to describing the hydrologic effect of the final fault geometry, it perhaps limits understanding of how materials evolve as they transition from the protolith to the mixed zone and finally into the fault core. For example, what differences are required for clays to reach the fault core rather than end up as clay veneers that bound lens-shaped slivers of intact coarse-grained sediments in the mixed zone? Heynekamp et al. (1999) observed gaps in the clay veneer (gouge holes) and speculated that these gaps might be transient features.

The work by Heynekamp et al. (1999) is significant in that it is the first example of a multitude of lithologies up to gravel incorporated into a fault zone with the clay component, and it is the first published example to consider clay smear in the context of a spectrum of fault zone elements whose geometry and distribution influence cross-fault flow.

### 3.1.3. *Verification and refinement of fault processes*

Subsequent studies include observations that largely fit into the framework defined by the early studies. In some instances the same areas or geologic settings were revisited, which offers the opportunity to independently verify the original observations. In other cases new observations help to further refine our understanding of process, either by bringing a new focus to the same outcrops or by visiting outcrops that preserve processes more completely.

*3.1.3.1. Shale incorporation processes.* Aydin and Eyal (2002) report detailed field observations around a fault tip and along the dip of a fault to more clearly elucidate the processes that incorporate shales into a fault zone; their results further support the importance of fault segments that overlap in a releasing bend geometry. Doughty (2003) and Faerseth (2006) similarly rely upon overlapping fault segments to entrain shale beds. Eichhubl et al. (2005) offer a more detailed look at fault propagation processes at a sandstone/shale bed interface and interpret incipient distributed shear across a deformation zone in bounding sandstone beds and increasingly localized deformation within the clay smear as a result of granular flow of the clay component. The critical observations in this interpretation include the recognition of sedimentary bedding contacts between sandstone and shale, which indicate incorporation of structurally coherent lenses via a fault relay process. However, it is unclear whether the interpretations of Eichhubl et al. (2005) are limited by assumptions about which fault segments are active in what order and whether multiple slip surfaces are active simultaneously.

Vrolijk et al. (2005b) documented a normal fault system developed over a 2 km strike length cutting stratigraphy that varies considerably over that length. They discovered a fluvial channel stacking pattern that promoted the extensive development of fault relays and lenses that increased the occurrence of folded and tilted coherent shale lenses and a fluvial sandstone-poor interval that results in a simple fault zone with limited fault relay development. Moreover, they documented shale-dominated fault lenses with limited extent along the strike of the normal fault (Fig. 8). Davatzes and Aydin (2005) similarly deduced that the geometry of the fault network was influenced by the geometry of the faulted sedimentary section based on evidence along the Moab Fault, and they concluded that a vertical relay was required to incorporate shales of the Morrison Formation into the fault zone.

One of the single most important insights derived from field studies is that clay smear is associated with a network of fault segments, many of them synthetic to the main fault, that result in the proliferation of fault relays and lenses (Fig. 9). This phenomenon appears at a multitude of scales (e.g., Childs et al., 2009a).

One observation that arises from time to time but escapes significant discussion is the observation that some shale beds are cleanly cut by a fault or contribute far less clay to the fault zone than nearby shale beds (e.g., upper versus lower shale beds of Aydin and Eyal, 2002; Doughty, 2003; faulted shallow marine deposits of Kristensen et al., 2013). Do shale beds that escape incorporation simply exist in a stratigraphic position for which fault relay formation is suppressed, or do they possess different mechanical properties at the time of faulting (i.e. with respect to other shale beds and surrounding sandstones) that promotes a simple fault zone? It is difficult to answer this question in most outcrop settings, but we note that the incorporation of shale into a fault may depend more on how the fault network develops, compatible with the observations of Foxford et al. (1998), than current clay smear models account for, which treat every shale bed as a potential contributor to the fault zone.

van der Zee et al. (2003) pursued further the idea of clay injection as observed in outcrops in Malaysia, Germany, and Oman to develop kinematic and mechanical constraints for the injection process that they subsequently explored with analytical and numerical models. From these models van der Zee et al. (2003) derived constraints on material properties and stresses necessary for clay injection to occur and constructed a model based on wireline logs to define the potential for which any shale bed in a sequence would inject clay into a fault zone (Mechanical Clay Injection Potential: MCIP). van der Zee and Urai (2005), reporting on the same Miri outcrops, provide a comprehensive description for how shale is incorporated into a fault as a result of an evolving fault relay system (Fig. 10), explore the mechanics of the contribution of deforming fault lenses to clay smear, and established a correlation between SGR and the average values of the highly variable measured clay content of the fault zone.

*3.1.3.2. Clay smear evolutionary processes.* A nearly universal theme of outcrop studies, either explicitly or implicitly described, is

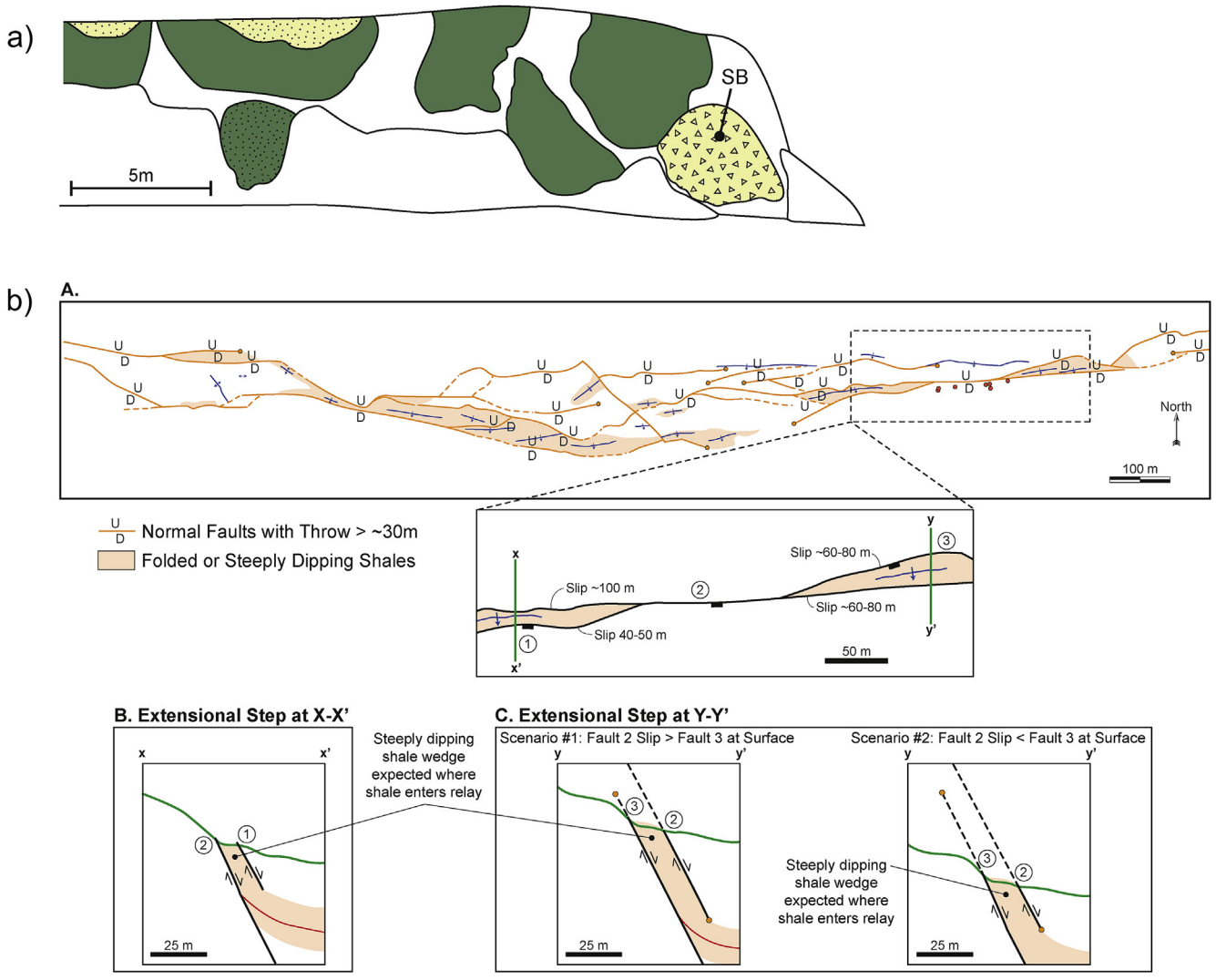


**Fig. 8.** Plan view illustrations of fault lenses developed on scale of meters to 100's of m. (A) modified after Childs et al. (1997). Note in this Lancashire mine exposure that both shale- (green) and sandstone-dominated (stippled) lenses develop on fault surface (with minor sandstone breccia lens: SB). (B) Reproduced from Vrolijk et al. (2005): mappable shale lenses develop along normal fault with 100's of meters of throw. Cross-sections illustrate geometry of overlapping fault segments (no vertical exaggeration). Note that observations along strike like these are essential for evaluating clay smear continuity for application to subsurface flow problems. Fig. 8a reprinted from Childs et al. (1997) with permission from Elsevier.

that clay smear exists in a layered fault zone structure (Fig. 5; Lehner and Pilaar, 1997; Foxford et al., 1998; Heynekamp et al., 1999; Lewis et al., 2002; Aydin and Eyal, 2002; Bense et al., 2003; Doughty, 2003; van der Zee and Urai, 2005; Eichhubl et al., 2005; Vrolijk et al., 2005b; Faerseth, 2006; Kristensen et al., 2013). Layering in the fault zone preserves the stratigraphic order of the faulted lithologies (Aydin and Eyal, 2002; Doughty, 2003), even if parts of the stratigraphic section are omitted in some locations (e.g., Davatzes and Aydin, 2005).

Stratigraphic omission appears to be accommodated by boudinage processes (Fig. 11) that may be assisted by small-scale, secondary faults (including Riedel shears). It appears that all lithologies from mudstone to gravels can create smears in a fault zone (e.g., Heynekamp et al., 1999; Bense et al., 2003; Doughty, 2003; Kristensen et al., 2013), but it is the winnowing of lithologies via a boudinage process with increasing fault throw that allows one lithology to become more abundant in a fault than the other lithologies. It is this variable evolutionary process that caused van der Zee and Urai (2005) to propose a 'preferred smear,' a process that accounts for the attenuation and boudinage of sand layers and thereby allows individual clay smears to amalgamate into a composite smear, enriching the fault zone in clay at the expense of other lithologies.

Numerous authors have described the occurrence of secondary faults adjacent to and within the fault zone, but these observations are made without a kinematic framework that would help compile and evaluate the importance of these small faults in the overall fault structure and in the clay smear evolution, in particular. For example, Aydin and Eyal (2002) conclude that small faults never degrade the integrity of the clay smear in the fault. Although Doughty (2003) interprets small faults in the studied fault zones as Riedel structures, he then neglects to apply the Riedel framework to his fault interpretation in spite of the fact that he attributes thickness changes and clay smear terminations to result from minor normal faults.

Kristensen et al. (2013) investigated the implications of different consolidation states and different stress conditions in a comparative study of three outcrop locations in Denmark. In the shallowest setting where recent (post-glacial) shallow marine deposits are faulted, the resulting fault zone includes smears of sand, silt and clay lithologies. Some sand grains are mixed into the clay smear, and some clay beds are cleanly cut by the fault without appearing to

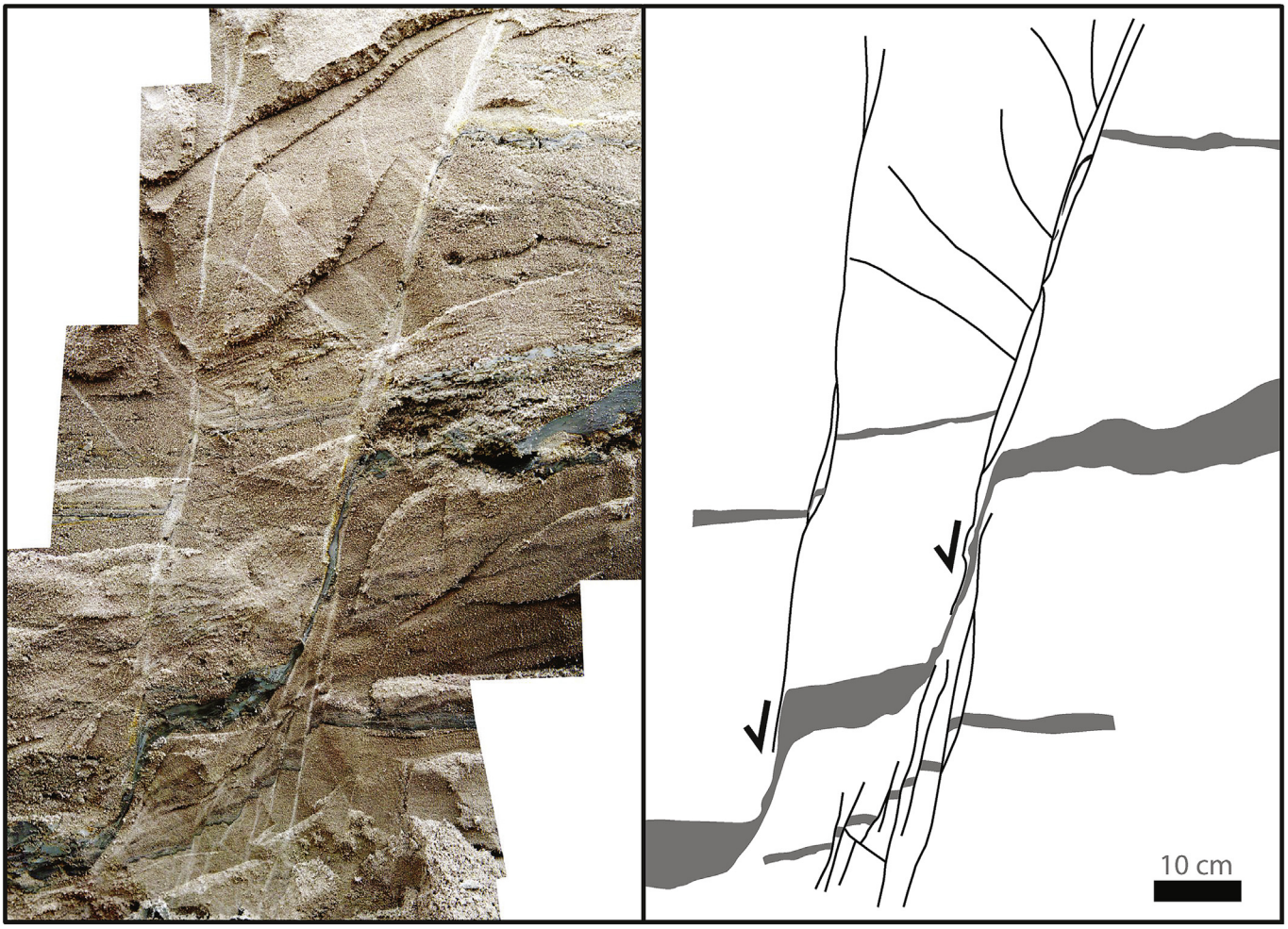


**Fig. 9.** Outcrop figure from Hambach mine, Germany, in which dark clay bed is smeared along two primary fault zones defined by white deformation bands in sandstone, forming fault relay structure. Between bounding shear zones multiple secondary faults develop (base of outcrop), resulting in formation of small fault lenses of relatively undeformed clay bounded by clay-filled shear zones.

contribute at all to the fault zone. In the deepest Jurassic outcrop the presence of cataclasis is a distinguishing characteristic. Kristensen et al. (2013) document progressive mixing of sand and clay components with increasing fault offset, although thin sandstone layers developed between thicker shale layers are absent in the fault. The intermediate depth example also defines a layered fault zone with little mixing of grains, and both brittle and ductile deformation of shale beds is observed. The implications of this work are that fault processes evolve as a function of the changing consolidation state of the faulted materials and the stresses available at the time of faulting.

*3.1.3.3. Clay smear in over-consolidated rocks.* Although clay smear is usually associated with soft, ductile shales, there is evidence that clay smear-like structures develop when fragments of stronger, overconsolidated shale are incorporated into fault zones. Holland et al. (2006) describe the evolution of highly over-consolidated shales into clay smear via fracturing, faulting, and abrasion processes. They document the creation of a high porosity, low permeability clay smear from an initially low porosity, low permeability shale, and because that transformation takes place without any significant chemical or mineralogical changes, the resulting clay gouge may look indistinguishable from a clay smear (e.g., sampled in a core); a reworked shale is a soft clay, while a reworked sandstone is a cataclasite although both are produced by purely mechanical processes. Although the examples shown by Holland et al. (2006) represent an end-member behavior, they offer a good example of how clay smear may arise in a fault zone from brittle processes.

*3.1.3.4. Clay smear applied to hydrologic problems.* The work by Heynekamp et al. (1999) illustrates how fault zone structures are defined for the purpose of investigating the effect of clay smear on cross-fault flow, but the focus on defining the final geometry and flow properties of various fault elements sometimes limits the insights for how that final geometry was achieved. Notwithstanding this limitation, these studies provide some of the most compelling observations for terminating clay smears.

For example, Bense et al. (2003) describe how: 'gravel pebbles trapped in the fault plane cause discontinuities in the clay smear.' The pebbles create asperities that can disrupt clay smear continuity when the pebble size approaches the thickness of the clay smear. Caine and Minor (2009) describe laterally persistent clay-rich fault cores (clay smears) in a sandstone-dominated setting but identify a few rare exposures where a clay-rich core is absent and hanging wall and footwall sandstones are juxtaposed. They recognize that a key factor is the: 'identification of the size and location of relatively high-permeability "hydraulic holes" in …faults' (Bense et al., 2003)

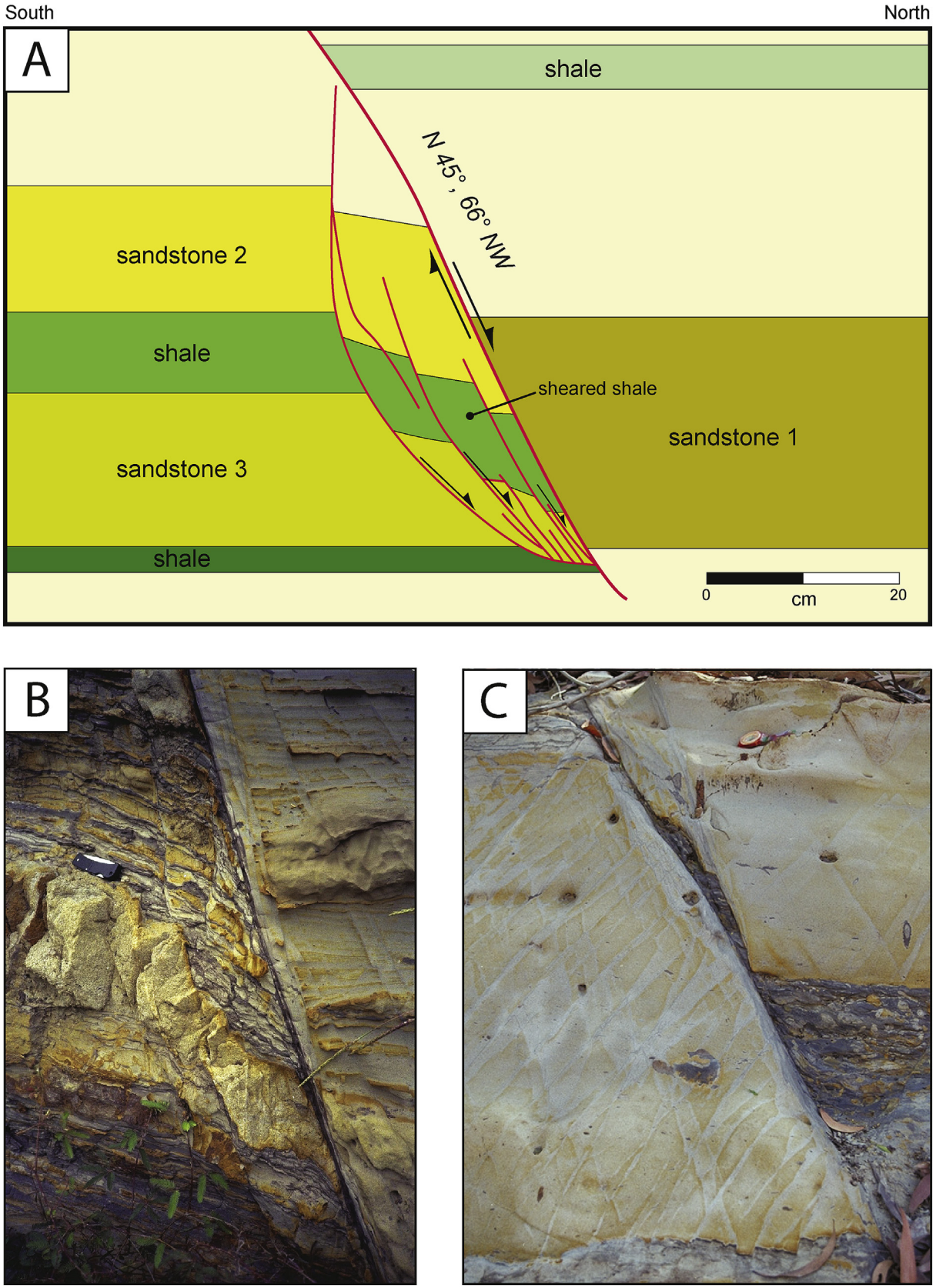


**Fig. 10.** Fault relays developed in Miri outcrops at bed scale illustrate early stages of shale incorporation into fault zone as result of fault relay development and bed telescoping. (A) Field drawing after Burhannudinnur and Morley (1997) showing progressive rotation and shearing of shale bed approaching main fault surface, possibly characterizing a fault outcrop (B) described by van der Zee et al. (2003). (C) Characteristic shale wedges described by van der Zee and Urai (2005) as result of fault relay evolution; see van der Zee and Urai (2005) for reconstruction of fault structure. Fig. 10c reprinted from van der Zee and Urai (2005) with permission from Elsevier.

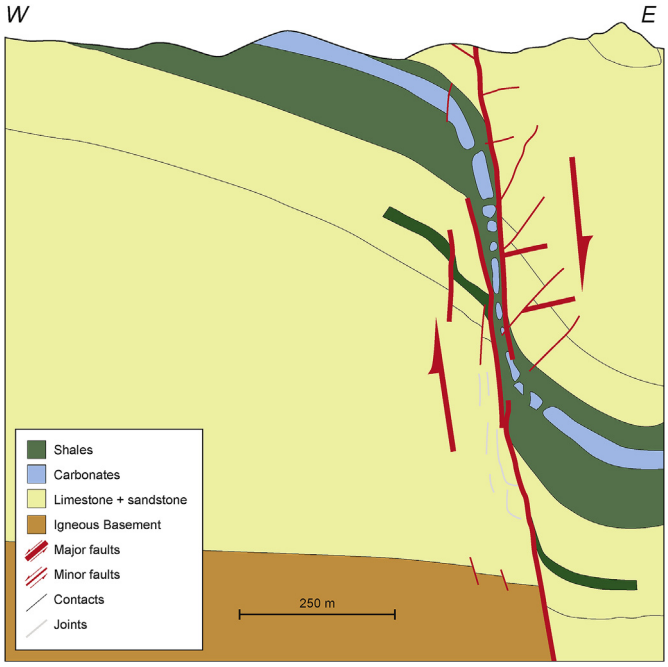


**Fig. 11.** Summary of fault zone structures documented by Aydin and Eyal (2002). Important fault structures defined at this scale include stratigraphically layered fault zone, with bed thickness in fault zone roughly proportional to original source bed thickness; minor faulting of footwall and hanging wall beds immediately adjacent fault; boudinage of carbonate-dominated interval contained within shale interval; and secondary (Riedel?) faults developed mostly in hanging wall. Note proximity of a rigid basement in footwall, making this a good comparison for sandbox experiments introduced in later Experimental Studies section (4.2.1).

that compartmentalize an aquifer and implicitly acknowledge the difficulty in outcrop studies for providing this characterization.

Loveless et al. (2011) describe many fault zone elements associated with clay smear processes: a fault zone consisting of multiple slip surfaces; drag of thinned lithologies in the fault zone; incorporation of coherent fault lenses into the fault zone; grain-scale mixing of different lithologies. All of this occurs in a stratigraphic section without shale, and thus there is no fault core containing clay smear. Although this outcome seems obvious, the ubiquitous development of similar fault structures shows that clay smear develops in the context of a more universal fault structure evolution.

*3.1.3.5. Processes that terminate clay smears.* Although this facet of the problem is the most important for determining cross-fault flow, there are few outcrop observations that address how this actually occurs. Firstly, holes are hard to find given the inherently 2D nature of outcrop exposures. Secondly, when they are described, they occur related to thinning and attenuation of the clay in the fault zone, but it is hard to say whether thinning is a necessary or just helpful condition. It is clear, however, that attenuation and thinning is by no means a sufficient condition for holes to form. There is as yet no explanation for why a hole in a clay smear forms at any particular point. Doughty (2003) pointed to small faults as the cause of observed holes, and Bense et al. (2003) attributed the holes they saw to gravel roughness elements in the fault zone. van der Zee and Urai (2005) claimed there were no holes observed in dip sections of faults investigated in Miri, Malaysia, but when they found holes in the clay smear in fault strike sections exposed on benches, they were unable to rule out the possibility that a parent shale bed was absent at that location and thus the cause of the hole.

Childs et al. (2007) studied clay smear processes in deep-water turbidite channel and fan deposits cut by normal faults in coastal exposures of New Zealand. The observations made at these outcrops appear to contradict generalizations made from previous studies in settings that are more dominated by sandstones, including the following:

- 'Clay smears maintain continuity for high ratios of fault throw to clay source bed thickness (c. 8; *approximately 8*), but are highly variable in thickness, and gaps occur at any point between the clay source bed cut-offs at higher ratios'
- 'data demonstrate that there is no clear relationship between distance from the source bed and smear thickness, and that thickness immediately adjacent to the source bed may be as low as those distant from the source bed'

The result of these observations is the definition of a Probabilistic Shale Smear Factor (PSSF) that attempts to account for heterogeneous fault zone structure by allowing the finite probability of a hole developing somewhere on a clay smear according to a specified probability density function. The rationalization for this approach is the inference that: 'the locations of smear breaching are controlled by strain distributions, and slip surfaces, within the fault zone' (Childs et al., 2007), a statement that is compatible with Foxford et al. (1998), although the precise structural mechanisms that cause these holes remain undefined. What is remarkable about this study, though, is that holes may form before there is any significant thinning by simple shear processes in the fault zone, the first realization of this fact since the original conceptualization of a clay smear as a taper from a source bed.

*3.1.4. Summary insights from outcrop observations*

Field observations describe fault structures resulting from processes that control the presence, morphology, distribution, and continuity of clay smears (Table 2). However, when broken down into the essential elements necessary to address the clay smear problem, it becomes clear that there is substantial room for improvement in all dimensions of the problem. A number of studies have shown that the path to a deep understanding includes outcrops that contain the source beds on both sides of the fault, but this in turn makes it very difficult to find outcrops that provide this exposure of a fault with as much as 25 m throw.

There has been reasonable progress toward developing an understanding of the processes that incorporate shales into faults and the processes that further deform those clays in the fault (Table 2), even though some elements like folding appear poorly defined by field observations, especially in light of potential folding associated with propagating fault tips. Perhaps a large part of this state is the difficulty in deducing kinematic histories of all the minor elements in a fault zone; for example, interpretation of folding and minor faulting interactions leading to sandstone boudinage (Fig. 12). With greater fault offset, the inference of these interactions becomes much more challenging. One important insight that does emerge from outcrop studies is that the kinematic fault network evolution, in the sense of Childs et al. (1997) and many other authors, is essential for defining how fault zones evolve. For example, Cilona et al. (2015) interpret clay smear in a fault with primary strike-slip offset and minor dip-slip displacement; is dip-slip of gently dipping beds necessary for shale incorporation in the fault with subsequent evolution dominated by the strike-slip component, and if so, did dip-slip occur before strike-slip displacement? The role of kinematics will be further developed in the discussion section.

Most remarkable, however, is the paucity of helpful observations for processes that terminate clay smears. This aspect of the problem has been recognized as critical for predicting the flow properties across faults since Weber et al. (1978), yet progress is


**Fig. 12.** Example of how folding and secondary fault development (synthetic to main fault surface) interact to both entrain shale into fault zone and begin to dismember and boudinage intervening sandstone layers. Photo of outcrop from Miri presented in van der Zee et al. (2003).

limited. Are outcrops poorly suited for investigating this aspect of the problem? It would appear that non-destructive 2D outcrop observations hinder investigation of structures associated with holes because there are always uncertainties that arise from the geology just beyond the outcrop surface; even studies with minor amounts of excavation (e.g., Kristensen et al., 2013) illustrate the benefits of seeking the three-dimensional geometry and continuity of fault zone components.

A composite view of the elements present in a fault zone with clay smear is becoming clear (Table 2), but the distribution of these elements in any individual fault zone is uncertain. It is also difficult or impossible to construct a detailed 3D block model that is retrodeformable, a fact which probably reflects an incomplete understanding of the kinematic evolution of the fault zone, especially the role of the secondary fault structures. Because insights into the material properties and stress conditions resulting in different structures are limited, it may be difficult to achieve much progress with outcrop observations alone. Moreover, the necessary observations for identifying the few most important processes that control clay smear evolution remain elusive.

The goal of outcrop studies is to define fault structures and associated lithologic components in a way that allows analyses comparable to subsurface studies and provides the structural and geometric characteristics necessary for comparison with laboratory and numerical models. We propose that the following observations are critical to achieving this goal:

1. Multiple transects with clay fraction determinations along the dip and strike of the fault zone (e.g., van der Zee and Urai, 2005)
2. Geometric aspects of fault (spatial components), including:
   a. Thickness of each of the structural and lithologic components
   b. Fault throw (in lieu of displacement vector)
   c. Stratigraphic column of the faulted section, including Vshale characterization
      i. N:G of section (proportion of lithologies on either side of Vshale cutoff)
      ii. Average bed thickness for each lithology (for a defined Vshale threshold)
   d. Number of shear zones in each fault transect
3. Comprehensive listing of diagnostic fault structures (developed in following sections; Fig. 27)
4. Detailed fault description of all fault components, including deformation in sand (stone); from one edge of fault zone to the other
5. Along-dip lengths (and continuity) of all structural and lithologic components (i.e. basis for subsurface fault zone mapping)
6. To the extent possible, 3D definition of fault systems (i.e. along fault strike)
7. All scales of observations from microscopic to largest scale possible in each outcrop (which must be defined)
8. Collect data in such a way that observations and measurements are reproducible

Outcrops will always be limited in the dimensions of observation and thus over-estimate the continuity of structural components. This limitation needs to be embraced in such a way that all clues in the outcrop that indicate further dimensions are observed and recorded.

### 3.2. Laboratory and numerical models of clay smear

Laboratory and numerical experiments are undertaken in order to elucidate physical processes that result in faults with clay smear. Because it is possible to follow the incremental strain history and to measure stresses and material properties in experiments, they form a crucial part of our understanding of clay smear processes. In this section we review the available literature on laboratory and numerical experiments, summarize what we think has been learned from these studies, and discuss where we think future areas of research may contribute to further advances in our understanding. Often the results of laboratory and numerical experiments are used to compare the effectiveness of clay smear algorithms in the subsurface – later in this section we discuss the many pitfalls of this approach.

Outcrop studies reflect three important stages in the development and maintenance of a clay smear: (a) an initial stage responsible for incorporating the necessary clay into a fault zone; (b) an intermediate stage where clay smear evolves as the fault accumulates large shear strain and initial holes may be closed; and (c) a final stage where clay smear is disrupted and holes form. As

was described in the Outcrop Studies section, this generic history of the continuity of a layer during fault evolution exists regardless of whether clay is involved in the faulted section. In our review of the experimental and numerical studies we follow this same scheme.

The search for the answer to the question – how does a clay layer in sand evolve into a more or less continuous clay smear in a fault zone? – should start with a thorough understanding of the relevant processes in homogeneous materials (for example by replacing the clay layer with sand, just colored differently). Fault evolution in pure sand is by no means understood, but what is known provides a useful baseline to study how the difference between clay and sand affects the process of clay smear evolution. Interestingly, experimental and numerical studies use similar model geometries and suffer similar problems with simulating localization and fault evolution processes.

If these processes are understood in the laboratory and numerical simulations, the next non-trivial task is to upscale these results to faults in nature. Does any individual experiment relate to nature at a scale of 1 m or 100 m in size? When does the grain size chosen in the laboratory or grid size chosen in the computer influence the observed fault processes in a way that biases the understanding of faulting when results are up scaled to nature? The final, most difficult question asked by subsurface flow applications is: when is the clay smear discontinuous in the subsurface? Keeping this in mind, experimental and theoretical modeling of clay smear can be seen as a truly challenging task. On the other hand, even if the results are incomplete, these studies shed light on processes or define structural domains which are otherwise difficult to identify from final, total finite strain examples represented in outcrops, and if one can demonstrate that the results are applicable or can be scaled to natural prototypes, they then prove useful. Our final task in this section is thus to summarize how the available laboratory and numerical experiments are appropriately used in nature.

### 3.2.1. Experimental study of clay smear processes

Experimental research on clay smear has been done in a range of configurations and corresponding boundary conditions. The short review below attempts a comparison of these different experiments, trying to identify structures and processes that are independent of the experimental technique and those that occur both in numerical simulations and in laboratory experiments.

A good starting point for this discussion is shear band formation in homogeneous granular material, which has been studied extensively since the late 1950's (Fig 13). It is well known that in triaxial tests (Vardoulakis and Sulem, 1995) development of a single well-defined shear band is complicated by the symmetry of loading; initially a complex failure pattern evolves of multiple incipient shear bands. Many studies of shear band formation in sands have been conducted using plane strain compression testing. Here, there are many uncertainties regarding when shear bands initiate, and at what stage of the loading history bifurcation and localization occur. 3D image correlation techniques to measure the full velocity field in the sample (Hall et al., 2010) are required to address these questions. In direct shear experiments, curved shear bands form a lens before a through-going shear zone is established. Shear bands also develop in ring shear experiments. Although the shear band is prevented from developing at any orientation in a ring shear apparatus, very large displacements are possible. In sandbox experiments, a multitude of shear band structures develop depending on boundary conditions. Balthasar et al. (2006) compared a number of experimental configurations and discussed existing constitutive models for shearing clays, concluding that there are no calibrated and validated models for the rheology of sheared clays at present.

*3.2.1.1. Ring shear experiments.* The classic papers on experimental study of shearing in granular aggregates and the development of clay smear are Mandl et al. (1977) and Weber et al. (1978). A ring shear apparatus was used to study the development of shear zones, together with in-situ stress measurements, microstructural study of the deformed materials and permeability measurements. The experiments were analyzed in great detail and clearly identified the limitations of such experiments in the study of fault zones in nature. Shear stress was applied to the samples by rough, permeable, ring-shaped plates at the top and bottom of the shear zone. A transparent annulus was illuminated from inside so that samples saturated with pore fluid of the same refractive index remained transparent, and the development of shear zones, clay smears and slip planes could be followed in real time. Materials and normal stress were chosen to either allow or suppress dilatancy and to cause grain crushing in the shear zone at high stress. Principle stress orientations were measured inside the samples using photoelastic cylinders. Deformed samples showed slickensides on the master slip plane and secondary slip planes in Riedel orientations. The photoelastic stress measurements show that in the beginning of the shearing process the direction of maximum compressive stress rotated from vertical into a position at an angle of 45° to the horizontal shear direction, and the authors concluded that: 'the shear band produced between the rigid platens of the apparatus is bounded by planes of maximum shear stress rather than by Coulomb-type slip planes.' At the same time the observations of oblique sets of minor shears indicate the tendency of the material to deform in accordance with Coulomb's slip concept, which obviously is suppressed by the specific type of kinematic boundary constraints (Mandl et al., 1977). Thus the trade-offs between the inherent nature of the fault structure and the structure imposed by the kinematic constraints of this particular experimental design, selected for the high shear strains allowed, became established.

For the clay smear experiments (Fig. 14), the apparatus was filled with alternating layers of sand and remolded clay (Weber et al., 1978). Results show the clay sheared to form a continuous, multilayered clay smear along the shear plane. An important observation was the formation of wedge-shaped sand intrusions in the clay (pointing into the shear direction). In movies of these experiments made through the transparent outer ring, these sand wedges were observed to move into the clay layer, producing a local thickening (injection) of clay in the shear zone as a result (G. Mandl, pers. comm. 1997). The clay smear was mixed with sand grains and had a low permeability to flow across the shear zone.

Sperrevik et al. (2000) used a ring shear apparatus at effective stresses corresponding to a depth of about 50 m to shear sand-clay sequences. They used different clay types, with undrained shear strength between 50 and 350 kPa, and water content between 19 and 50%. Removing the upper sand exposed the clay smear, allowing measurement of its continuity (Fig. 15). The development of clay smear was discussed as a function of the competence contrast between the clay and sand. Many of their results are comparable to those of Weber et al. (1978). Clay, which was less competent than sand, was interpreted to be ductile, and formed clay smears along the shear zone. The compaction of the sand during deformation led to work hardening and increased its competence contrast with the clay, which smeared along the shear zone in a ductile manner. In experiments where the sand compacted during deformation, a clay wedge formed by drag of the clay into the shear zone. The thin (1.5 mm) clay smear was continuous, in some cases along the whole shear zone. With increasing distance to the source clay, increasing amounts of clay mixed with sand were found, together with discontinuities in the clay smear. In some

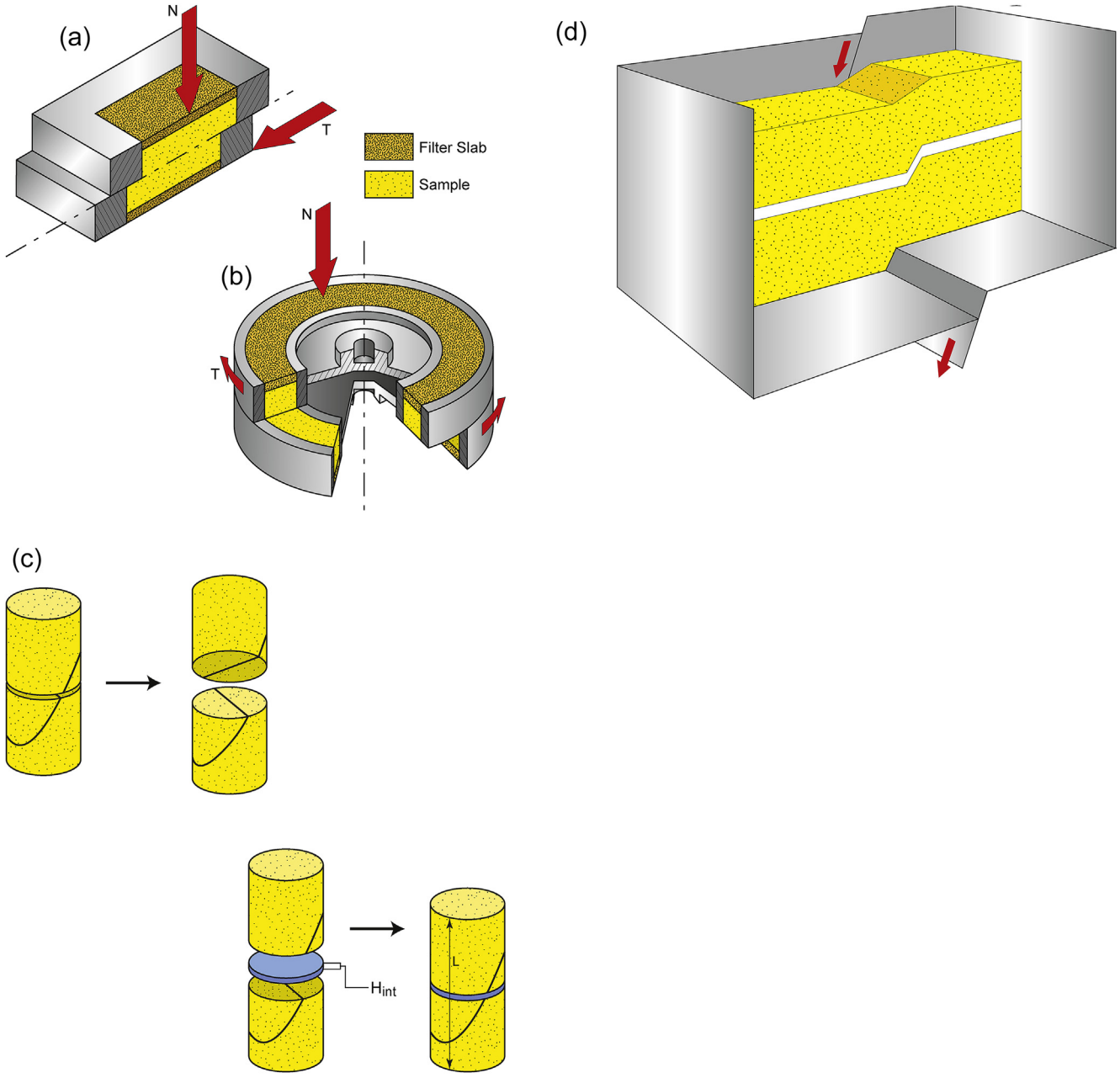


**Fig. 13.** Schematic illustration of different experimental configurations to model claysmear. (A) Direct shear (red arrows indicate stresses); (B) Ringshear (red arrows are applied stresses); (C) Triaxial sample, illustrating how a pre-cut fault cylinder is separated into two, a sandwich of siltstone inserted to simulate fine-grained smear material, and sample reassembly; (D) Sandbox deformed over rigid basement fault with red arrows indicating displacement imposed by apparatus.

cases the clay formed undulatory bumps over Riedel shears in the sand, but in other cases it lost its continuity in these structures. Multiple initial clay segments led to a composite, layered clay smear, which was sometimes discontinuous in 3D with a thin sand wedge connecting the sand on both sides of the clay.

When experimentally deformed clay was more competent than sand, it behaved in a brittle manner and formed isolated angular fragments. Here, the shear zones dilated and the sand strain-softened and became less competent than the clay. Sperrevik et al. (2000) propose that the transition is a function of the stress conditions, initial porosity of the sand, and the mechanical properties of the clay. Unfortunately the full mechanical properties (e.g., dilatancy transition) of the individual clays were not determined so that it is difficult to establish the exact deformation mode of the clay. Based on rock mechanics considerations, the absolute value of the clay's brittleness must also play a role, not only its contrast to the sand. An additional problem that Sperrevik et al. (2000) could have discussed is the initial state of stress (e.g., as can be visualized using photoelastic techniques) because it is difficult to pack and load a sample such that initial stress is homogeneous.

Clausen and Gabrielsen (2002) and Clausen et al. (2003) built on the work of Sperrevik et al. (2000) using the same apparatus and sand with a wider range of clays (undrained shear strength between 20 and 700 kPa) in drained shear experiments which have shown good reproducibility. Detailed measurements of the shear stress and volumetric strain in the samples are accompanied by thin section analyses of deformed samples. The authors classified three types of structures: absence of a clay smear with only clay

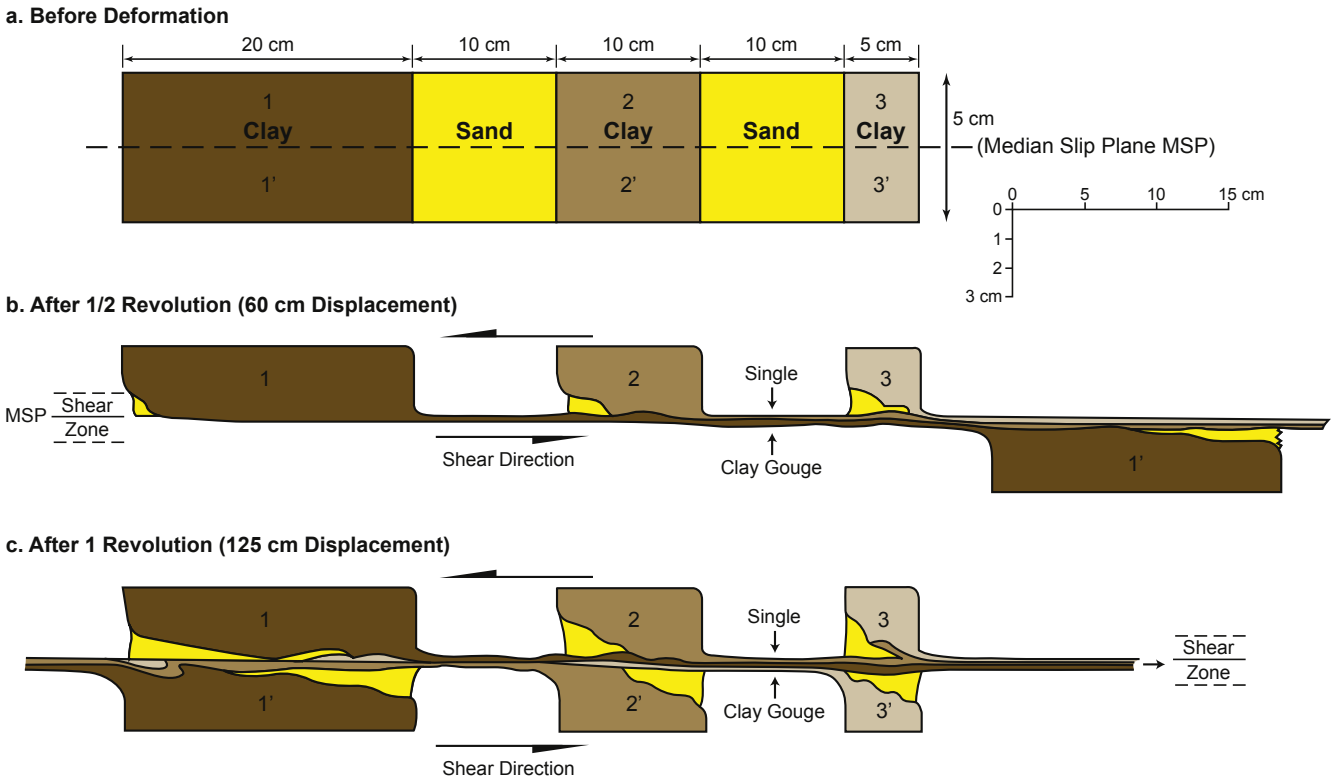


**Fig. 14.** Development of multilayered composite clay gouge in sand-clay sample deformed in ring-shear apparatus (redrawn after Weber et al., 1978). Note how layers in clay gouge are correlated with their source layer, and sand wedges (squeezing blocks) which move into clay layer and are associated with transport of clay into shear zone. Copyright 1978, Offshore Technology Conference. Reproduced with permission of OTC. Further reproduction prohibited without permission.

fragments at low stress, a mixture of clay and sand or patchy clay in a sand matrix at intermediate normal stress and a semi-continuous clay smear at high normal stress. The normal stress required for the transition between these continuity domains depends on the clay type and is higher for stiffer clays, as expected. Clay wedges or lenses were observed close to the source layer in many experiments, interpreted to be associated with initial fracturing of the clay with the assistance of Riedel shears. Clay smear continuity and area of shear plane covered with clay became larger when the normal stress was increased. The water content of the clay decreased with increasing strain in compacting samples. Thin sections of deformed samples show that both sheared clay and mixed sand-clay are present in the clay smears.

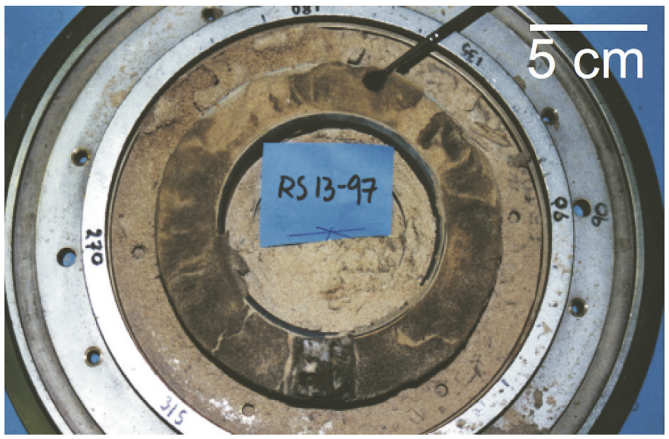


**Fig. 15.** Top view of a clay smear formed in ringshear experiment (Sperrevik et al., 2000) after brushing away top sand layer. Dark block at bottom of photo (inner ring) is source clay layer.

Cuisiat and Skurtveit (2010) presented results from a high-stress ring shear apparatus using uncemented, normally consolidated sand and clay at stresses corresponding to burial depths up to 1500 m. The samples all reached a steady shear stress during the experiments and compacted progressively. It is unclear if compaction is due to grain rearrangement in the different phases or mixing of sand and clay (cf. Schmatz et al., 2010 a,b). Sectioning of the samples after the experiments, corresponding thin sections, and permeability measurements across the shear zone were used to investigate clay smear continuity, thickness and evolution of permeability (Cuisiat and Skurtveit, 2010). Granular flow, grain mixing and cataclasis all contribute to the resulting clay smear structure as a function of effective mean stress. Under conditions of granular flow, clay smear led to strong permeability reduction across the shear zone. At greater effective stress, permeability reduction by grain crushing was of a similar order as by clay smearing. Cuisiat and Skurtveit (2010) interpreted that in addition to clay smearing, drag and injection of clay along the fault plane also occurs, together with mixing of clay and sand in the fault core, although the evidence for this seems inconclusive. The thickness of clay smear was higher for thicker clay source layers, while reducing the clay layer thickness to one half of the reference layer produced a thin and discontinuous clay smear. Shearing of multiple clay layers produced a layered, composite clay smear 2–3 times thicker than that for a single clay layer. The authors concluded that the experiments were consistent with a first order correlation between SGR and seal capacity.

Sadrekarimi and Olson (2010) studied sand samples with colored marker layers in a ring shear apparatus that had a transparent outer ring to allow direct observation. The samples deformed homogeneously before peak stress, followed by

localization and slow widening of the shear band until a stable thickness of one grain diameter was reached.

In summary, the main advantage of ring shear experiments is the very large shear strains allowed by the apparatus. Intensive shearing in the thin shear zone imposed by this design occurs by granular flow and mixing of sand and clay, by abrasion of brittle clay fragments, or by cataclastic flow at high normal stress. The full spectrum of clay smear continuity from discontinuous clay fragments to continuous clay smear was found in the shear zone, depending on effective stress, and the transition from discontinuous to continuous occurs at higher stress for stronger clays. The key parameter for overconsolidated clay in cohesionless sand is the effective stress, which suppresses brittle failure of the clay and enhances shearing. Cataclastic flow produces similar geometries. A disadvantage of ring shear experiments is the strong kinematic constraints imposed by the fixed geometry of the apparatus. Localization patterns are prescribed by the rotating outer rings so that the sample can only develop the thin shear zone in the plane of the forcing rings.

*3.2.1.2. Direct shear experiments.* Karakouzian and Hudyma (2002) present a novel apparatus for investigation of clay smears. Samples consist of alternating layers of sand and clay, encased in a transparent tube, and an axial plunger with a half-circle cross section which pushed half of the sample past the stationary part. Deformed samples show deformation bands with sheared clay and the development of lenses, similar to the structures that develop in a direct shear configuration (Thornton and Zhang, 2003). The authors conclude that direct (real time) observation is a useful addition to more sophisticated deformation experiments.

Urai et al. (2003) used artificially prepared layered samples with sand, kaolinite, illite and smectite. Samples were deformed to shear offsets up to twice the layer thickness in a geotechnical direct shear apparatus. After saturation and initial compaction the sample was inserted in the shear apparatus and deformed under drained conditions. Besides recording the stress-strain behavior of the aggregates, a detailed study of the internal structure of the fault zones was done by serial sectioning of the deformed samples.

Structures developed in end-member samples were quite different, with relatively wide deformation bands in the sand and much sharper deformation bands in the clays. Shear bands were initiated at the edges of the moving sample chamber and propagated towards the center of the sample. The primary effect of inserting several layers of clay was to increase the width of the deformation bands by creating an additional degree of freedom of the system due to layer-parallel shear in the clay layers. Changing the type of clay layers caused less dramatic changes in the final structure. In general, continuity of the sand layers across the shear zone was maintained in experiments with thin multilayers. However, in experiments containing one layer of clay sandwiched between much thicker layers of sand, Urai et al. (2003) observed loss of continuity of the clay layer.

The experimental study of clay smear has made surprisingly few links to the extensive body of literature on shear deformation and the evolution of frictional behavior in clay gouge (e.g., Rathbun and Marone, 2010). In this study, water-saturated layers of a granular material analog to a fault gouge were deformed in the double-direct shear configuration. Strain markers helped define shear localization as a function of dilation in response to perturbations in shear stress and rate/state friction response to shear velocity perturbations. Although the different layers only differed in color and had the same mechanical properties, the deformed layers had a complex attenuated shape. These experiments show the complexity of the shearing process and the wide range of parameters that affect the final geometries of fault zones.

Giger et al. (2011) present a novel design of the direct shear experiment to deform large ($0.3 \times 0.3 \times 0.6$ m) rock samples under high pressure up to 36 MPa, fluid-saturated and with the possibility for fluid flow measurement across the shear zone. The most important innovation in design was the relaxation of the sharp displacement boundary condition at the edge of the sample. They use a high viscosity fluid to seal the sample around a 1 cm wide gap in the contact between the sample and the loading plates so that the shear zone localizes more broadly than in conventional direct shear tests. The philosophy behind this adaptation is that: 'the increasing complexity and inaccuracy of the mechanical results … were deliberately accepted … in exchange for producing a more realistic fault zone' (Giger et al., 2011). These boundary conditions determine the width of the shear zone, which does increase towards the middle of the sample, but far less so than in conventional direct shear tests. There is a small rotation of the sample's lower and upper halves with respect to each other, and it is not completely clear how this influences the displacement field in the shear zone and the formation of Riedel shears.

Çiftçi et al. (2012), Giger et al. (2013), and Çiftçi et al. (2013) used this apparatus in a series of experiments to measure transport properties and stress-strain behavior as a function of clay content and strength contrast between the sand and clay. Artificial and natural rock samples were studied by CT-scans to image the geometry of the sheared clay layer (Fig. 16), which was found to depend on stress and on material properties; brittle clay forms segmented smears while ductile clays form more continuous smears. No tapering of the smear away from the source layer was observed. Increasing normal stress increased shear zone width slightly (width is mainly controlled by the gap between the loading grips) and correspondingly there was more clay in the shear zone. The authors interpret their results to be in reasonable agreement with the SGR model. The main processes in the generation of clay smears are interpreted to be brittle processes of 'slicing' and wear rather than 'ductile drag or plastic flow' (Çiftçi et al., 2013). Highly overconsolidated and cemented clay deforms by dilatant fracturing at low displacements. Clay, with Unconfined Compressive Strength (UCS) equal to or greater than the UCS of the matrix sandstone, forms continuous clay smears. Morphology of the clay smears thus vary widely, depending on stress and brittleness of the clay. However, the authors point out that initial segmentation of the clay layer sometimes evolves into a continuous clay smear because the clay fragments in the shear zone are reworked to clay in critical state. The smearing in strong clays can start with brittle failure producing fragments of clay in the shear zone which are then abraded during progressive shearing, as described by Holland et al. (2006) and Schmatz et al. (2010b), and followed by the formation of clay smears along Riedel shears (Fig. 17). With softer clays, a more uniform clay smear is formed, with lower average thickness of the clay smear.

In summary, the advantage of direct shear experiments over the ring shear apparatus is the benefit of larger samples, which yields results that are closer to the heterogeneous structures observed in nature. The geometry of localization is complicated in direct shear devices, starting from the lines of discontinuity around the central plane in the sample propagating inwards, forming a lens-shaped zone of deformation in the samples. This lens has some resemblance to lenses observed in outcrops, and in the center of experiment the sample has more freedom to develop a complex localization pattern than in a ringshear device. Interestingly, the relaxation of the sharp discontinuities at the sample boundary by Çiftçi et al. (2013) produces a much more diffuse lens in the sample.

*3.2.1.3. Triaxial shear experiments.* In triaxial experiments the suppression of strain localization by rotational symmetry in the

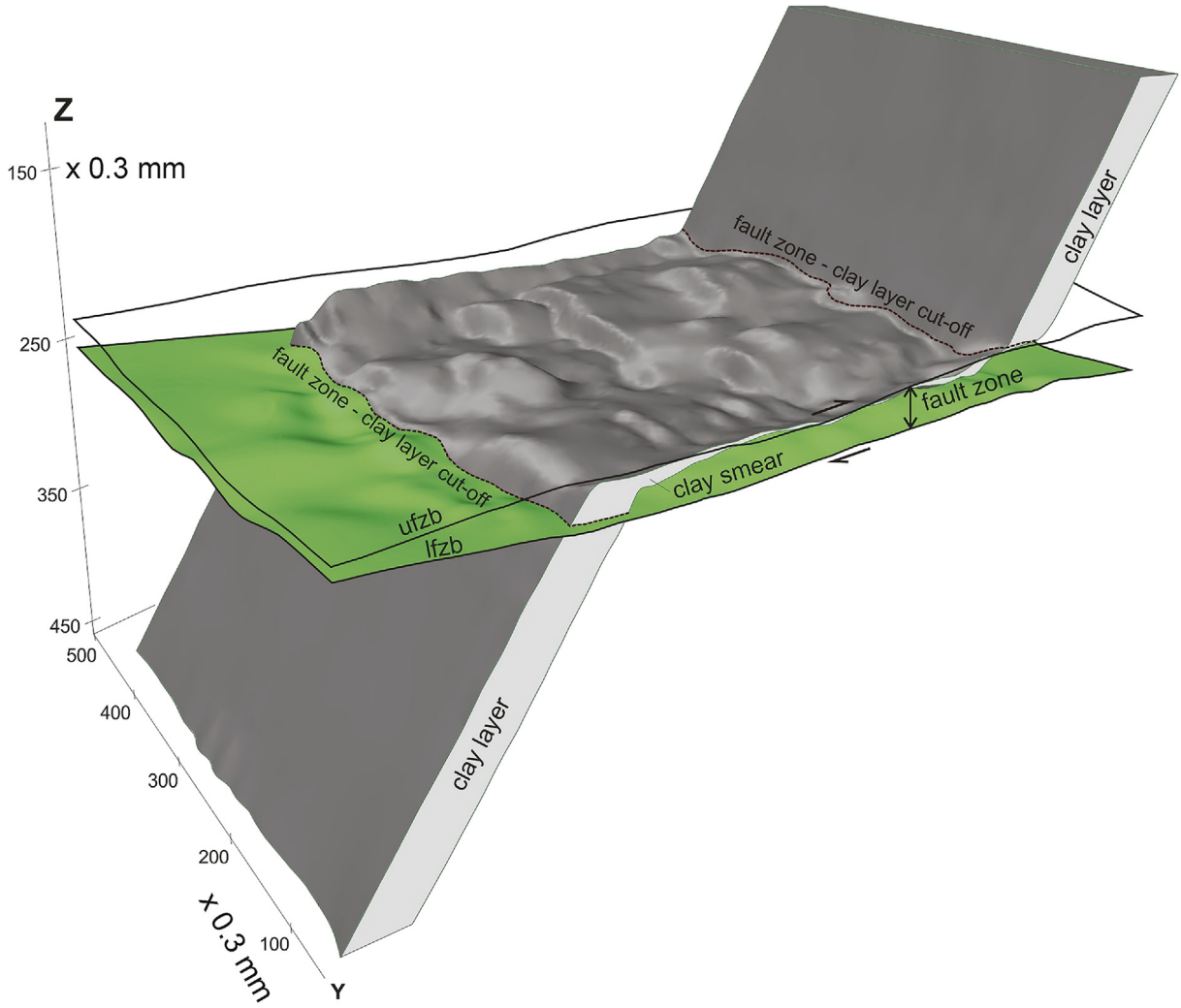


**Fig. 16.** Three dimensional structure of clay smear formed in a large modified direct shear experiment (Çiftçi et al., 2013), showing sheared clay layer and shear zone boundaries. Note that although simulating normal fault processes, direct shear system creates horizontal displacement. ufzb and lfzb are upper and lower fault zone boundaries, respectively.

sample is usually solved by using pre-cut cylinders that are subsequently sheared (e.g. Savage et al., 1996). Takahashi (2003) used a variation on this geometry and presents a detailed study of the shearing of a siltstone layer embedded in sandstone, deformed by sliding along pre-cut shear planes in the sand. Thickness of the sheared layer was measured together with displacement, microstructure of the deformed samples was studied by optical and electron microscopy, and fluid flow across the sheared layer was monitored during the test.

The sandstone deformed by cataclastic shearing with the shear zone widening during deformation, and the sheared siltstone varied from thick and continuous to thin and discontinuous. Takahashi (2003) proposes that the sealing of the fault was mainly a function of effective stress. Permeability measurements indicate three permeability regimes that arise out of the deformation. In regime 1, permeability is rapidly reduced by 1–1.5 orders of magnitude by

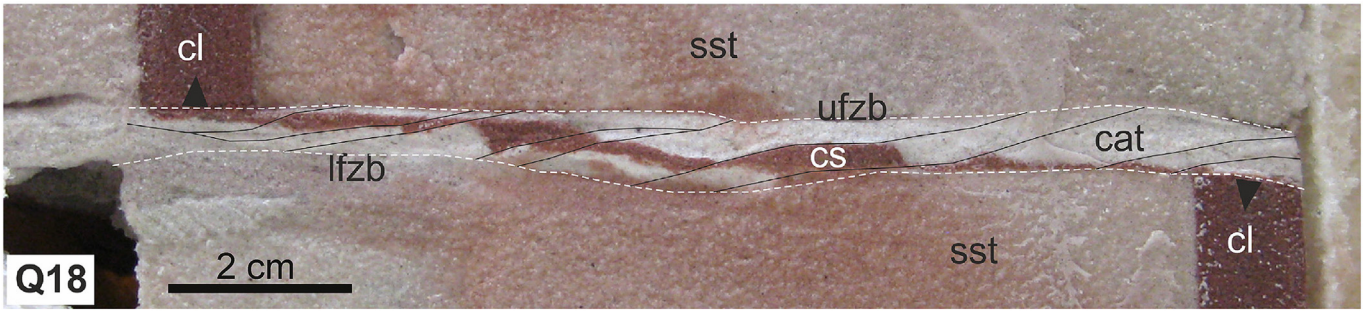


**Fig. 17.** Photograph of sawcut of deformed sandstone–clay sample (Çiftçi et al., 2013). Clay layer is 12 mm thick. Note secondary shear zones dissecting sheared clay in wider shear zone. Sheared clay layer has highly variable thickness. sst = sandstone; cl = clay; ufzb and lfzb = upper and lower fault zone boundary, respectively; cat = cataclasite; cs = clay smear.

compaction until the sample reaches its yield stress, at which point inelastic deformation starts. In regime 2, permeability decreases, while it gradually increases in regime 3. The transition between these regimes depends on effective normal stress; higher stresses are proposed to enhance abrasion of the siltstone and incorporation of more smear into the shear zone.

Permeability increase in regime 3 is due to thinning of the smear by sand grain erosion. Post-mortem observations suggest that the amount of cataclasite and gouge derived from the sandstone increases after loss of continuity in the siltstone smear and that cataclastic sand gouge keeps the permeability lower than the initial permeability. The thickness of the zone of sheared siltstone plays an important role in the hydraulic properties of the sample. We note that it is not clear if the two pre-cut planes in the sandstone were slightly misaligned and thus non-coplanar after assembly with the siltstone layer sandwiched in between (cf. the top block in the sandbox experiments of Schmatz et al., 2010b).

Crawford et al. (2002, 2008) report experiments on mixtures of fine-grained quartz and kaolinite gouge to establish their strength and fluid flow properties. In general, permeability decreases with increasing kaolinite content. Porosity shows a minimum that evolves with increasing effective pressure as predicted by an ideal packing model. Sheared gouge samples show a reduction in frictional strength with increasing clay fraction. Permeability variations as a function of clay content and shear deformation are explained reasonably well with simple models based on theory of mixtures (c.f. comparison of laboratory data with models in Crawford et al., 2002). Clay content had the largest effect on permeability, and shear deformation affects permeability of quartz-rich gouges more than clay-rich gouges. Shearing mechanism, as defined by Lupini et al. (1981) is in three modes: a turbulent mode, a transitional mode, and a sliding mode, depending on dominant particle shape and the coefficient of interparticle friction. Crawford et al. (2002, 2008) conclude that clay mineralogy is as significant as clay content in controlling fault rock permeability, and strain is of secondary importance for permeability evolution.

In summary, triaxial experiments show results similar to the ring shear and direct shear experiments: different failure modes of the clay layer lead to either macroscopically ductile shearing or initial fragmentation followed by reworking of the fragments during shearing in the sand. Probably the strong boundary conditions in these tests prevent deformation modes other than shearing in the shear zone pre-defined by saw cuts, although increasing the thickness of the zone of shearing has also been shown to lead to thicker clay smear. Granular mixing is recognized as an important process in many experiments, and the measurements of shearing in artificial gouges provide important clues on this process. However, the rates of this process and the properties of the mixture are far from understood.

*3.2.1.4. Sandbox experiments.* Sandbox experiments, (dry or water saturated) of clay smear evolution are done at the lowest effective pressure of all experiments discussed in this review, with well characterized nonlinear rheology of model materials. In spite of these limitations, they offer the most realistic set of geometric boundary conditions because of the significant body forces and the large degree of freedom of the models to develop fault geometries like relays and lenses, which are common in nature.

van der Zee et al. (2003) present analog models of dry sand above a basement fault dipping at 45°, with a layer of relatively very soft (yield strength 20 Pa) oil-water emulsion with an elastoplastic rheology to model clay. Movement on the basement fault creates normal faulting in the multi-layered sedimentary overburden with small apparent cohesion (Maksimovic, 1989) and a friction angle of around 35°. In experiments with a thin overburden of 1.5 cm, the fault zone develops with the soft layer derived from the hanging wall sheared along the fault, creating a continuous and asymmetric smear that becomes discontinuous at high strain. With a thick overburden of 9.5 cm, a locally thick fault zone of soft clay analog was created by injection into the fault zone from the layer in the footwall (Fig. 18). The basement fault formed a releasing step in the soft layer, and a second fault was initiated to form the squeezing block, causing the soft layer to become injected into the fault. The differences between the thin and thick overburden cases are explained by considering the contrast in strength between the sand and the emulsion at the given overburden stress. For a thick overburden the strength contrast between sand and soft emulsion is much higher. At a certain overburden thickness the squeezing block is spontaneously initiated in the footwall, leading to injection of the soft layer, but the mechanism needs more study.

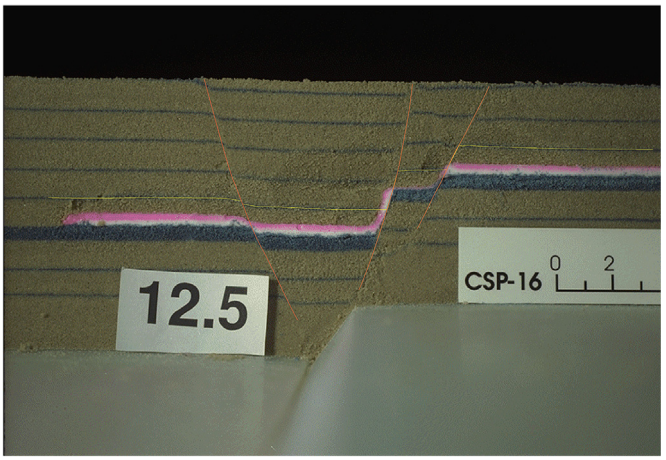


**Fig. 18.** Lateral clay injection in sandbox experiment with very soft clay analog under relatively high overburden stress. Note almost complete injection of clay layer under squeezing block into dilatant fault. Experiment by P.D. Richard and J.L. Urai (2001).

Schmatz et al. (2010 a,b) deformed water-saturated, layered sand–clay models above a rigid basement cut by a fault. The models had a free top surface or a faulted top block, resembling weaker layers (sand and clay) sandwiched between two strong and stiff layers cut by two co-planar faults. Models were deformed between two lubricated glass plates to allow real time observation and measurement of the velocity field by Particle Image Velocimetry (PIV). The thick clay layers were undrained, while pore pressures remained hydrostatic in the sand. Material properties were characterized by a series of standard geotechnical measurements. The experiments were all in the 'precursor structural domain' defined by Nollet et al. (2012) in which the initial deformation is accommodated on a steep antithetic fault to the basement fault. After the first increments of deformation, the fault migrates toward the kinematically preferred plane coplanar with the basement fault (Fig. 19). Thus, different segments of the final shear zone have moved at different times, and the clay smear increases the shear zone's thickness. The models are sufficiently large to form releasing or restraining relays in the clay layer, which have a major control on fault-zone structure. In general, high strength contrast between sand and clay leads to a more complex fault zone. Because sand undergoes boudinage while weak clay layers continue to shear and become amalgamated, clay is found in greater abundance in the fault zone than in the faulted stratigraphy. Fragments of brittle clay (Fig. 20) may be reworked with ongoing deformation following an initial loss of continuity during an earlier stage of deformation. Thus, the continuity of a clay smear within a layered sequence can increase after an initial decrease. Thin, weak clays deform

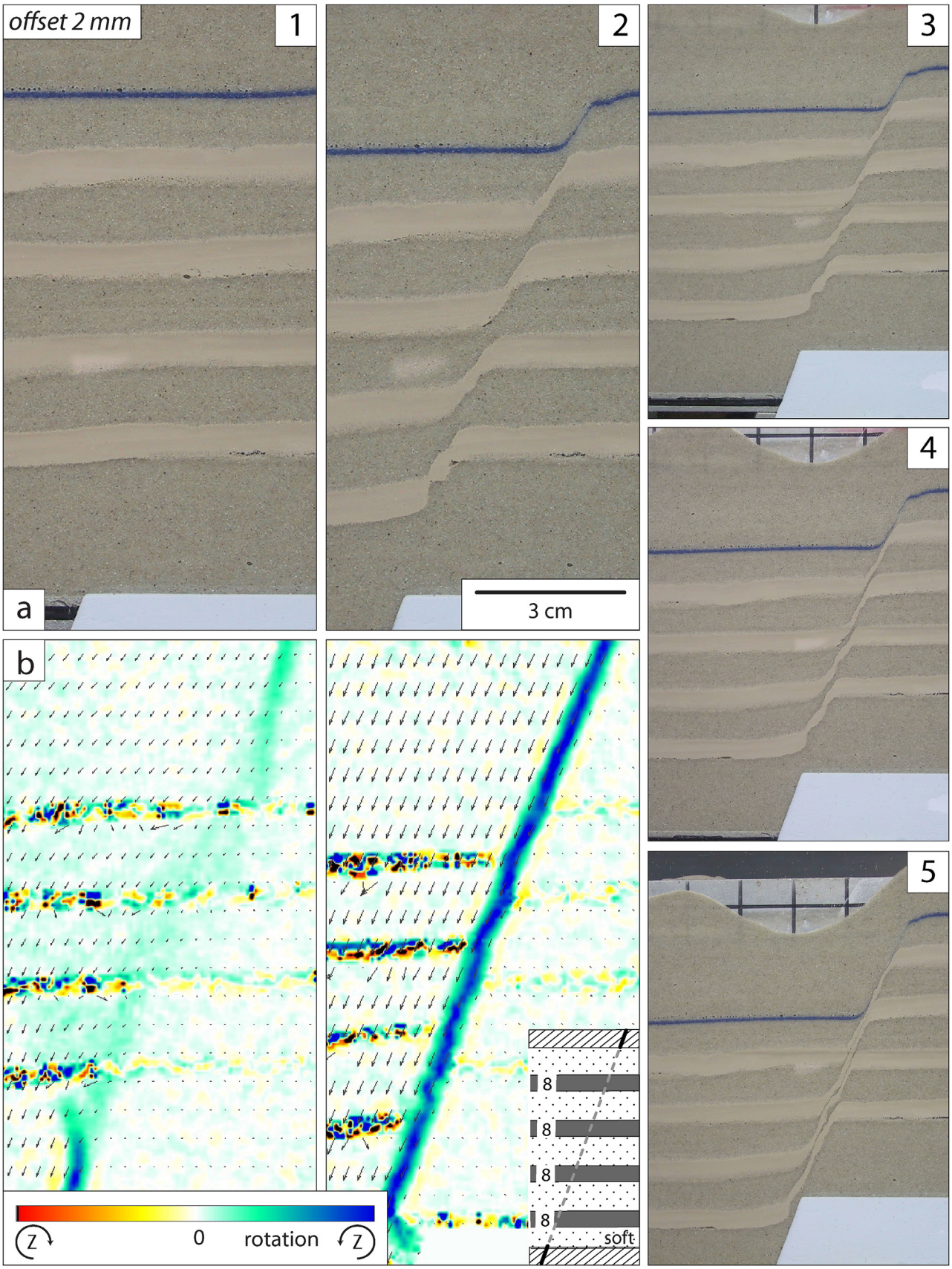


**Fig. 19.** Stages of sandbox experiment with sand (gray) and clay (tan) deforming in shear and having similar strengths. First two stages are from experiment discussed in Fig. 16 of Schmatz et al. (2010b), showing PIV derived strain rate contours to illustrate lateral migration of zone of shearing. Last three stages show how progressive deformation of initially layered sand-clay shear zone results in one coherent sand-clay mixture band. Figure reprinted from Schmatz et al. (2010b) with permission from Elsevier.

continuously over large displacements, and the volume of clay smear increases as sand mixes into clay at the margins of the shear zone.

An unexpected outcome of the Schmatz et al. (2010a,b) experiments arises from the evolution of clay thickness in the shear zone with increased fault offset. That thickness should decrease by simple shear, yet thickness varies little with offset. This led to the observation of sand grain incorporation at the margins of the sheared clay, effectively inflating the clay volume by a process of sand-clay mixing. Based on these observations, we think mixing is an integral part of clay smear processes.

Noorsalehi-Garakani et al. (2013) present observations of clay smear continuity in water-saturated sandbox experiments similar to those of Schmatz et al. (2010a,b), but in this follow-up study the sheared clay layers were excavated after deformation (Fig. 21). Standardized model materials were characterized in detail. The sheared soft clay layer above a 70° dipping basement fault reveals a complex, natural-looking fault zone architecture with relay ramps, breached relays and fault lenses. The clay smear shows clear variations in composition and thickness and becomes locally discontinuous, forming holes at throw-thickness ratios >7. In addition to fault segment migration into the footwall and/or hanging wall and tectonic telescoping in the relays, the thin, continuous parts of the clay smear is formed by mechanical mixing of sand and clay. Deformation in the hanging wall was stronger and more complex than in the footwall.

A complementary perspective on the clay smear problem is provided by van Gent et al. (2010) and Kettermann and Urai (2015) who deformed thick, brittle hemihydrate layers with thin, weaker sand between them. These experiments may provide clues for faults where the sand is cemented and the clay is weak. In these experiments, the fragmentation of the brittle layers made the fault zone wider and more complex (cf. Schöpfer et al., 2007a,b) with the weak sand flowing around the blocks. An interesting observation is the gravity-driven downward flow of sand into open fractures, a process which may be relevant in faults in some carbonate-clay sequences.

In summary, the main advantage of sandbox experiments over other experimental designs is that the boundary conditions allow a much more realistic development of a network of fault segments that evolve into a thoroughgoing fault zone by coalescence of segments and by migration of the zone of shearing. As observed in all other experimental setups, a key parameter in sandbox experiments is the failure mode of the clay layer; if the compressive strength of the material is much stronger than the mean effective stress, the clay layer will fail in extension and fragment, with reworking of the fragments during further shearing. A disadvantage of sandbox experiments is the low effective stress, which prevents simulation of cataclastic flow.

*3.2.1.5. Discussion of experimental studies.* Since the pioneering work of Mandl, Lehner and coworkers, forty years of experiments on clay smear processes have produced many interesting results. There have been important developments in technology and measurement techniques, such as image correlation, 3D modeling, etc. It has also become clear that full analysis of many different

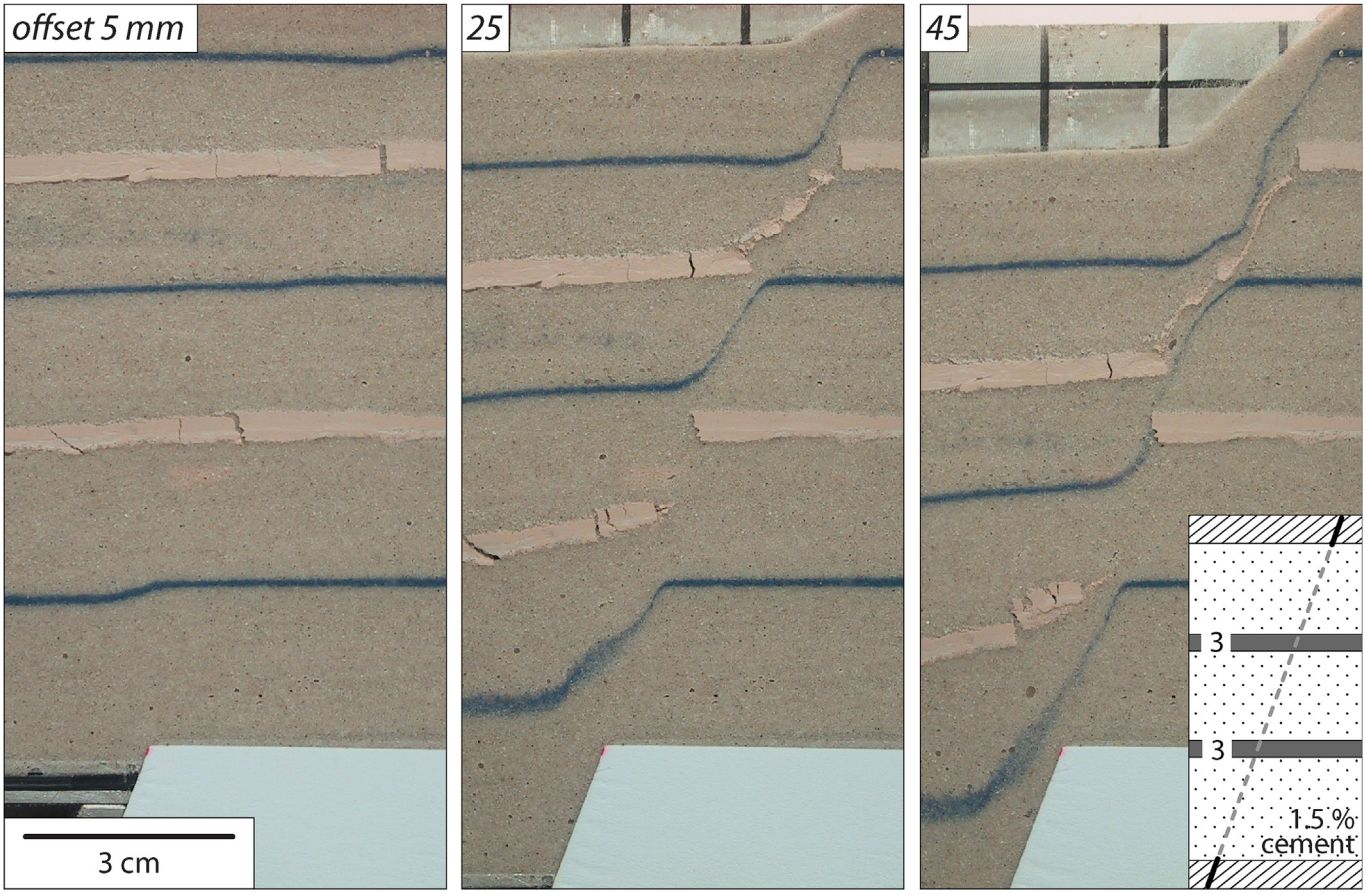


**Fig. 20.** Image sequence showing experiment with two cemented clay layers and top plates Schmatz et al. (2010b). Basement fault offset is 5, 25, and 45 mm. Rigid footwall block (off-white) is stationary, and rigid hanging wall top-plate (silver with black grid) falls into view with displacement. Note initial fragmentation of upper clay layer followed by subsequent shear and abrasion, developing towards more continuous clay gouge. Figure reprinted from Schmatz et al. (2010b) with permission from Elsevier.


**Fig. 21.** Excavated surface of sheared clay layer showing different degrees of mixing of clay with sand from both sides of the clay (light blue areas of fault) and holes in clay gouge (center of dark blue areas). Technique described by Noorsalehi-Garakani et al. (2013). Note sheared lenses in the master shear zone (thicker, pure white sections on fault surface).

parameters, such as fluid flow, velocity field, stress field, in real time and 3D, is required to learn more about the complex, nonlinear fault processes. It is also clear that to understand clay smear, one needs to understand the whole fault zone, including the structures in the adjacent sand as well as those in the clay.

All experiments produce shearing in a sample with a shear zone at high angle to layers embedded in sand. However, there are large differences in boundary conditions, leading to very different geometries of localization. The challenge in experiment design is to produce a large displacement in a small sample (Table 3). Thus experimental geometries like the plane strain biaxial test, which would allow the localization of deformation to be mainly determined by the mechanical properties of the sample, have been underexplored. The boundary conditions chosen to reach high strains place different restrictions on how the zones of shearing are localized. The strongest restrictions are probably present in the ring shear and pre-cut triaxial experiments. In both of these systems, a thin (of the order of several grain sizes thick) zone of shearing is forced at both edges of the relatively small sample, from where the shear zones propagate towards the center.

The direct shear experiments and sandbox experiments have samples almost an order of magnitude larger than in other experimental designs, and the structure of the shear zone is correspondingly more complex and more similar to fault zones in nature. In these larger set-ups, the shear zones develop more segmented faults and fault lenses, relays and Riedel shears. The sandbox experiments have the least restrictive boundary conditions because the shear zones are allowed to migrate laterally with an unconstrained width. It is interesting to note that granular flow and cataclastic flow of clay seem to produce similar geometries as long as the boundary conditions are comparable.

In all types of experiments, shearing in the thin high strain shear zone occurs by granular flow and mixing of sand and clay, and by abrasion of brittle clay fragments if present. Cataclasis of sand occurs at higher stress and produces similar geometries. Thin multilayer clay smear forms if several clay source layers are present, and in those instances where mixing and abrasion are sufficiently active, the sand-clay layered gouge will transform into a more homogeneous sand-clay mixture (the volume change caused by this process is an additional driving force). The evolution of the internal structure of this thin shear zone is poorly known as little of

**Table 3**
Comparison of main parameters in clay smear experiments.[a]

| | Sandbox | Ringshear | Direct shear | Triaxial | Comments |
|---|---|---|---|---|---|
| Effective mean stress | ★★★★ | ★★★★ | ★★★★ | ★★★★ | Triaxial cell can reach highest stress |
| Shear offset | ★★★★ | ★★★★ | ★★★★ | ★★★★ | Up to 40 cm in ringshear |
| Fault zone area | ★★★★ | ★★★★ | ★★★★ | ★★★★ | Up to 40 × 40 cm |
| 3D geometry of fault zone | ★★★★ | ★★★★ | ★★★★ | ★★★★ | |
| 3D geometry of clay smear | ★★★★ | ★★★★ | ★★★★ | ★★★★ | |
| **Freedom to localize** | ★★★★ | ★★★★ | ★★★★ | ★★★★ | Improved in Çiftçi et al. (2013) |
| Dilatancy measurement | ★★★★ | ★★★★ | ★★★★ | ★★★★ | |
| Stress measurement | ★★★★ | ★★★★ | ★★★★ | ★★★★ | |
| Velocity field | ★★★★ | ★★★★ | ★★★★ | ★★★★ | Using DIC |
| Microstructural investigation | ★★★★ | ★★★★ | ★★★★ | ★★★★ | Direct observation and post mortem microscopy |
| Fluid flow measurement | ★★★★ | ★★★★ | ★★★★ | ★★★★ | |
| Body forces | ★★★★ | | | | |

Note: Star rating reflects score (red stars) out of maximum potential score (blue stars).
[a] Higher rating represents a parameter closer to subsurface prototype or better access to measurement.

the process is resolved in today's experiments, by for example electron microscopy.

All experiment types point to the importance of the failure mode in the clay layer – if the relative values of mean effective stress and strength are such that extensional fracturing or shear fracturing result in clay fragmentation, continuous clay smears may only form after abrasion of the fragments in the shear zone. In other words, after an initial phase of fault permeability that is little reduced from the juxtaposed sandstone permeability, permeability of the fault decreases as clay fragments become abraded and distributed along the shear zone.

Lateral injection of clay into the fault is shown to occur when clay is much weaker than sand. This process can locally produce large increases in the amount of clay in a fault, but many questions about the process remain. Even less studied is the effect of brittle fragmentation of sand layers with soft clay redistributed around the sandstone fragments.

To a first approximation, deformation in thin shear zones is heterogeneous simple shear. A number of workers have calculated the deviation from this simple shear as a measure of strain heterogeneity (Schmatz et al., 2010b). It is also surprising that in most experimental studies the thickness of shear zones is overlooked as an important parameter (Fig. 22), although simple geometrical arguments illustrate how this parameter affects the shear strain and the fault zone geometries that result from that shear strain.

In faulting at upper crustal temperature and pressure, there is extensive evidence for solution transfer processes and frictional healing (e.g. Gratier, 2011). The role of these processes is unexplored in the clay smear community. Also, the extensive literature on clay gouge dynamics has yet to find its way into the clay smear literature (e.g., Byerlee, 1978; Haines et al., 2013; Vrolijk and van der Pluijm, 1999), although we recognize that these processes represent an extension of the clay smear problem beyond its classical definition.

### 3.2.2. Analytical models of clay smear

The first mechanical model of clay smear was developed almost 40 years ago (Lehner and Pilaar, 1997; Weber et al., 1978). Based on detailed field observations, these authors argued that the mechanism of clay smear emplacement must involve both shearing in the

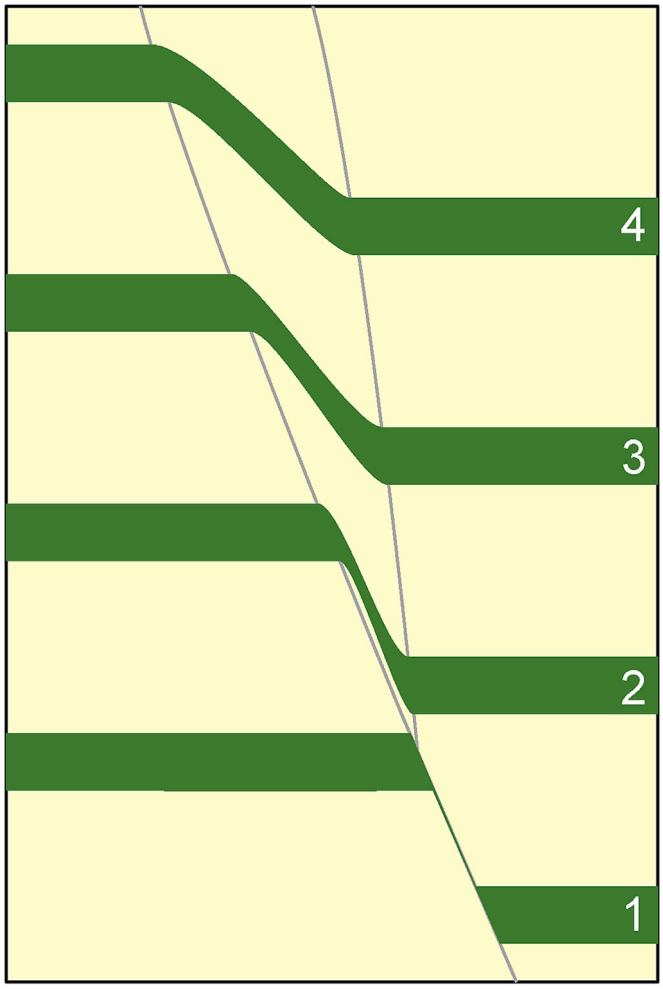


**Fig. 22.** Schematic drawing to illustrate effect of fault zone thickness on clay smear. In fault zone that progressively widens and subjected to homogeneous simple shear for each of four clay beds, clay smear thickness increases with shear zone thickness.

fault zone and continuous supply from the source bed. Lehner and Pilaar (1997) proposed that 'traversing a shale source bed, a normal fault has to be offset in the direction of the downthrown block in order to make room for the emplacement of a clay smear. Evidently, this mechanism can also provide an effective way of unloading the source bed along the rupture faces, thus facilitating the extrusion of plastic clay material. The extruded material will fill the gap created by the pull-apart mechanism. It will thereby enter the shear zone proper, where it will be subjected to the slow shearing imparted by the relative displacement of the fault blocks, to be smeared out along the fault.'

To model the extrusion process, the authors assumed that the clay layer has an effective viscosity, which implies that under otherwise identical conditions, one thicker clay layer extrudes more clay than two thinner layers with the same total thickness, expressed by the often cited $w \sim h^2$ relationship (Lehner and Pilaar, 1997). In many ways, this paper was far ahead of its time, combining detailed field observations with a kinematic-mechanical model, clearly distinguishing between the initial localization process and the shearing in the fault zone.

van der Zee et al. (2003) investigated the model of Lehner and Pilaar (1997) further, this time using a time-independent Mohr Coulomb rheology for the clay. Based on field observations van der Zee et al. (2003) propose that clay injection is associated with footwall collapse and the formation of a 'squeezing block' above the clay layer. For this model it was shown that no injection occurs when the horizontal stress in the releasing segment reaches zero if the differential stress fails to achieve a state of failure in the hard clay bed. No explanation is given for the origin of the squeezing block. They propose the Mechanical Clay Injection Potential (MCIP) condition for the onset of injection, defined as follows:

$$C = \frac{\sigma_1' \times (1 - sin\ \phi)}{2cos\ \phi} \quad (1)$$

where C = cohesion (MPa), $\sigma_1'$ = maximum principle effective stress (MPa), and $\phi$ = angle of internal friction (degrees). This expression states that above a certain cohesion value, a clay layer will be prevented from extruding into the fault zone. Finite element models (with pre-existing contact elements) are in good agreement with the equation above. This equation also describes the transition in failure mode from extension to shear failure found to be important in many experiments. An interesting conclusion described by van der Zee et al. (2003) is that if the lateral dimension of the squeezing block scales with clay layer thickness, the $w \sim h^2$ relationship proposed by Lehner and Pilaar (1997) also follows. The formation of the squeezing block is seen as another example of the increasing fault zone complexity with competence contrast, as discussed by Schöpfer et al. (2007a,b).

Welch et al. (2009) adopted the idea of the trishear kinematic model of fault propagation folding and developed a 2D, kinematic, quadshear formulation to model fault-related folding in a ductile interval sandwiched between brittle layers. The models offer interesting ideas of the different possible kinematic styles formed as a function of the location of the faults on both sides of the layer and of the geometry of the localized zone in the quadrilateral lens of deformation between the two faults. However, the model offers no mechanical understanding of why the localization stops with progressive deformation, nor a way to predict when a fault's deformation will delocalize into the shear zone.

### 3.2.3. Numerical simulation

The simulation of localization in shear zones and extension fractures in general is as challenging a numerical problem as is the experimental investigation of large shear deformation in geomaterials. Besides the continuum mechanical approach, improved by extension to polar continua and adaptive remeshing, numerical methods with discrete particles are used to explore these problems. In general, there is agreement that numerical models in the state of the art are unable to accurately reproduce the details of patterns of localization, and the same holds for patterns of shearing and evolution of Riedel shears in a fault zone. However, numerical models are nevertheless helpful for gaining insights into the complex evolution of stresses in a layered section with contrasting mechanical properties, an area of investigation where analytical models offer little benefit.

*3.2.3.1. Discrete element modeling.* Numerical modeling in geomechanics with discrete particles is based on Cundall and Strack (1979). Material properties are defined at the particle level, and macroscopic properties result from interactions between the particles. Cundall et al. (1982) show that the method yields good correspondence with theoretical models of bifurcation (Rudnicki and Rice, 1975; Vardoulakis, 1989) and with experiments on sand (Thornton, 2000; Zhou and Chi, 2002). Tensorial variables such as stresses and strains are also calculated (Cundall et al., 1982; Luding and Herrmann, 2001; Hardy and Finch, 2005, 2006; Finch et al., 2004; Zhao et al., 2007; Egholm, 2007; Egholm et al., 2007). Deformation to very large strains in fault zones has been modeled using discrete elements, including dynamic rupture processes by Wang et al. (2006), Abe et al. (2006), and Latham et al. (2006). Compared with continuum methods (Section 3.2.3.2), the discrete methods hold significant advantages when it comes to modeling very large deformation in granular flows. Local dilation, localization of strain and fragmentation is easily simulated. The disadvantage is that the complex constitutive models required to accurately model real geomaterials are implemented only with difficulty. The stress-based discrete element method (SDEM: Egholm, 2007) solves some of these problems. By reproducing the 'Benchmark' sandbox models they show that the method generates shear zones at angles in agreement with general observations. Additional limitations for clay smear modeling include the number of particles and thus resolution of the model, as well as the shape of particles which are round rather than typical clay flake forms. Recent developments such as the SPOT method (Rycroft et al., 2010) promise large increases in computation speed.

*3.2.3.2. Continuum modeling.* Herle and Feda (2001) give a fundamental overview of the different finite element simulation methods and discuss problems related to shear zone growth, such as singularities and strain gradients at the tips of shear zones and mesh dependency in classical non-polar continua. For softening materials the problem is ill-defined. The effect of different material properties on localization is poorly understood (e.g., Herle and Feda, 2002; Hügel, 1995; Belytschko et al., 1994). A method to keep the shear zone thickness independent of discretization is proposed by Cosserat and Cosserat (1909), who introduce a characteristic length. Apart from additional degrees of freedom, which are defined at the level of elements, material characterization also needs to be extended (Mühlhaus, 1986) to properly address the localization problem. The calculated shear zone thickness is thus adjusted to correspond to experiments. Another approximation to softening is achieved by hypoplasticity (e.g., Kolymbas, 1988; Niemunis, 2003; Nübel, 2002; and Gudehus and Nubel, 2004). A recent approach to address localization is ELFEN by Rockfield (Crook et al., 2006) which uses Lagrangian methods and adaptive meshing, together with a constitutive model based on critical state concepts and global energy dissipation regularized by fracture energy. These models also compare well with the Benchmark tests (Buiter et al., 2006; Santimano et al., 2015).

*3.2.3.3. Discrete element models of clay smear.* Schöpfer et al. (2006, 2007a,b) present a major study of the localization of deformation in mechanically stratified multilayer sequences above a basement fault, using the PFC3D Discrete Element code. They show that deformation first localizes in strong, brittle, layers with dip relays in weak, ductile, layers. Faults under sufficiently low pressure-high strength conditions form by initial Mode I fractures in the brittle layers, together with low amplitude monoclinal folding. The fractures are linked by shallow-dipping faults in the weak layers. The models are similar to geometries observed in natural faults with brittle layers, including large changes in fault dip, fault branches, normal drag, and progressive linkage of fault segments. Fault zone width increases with increasing displacement. Faults in models with high strength contrast and low confining pressure are strongly segmented because of different modes of failure in the different layers (Fig. 23). At higher pressure and lower strength the models show a transition from extension to hybrid failure to shear fracture and an associated decrease in fault zone width and complexity.

Egholm et al. (2008) considered the case where an upward propagating fault in sand above rigid basement intersects a weak clay layer (with lower friction angle), refracting to a shallower dip in the clay and continuing at the initial angle in the sand above. This creates a contractional relay in the clay and locally increases the mean stress in this zone, promoting flow of the clay into the fault zone (Fig. 24), similar to the squeezing block of van der Zee et al. (2003). In this model, the volume of clay available for injection also scales with the thickness of the clay layer. SDEM models with the dimensions of sandbox models were run above a rigid basement fault dipping 65°, and with large rheological contrast between sand and clay (35° and 5° friction angle and a low cohesion). Comparison of the results produced with and without a clay layer show that in the case of a weak clay layer, shearing in the sand above the clay migrated into the footwall, progressively eroding the clay layer and transporting it into the fault zone. Initially, deformation in the lower sand localizes in a steep precursor fault, which migrates into the footwall. The thickness of the sheared clay in the fault zone increases with decreasing clay friction angle. The Egholm et al. (2008) results are thus at variance with the model of Lehner and Pilaar (1997) who proposed that the zone of localization steepens in the clay layer. In both cases, however, the deviation from a planar fault effectively widens the fault zone and increases its complexity. Egholm et al. (2008) propose that if clay beds are cohesive, steep tensile joints could produce the pull-apart of Lehner and Pilaar (1997). In this case, however, the model of van der Zee et al. (2003) predicts that the clay will not fail and should support an open fracture. Consequently, van der Zee et al. (2003) expect that the clay will fragment in this case and flow into the fault zone where it is eroded and smeared along the fault, as in the experiments of Sperrevik et al. (2000). Clearly more work is needed to explore how fault propagation creates a segmented fault network that affects the incorporation of clay into a fault zone and its early deformation.

Raith (2012) investigated models similar to Egholm et al. (2008) and Schöpfer et al. (2006, 2007 a,b), and studied the effect of cohesion of a simulated cemented clay layer and the angle of the basement fault. However, in these models the clay was stronger than the sand. Results from these numerical simulations reproduced the graben and precursor domains of Nollet et al. (2012). In both domains, the increase in cohesion of the cemented layer produces large differences in the structural evolution. When clay cohesion is sufficiently high, tensile stresses in the cemented clay layer lead to fragmentation, discontinuous clay and a complex fault

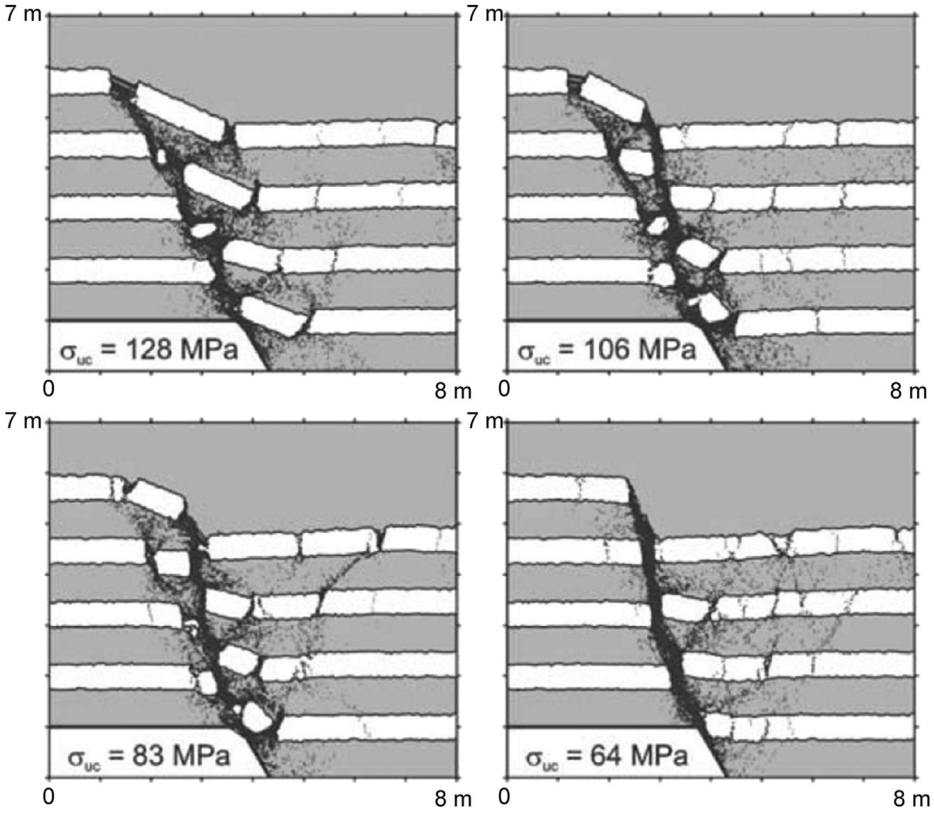


**Fig. 23.** Discrete element models of multilayer faulting above basal fault, with different strength contrasts between layers, showing how complexity and width of fault zone increases with increasing strength contrast, especially when strong layer fails in extension. From Schöpfer et al. (2007b). $\sigma_{uc}$ is unconfined compressive strength of stronger (white beds) lithology; example for same fault throw and same confining pressure.

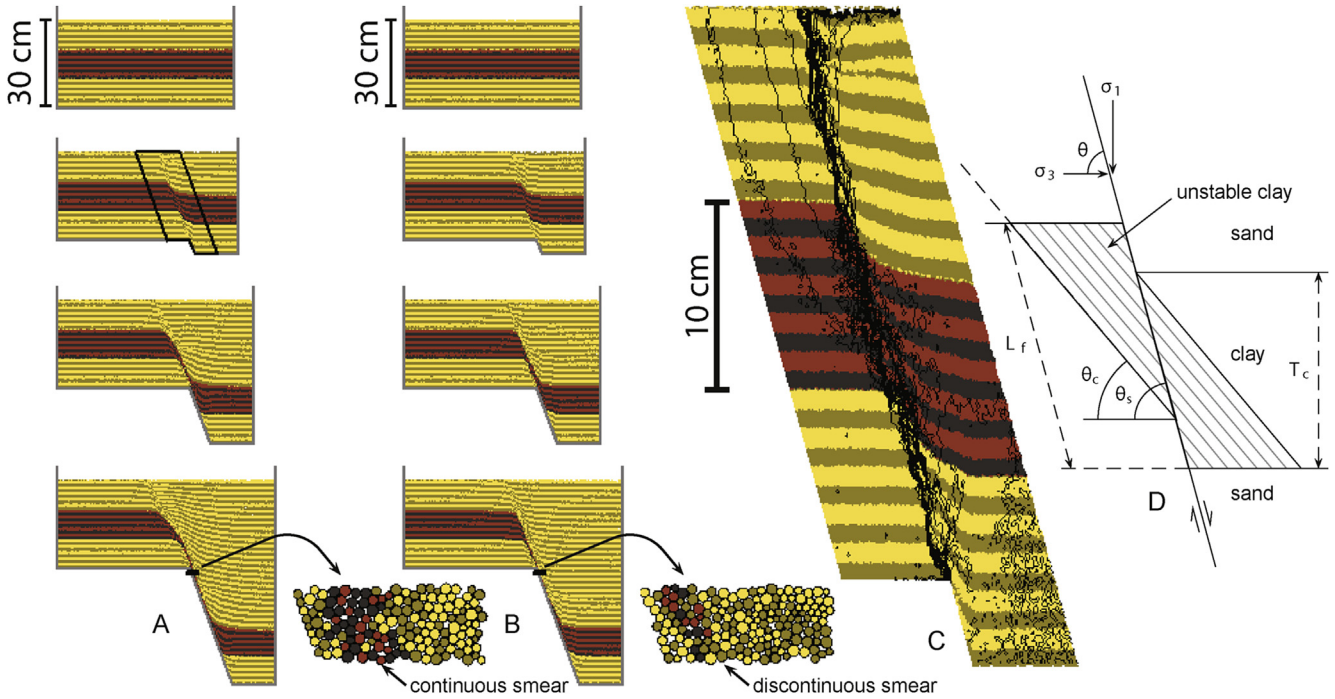


**Fig. 24.** Discrete element models of normal faulting above basement fault (Egholm et al., 2008). B series is model where dark brown layer has same properties as surrounding sand, while in A-series dark brown layer is much weaker (lower friction angle), leading to change in direction of shear zone in soft layer and transport of eroded material into shear zone. Note that in A-series during intermediate displacements, an antithetic fault develops in hanging wall that creates squeezing block geometry.

zone (Fig. 25). When cohesion in the clay layer is low, it softens and is distributed along the fault zone.

TerHeege et al. (2013) used a 2D DEM code to model direct shear experiments in large samples of Çiftçi et al. (2013) and Giger et al. (2013) discussed above. Numerical results were discussed in terms of four processes: drag of the clay layer, with tapering towards the fault, 'slicing' of the clay layer along slip planes, abrasion of the clay fragments and mixing of clay with rock fragments, and lateral flow of clay associated with dilation in the fault zone. Micromechanical parameters were calibrated by simulating 2D biaxial tests. The choice of the 2D direct shear setup was justified by arguing that (1) the clay smear is only passively loaded by the applied normal stress so that deformation of the source layer and associated changes of mechanical properties prior to the onset of displacement is limited; (2) entrainment of clay in the fault zone can be better studied in terms of end-member mechanisms, such as slicing, drag, wear and flow; (3) geometrical effects influencing the volume of clay entrained in the fault zone are minimized. Results of the simulations were similar to the experiments, but with shear zones less sharply localized. The authors used critical stress ratios (proximity to mechanical failure, see Eq. (1)) to define a criterion for clay smear failure and the construction of a smear breach diagram to constrain the sealing capacity of faults containing clay smears, which was higher for higher clay content of the source beds and for higher normal stress. One important point about this paper is that for realistic description of the mixing of sand and clay during shearing, a 3D model is essential, because the flow of clay into the pore space in the sand occurs through the pore throats, even when two sand grains touch (in 2D grain-scale mixing is prevented by the geometry of the experiment).

*3.2.3.4. Continuum models of clay smear.* Simulations of normal faults with clay smear caused by hypoplasticity (Gudehus and Karcher, 2007) present examples of deformation of sand-like and clay-like materials including creep terms for clay. First results show shear band patterns, which are compared to model experiments and natural fault patterns. The model uses a normal fault with a clay layer in sand above a basement fault. A simulation of shearing of the sand-clay layers is presented, but unfortunately the information provided about the models (Gudehus and Karcher, 2007) prevents critical evaluation of the results. An interesting first result is that with increasing offset the clay smear thickness stabilizes at ca. 15% of the source layer thickness, whereas the fault zone gets wider. The authors propose that local remeshing with polar quantities could resolve finer details of the fault zone structure.

Nollet et al. (2012) used ELFEN to study the effect of basement fault dip on the evolution of shear band patterns in sand as observed in sandbox experiments. Results reproduced the range of structural styles observed: a basement fault dip of 60° and lower results in a graben structure with antithetic shear bands, while a basement fault dip of 70° and steeper initiates a precursor shear band followed by a synthetic shear band close to coplanar to the basement fault. The authors propose two structural domains in which the first-order structural style and deformation patterns are only weakly dependent on the details of the rheology of the model materials and are also observed in sandbox experiments for the same set of boundary conditions but with different material properties. Note that the internal structure of the shear zones is only generally resolved by these models; the shear zones essentially deform by simple shear, and the layered display is an attractive demonstration for what one may expect in a homogeneous material.

Kleine-Vennekate et al. (2014) and Kleine-Vennekate (2013) used ELFEN to model the evolution of localization. The first numerical model series used a homogeneous model extended laterally until a shear band initiated from a soft element (i.e. a single node within the model with artificially weak mechanical parameters assigned to insure that failure occurs first at this node). Results show a shear-band dip arising as a function of friction angle and a weak function of dilation angle. The shear band becomes one

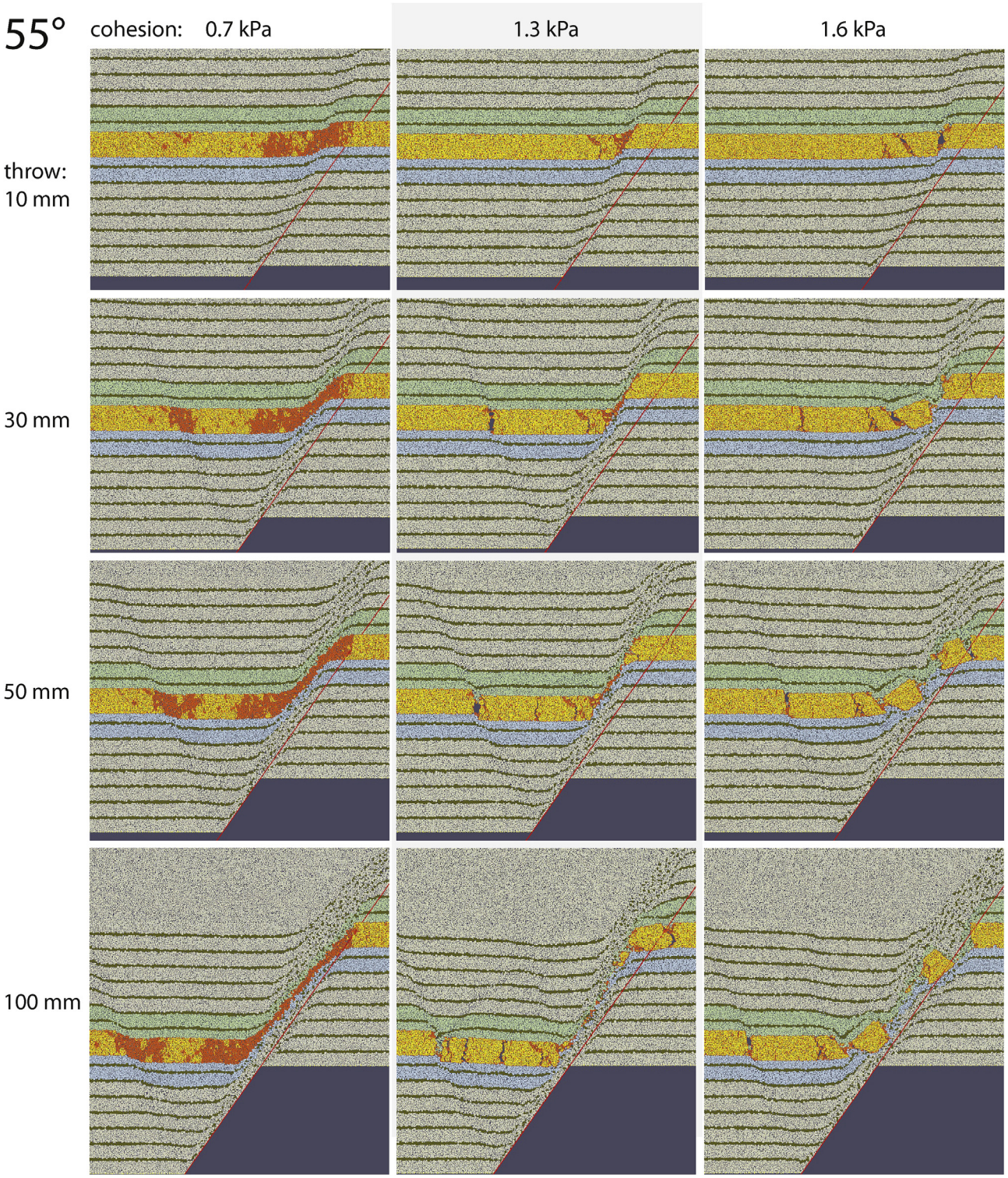


**Fig. 25.** DEM models of normal faulting above basement fault (graben domain) with contrasting strength between clay and sand layer and with different failure modes in clay layer (varying cohesion). Note strong changes in morphology in clay layer for same throw values. Yellow elements are intact; orange elements have failed bonds. From Raith (2012).

element wide during fully developed shearing, while the fracture energy is kept constant by regularization. The ratio of maximum displacement to shear band length is much larger than for faults in nature, perhaps because the ELFEN model allows no work hardening phenomena. Two non-coplanar shear bands coalesce in a relay, while closely spaced shear bands develop a lens structure. In mechanically layered models the shear band can change dip (as expected from friction angle and dilation angle) when the shear band propagates continuously. In models where localization is discontinuous and the shear band jumps across layers, coplanar shear zones are formed on either side of the clay layer, elegantly explaining why in many sand-clay sequences in nature faults

maintain a single orientation across layer boundaries. Such models have the potential to capture the initiation of the clay smear process as purely as possible, but unfortunately numerical problems encountered when running models to very large displacement have so far prevented this result. For modeling of sand-clay experiments above a basement fault in a sandbox, material properties were carefully calibrated based on tests of the model materials, and simulations of experiments without a clay layer also showed close correspondence with measurements. In models with a clay layer, different clay strengths were investigated. Although the continuum formulation fails to simulate the breakup of the clay layer, models with higher strength clay show a much stronger thinning with increasing displacement (Fig. 26), especially when the clay layer is so strong that tensile stresses are generated.

*3.2.3.5. Discussion of numerical simulations of clay smear.* Numerical modeling of clay smear processes has been less intensively explored than laboratory experiments. Numerical studies have the advantage of detailed and systematic parameter studies. Interestingly, some of the same problems of scale (e.g., shear zone thickness and development of secondary Riedel shears in the shear zone), resolution, and boundary conditions which are present in experiments are present in numerical models as well. Thus, in many ways experimental and numerical modeling of clay smear are complementary, and it would be very helpful in the future to develop benchmark models which are investigated by both methods to allow comparison and cross-fertilization.

In numerical models it is less clear what aspects of clay are included in the description of the material – this is true for both FEM and DEM models. For example, in a DEM model one may include a reasonable description of macroscopic mechanical properties, while the particle size of the Discrete Elements hinders the effects of grain scale mixing. Or, in a FE model clay softening and localization may be included in the formulation without a correct description of the thin shear zones that develop in clay or of the slicing and fragmentation often observed in experiments. As in experiments, benchmarks to compare the results of different codes would be very helpful to evaluate the results of different calculations.

One problem that clearly requires more numerical work is the evolution of Riedel shears, which are yet to be produced in the numerical models discussed above. Mixing of sand and clay is modeled poorly with existing DEM models; a much larger difference in grain size between sand and clay and construction of 3D models are needed to allow clay particles to migrate through sand pore-throats. Failure mode in one of the layers has a major control on the results of numerical simulations, but very little systematic work has been done on the rates of reworking of

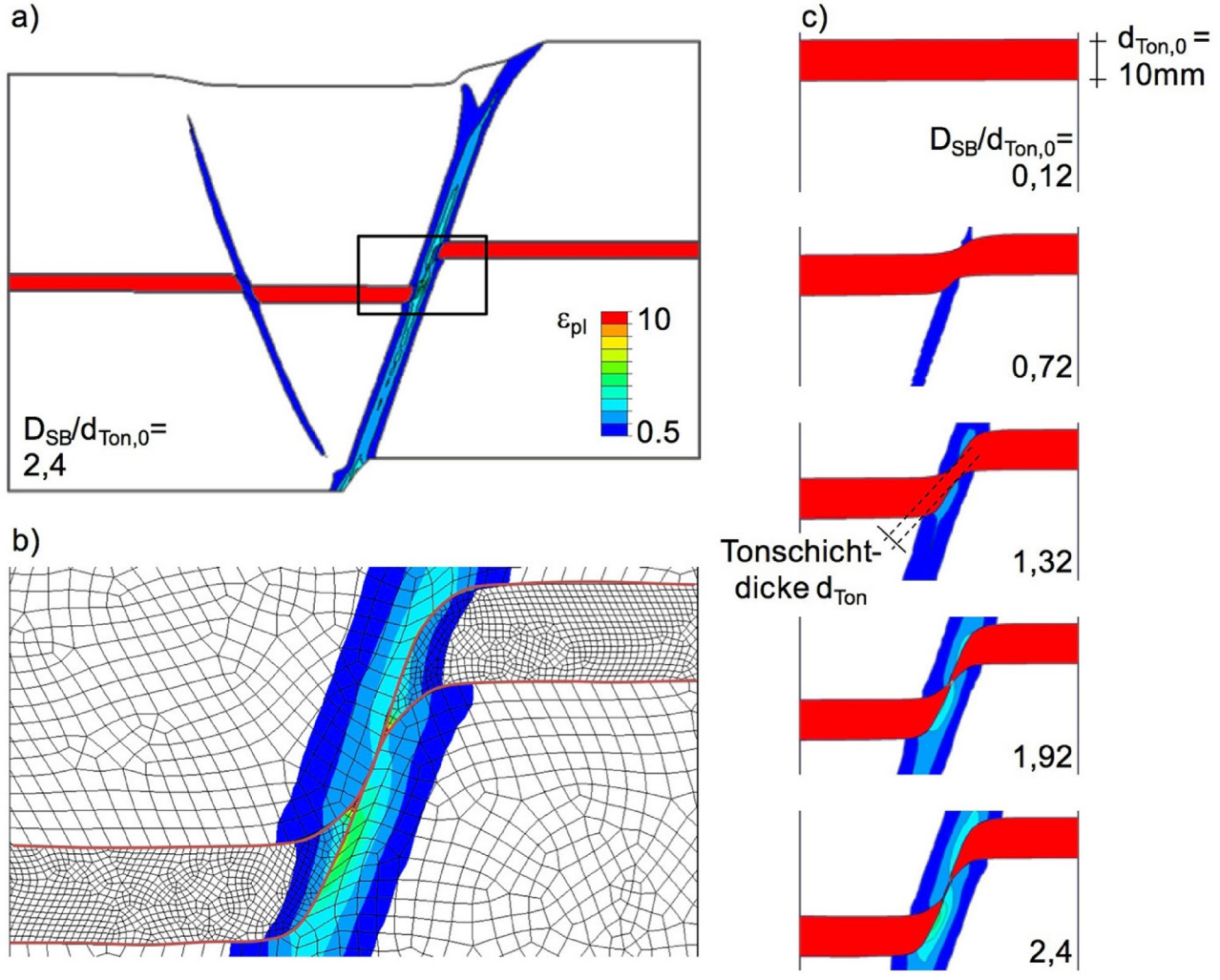


**Fig. 26.** ELFEN model of strong clay layer embedded in sand, sheared in numerical sandbox model above basement fault. Note strong boudinage of clay (Ton) layer. From Kleine-Vennekate (2013).

brittle fragments during shearing in the fault core (i.e. representing an evolution in the failure mode during progressive shear deformation).

### 3.2.4. Discussion and summary: laboratory and numerical models of clay smear

We set out in this section to summarize the literature about fault processes that create and disrupt clay smear. There are a multitude of laboratory and numerical approaches applied to the problem, and each approach enjoys advantages and suffers limitations imposed by either a laboratory or numerical experimental design. No single approach describes the entire mechanical and kinematic evolution of a fault zone, but rather that understanding lies at the intersection of all these approaches where the physical insight contributed by each method is free of design limitations. Unfortunately there is uncertainty about the limitations of all of these methods.

An important process revealed by the existing laboratory experiments is heterogeneous shear to large strains. This plays an important role in developing layered gouge in sandbox experiments. Grain-scale mixing (grain-scale abrasion) is important in many experiments, as shown by microscopy. More coherent fragments of clay are also observed to disaggregate during shearing under sufficiently high mean effective stress, reflecting a strain-softening evolution.

Sandbox experiments also provide information about the initial localization processes, reflecting an early history of fault segment evolution as fault orientation adapts to the changing stress state and misaligned fault segments coalesce and evolve into a geometrically simpler fault zone, including fault relays and fault lenses. Secondary faults, such as Riedel shears, are less common in laboratory experiments and numerical simulations than they are in outcrops. Secondary fault structures may also contribute to the rupture of a clay smear and the development of holes, but experiments also reveal the development of holes early in the fault development if brittle clay fragments are fractured and plucked from the source bed. This idea of initial clay fragmentation and evolution into a clay smear via strain-softening processes is a more recent insight that has presumably influenced the development of probabilistic clay smear approaches as applied to subsurface predictions (e.g., Childs et al., 2007; Yielding, 2012).

*3.2.4.1. Proposed mechanical framework.* We propose a matrix of deformation regimes that predict where clay smear may form and the processes that contribute to clay smear in each of those regimes (Fig. 27). The matrix is developed in terms of the relative properties of sand and clay; absolute properties are normalized to the stress state at the time of fault deformation. For example, an uncemented clay layer may fail in shear at low effective stress, while a stronger, stiffer, and more cohesive clay may fail in a similar deformation mode if effective stresses are high. In this way both the relative and

| | | Clay | | | | |
|---|---|---|---|---|---|---|
| | | <<= Failure in Shear Ductile* | | Failure in Extension =>> Brittle* | | |
| Sand | Failure in Shear =>> Ductile* | Much softer | Comparable | Stronger | Much stronger | Relative Strength (clay/sand) |
| | | Clay injection | Shear bands coalescence; fault gouge shearing | Fragmentation; abrasion | Fragmentation of clay in sand | Distinguishing Process(es) |
| | | Clay in fault exceeds clay in section | Layered fault gouge with secondary shear bands | Abraded clay fragments in fault gouge | Clay fragments in sand gouge | Diagnostic Fault Structure(s) |
| | <<= Failure in Extension Brittle* | Very much softer | Softer | Comparable | Stronger | Relative Strength (clay/sand) |
| | | Clay injection; clay flows around sand fragments | Shearing of clay; sand fragmentation; sand abrasion | Abrasion/ fragmentation of both sand & clay | Fragmentation | Distinguishing Process(es) |
| | | Sand fragments surrounded by clay | Clay gouge with sand fragments | Sand-clay breccia with fault gouge | Sand-clay breccia; no clay gouge | Diagnostic Fault Structure(s) |

NB: Clay in each column has the same absolute strength, and sand in each row has the same absolute strength.
Both classes of sand behavior encompass a range of subclasses not distinguished here.
Fault structure also changes with displacement.

* Ingram and Urai (1999)

**Fig. 27.** Matrix of deformation domains for layered sandstone and shale sequences. Matrix defined in terms of relative strength of clay and sand components and corresponding shear or extension failure modes. Table lists distinguishing processes that occur under different conditions and resulting diagnostic fault structures.

absolute properties of sand and clay are considered in the context of the stress state of fault deformation.

Within this matrix (Fig. 27) we recognize that much of the existing work on clay smear is concentrated in the upper left-hand corner of the diagram where both clay and sand fail in shear and where clay is softer (weaker) than or comparable to the associated sand. If effective stress is relatively high and stresses in the clay remain compressive, the sheared clay is initially continuous with its thickness variable over the different segments of the shear zone. With progressive shearing a layered gouge will develop, potentially assisted by lateral fault migration, telescoping and an increasing amount of mixing. Ultimately the clay smear may become discontinuous by attenuation and additional processes like Riedel shears that produce a hole. If clay is very weak, lateral injection may locally increase the amount of clay in the fault.

However, the other parts of this matrix are also relevant in nature. For example, the lower left-hand corner may reflect a calcareous sandstone with some early calcite cement resulting in a high cohesion for the sandstone. The upper right-hand corner may reflect conditions associated with sand injections in which sand failure in shear is dominated by fluidization processes while clay with minimal but finite cohesion fails in extension at the low effective stress levels that arise with sand fluidization and mobilization. If the ratio of effective stress and strength are such that extensional fracturing leads to clay fragmentation, a fault zone with clay fragments embedded in sheared sand is formed. Continuous clay smears may form only after shearing and abrasion of the fragments, although the rates of erosion, abrasion and reworking of fragments to produce continuous gouge are very poorly known. The lower right-hand corner represents the case of faulting over-consolidated rocks that are sufficiently cohesive to fail in extension under the relevant effective stress.

We view this matrix as an initial framework of processes because we recognize that current understanding is incomplete. We expect future research will modify this matrix while in the meantime it provides a basis to motivate that research. Moreover, this framework can also serve as an initial basis for an evaluation of what conditions, expressed as failure mode, are best suited for different clay smear algorithm approaches.

*3.2.4.2. Outstanding technical issues.* There are four general areas where the current laboratory and numerical experimental approaches face limitations:

1. Erosion and reworking of fragments to produce continuous gouge. Reworking of claystone at sufficient mean stress produces clay at critical state, while reworking sandstone produces a cataclasite. The higher the initial cohesion, the greater the softening in the fault zone. Although the mechanical and transport properties of quartz/clay mixtures is known to some extent (Lupini et al., 1981; Crawford et al., 2008; Tembe et al., 2010), the mechanics of the abrasion process are ill-defined, yet this is what determines the mechanical properties of faults with evolving clay-rich gouge. Faults with patchy and layered shear strength are probably the rule.
2. Scaling experimental results to nature: Careful reading of the literature on experimental and numerical modeling of clay smear often brings up the questions about the scale and level of detail one aims to understand in a study. Keeping in mind the enormous literature on fault zone evolution and our still rather incomplete understanding of this important domain, this question is important but often not well answered in the different studies. Considering a natural example of a normal fault zone with perhaps 20 m throw in a sequence of claystone and sandstone, it remains unclear which aspects of this fault zone are lacking in the present set of models. Moreover, fault zone thicknesses vary in nature and laboratory experiments, but this facet of the problem is rarely measured or reported.
3. Incomplete definition of fault processes: For example, rates of mixing of sand and clay are poorly modeled with existing DEM simulations because a much larger difference in grain size between sand and clay is needed to allow clay to go through sand pore throats. Moreover, the effects of diagenesis, pressure solution, and other deformation mechanisms in clay play an unknown role in the evolution of clay smear, and little of this has been systematically investigated.
4. Fault geometric evolution: Before much progress can be made in experiments and numerical simulations of clay smear, a better understanding of the effect of model geometries and boundary conditions on the evolution of fault zone architecture is required. We need well-defined benchmarks to compare experiments and simulations. If a numerical model can predict the evolution of structures in sandbox experiments then perhaps upscaling to nature is possible.

Experiments and numerical modeling are complementary, and the deliberate pursuit of both in concert offers the opportunity to achieve greater confidence in the developing understanding of physical fault processes and the means to extend results beyond which the laboratory or computer easily allows. In addition, it is clear that the ability to compare mechanically layered models with homogeneous systems in order to understand the difference caused by the clay layer could yield substantial insights by better clarifying when the presence of a clay layer matters. Lastly, a mechanism for incorporating an improved physical understanding of fault processes needs to be implemented for predicting the effects of clay smear development for subsurface flow problems. Comparing existing algorithms against experimental results has limited value if the comparison is done without careful scaling and outside of the context of geometric and geomechanical boundary conditions.

### 3.3. Field studies

Field studies include the subsurface application of clay smear models to oil, gas, and water flow. Clay smear processes are among the most important mechanisms to alter cross-fault fluid flow because they introduce the lowest permeability component of a stratigraphic section into a fault zone that cuts that stratigraphy at high angles.

Field studies contribute to our understanding of clay smear products because fluid flow interrogates the entire fault zone, seeking out the most permeable part of a fault where clay smear is least developed or continuous. However, field studies are limited in that the clay smear process is generally inferred rather than observed, and other processes may yield similar results. Moreover, most of the reported subsurface field studies fail to document many of the critical observations necessary to reproduce the presented interpretation (a criticism levied by those attempting to perform clay smear calibration studies; e.g., Bretan et al., 2003). While knowledge has been gained by the field studies reviewed here, there is the potential to learn far more from well-designed, comprehensive subsurface studies as two recent examples illustrate.

*3.3.1. Definition of cross-fault flow*

A common usage in the literature and the petroleum industry is to describe faults as either 'sealing' or 'leaking.' Seals are well defined when capillary properties in fine-grained rocks create no-flow boundaries for non-wetting oil and gas fluids (e.g., Urai et al., 2008) and lead to subsurface oil and gas accumulations (Fig. 28). Failure to hinder oil and gas migration is caused by 'leaking' faults that fail to trap 'significant' oil or gas accumulations.

Unfortunately the seal/leak terminology is also loosely applied to cross-fault flow problems when wells create fluid potential differences that lead to fluid flow (Fig. 28). In this instance a fault becomes sealing when flow rates at a well are deemed 'insignificant,' a threshold that may be problem specific. As a practical matter if often turns out that substantial differences in well flow rates are achieved with a limited range of fault flow properties, but it is nevertheless more informative to consider the problem of cross-fault flux in terms of a continuous spectrum of flow properties rather than the binary leak/seal properties useful for the capillary seal problem (Fig. 28).

Most workers (e.g., Yielding, 2012) agree that the geometry of juxtaposed permeable intervals is the primary control on cross-fault flow as Smith (1980) originally proposed, but where debate remains is in reconciling the apparent ubiquitous presence of clay smear in some fault zones with the inherent uncertainty in juxtaposition geometries. For the case of capillary seals in fault zones, two approaches developed: (1) a probabilistic method that simulates many fault juxtaposition geometries in a complete trap system of leaks and spills (James et al., 2004); or (2) a method using one of the clay smear algorithms (Fig. 3) 'calibrated' for local oil and gas accumulations. The result is a discrepancy in the area of a fault juxtaposition window that may be covered by a capillary clay smear seal (Fig. 29). We think that juxtaposition uncertainty has been

| | Migration and Accumulation | Aquifer Flow | Dynamic Two-Phase Flow |
|---|---|---|---|
| **Large Scale Process** | 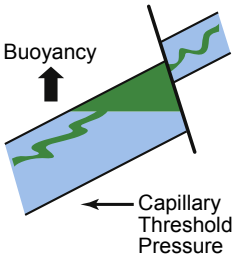 | 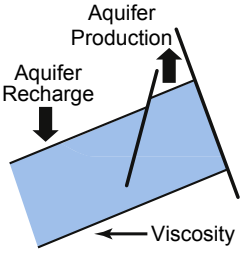 | 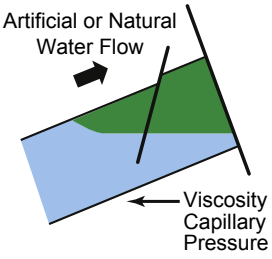 |
| **Implicit Treatment** | Two Phase Static | Single Phase Dynamic | Two Phase Dynamic |
| **Resistance** | Capillary Threshold Pressure | Fluid Viscosity | Fluid Viscosities and Capillary Pressure |
| **Small-Scale Process** | 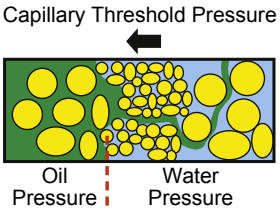 | 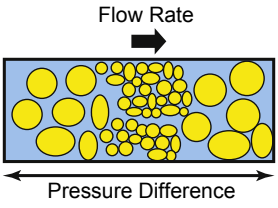 | 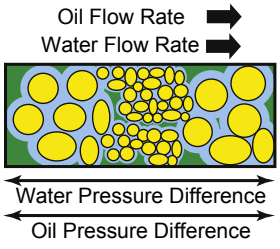 |
| **Principal Fault Rock Properties** | Capillary Threshold Pressure | Permeability and Thickness | Permeability, Thickness, Relative Permeability and Capillary Pressure Curves |
| **Governing Equations** | Capillary Pressure Leakage Criterion | Darcy's Law | Two Phase Darcy's Law, Capillary Pressure |
| **Flow-Rate (Time) Dependence** | Independent | Dependent | Dependent |

**Fig. 28.** Illustration of various cross-fault flow problems occurring in sub-surface describing physical phenomena that contribute to flow problem and manner in which these phenomena are evaluated. Modified from Manzocchi et al. (2002). Copyright 2002, Geofluids. Reproduced with permission of John Wiley and Sons.

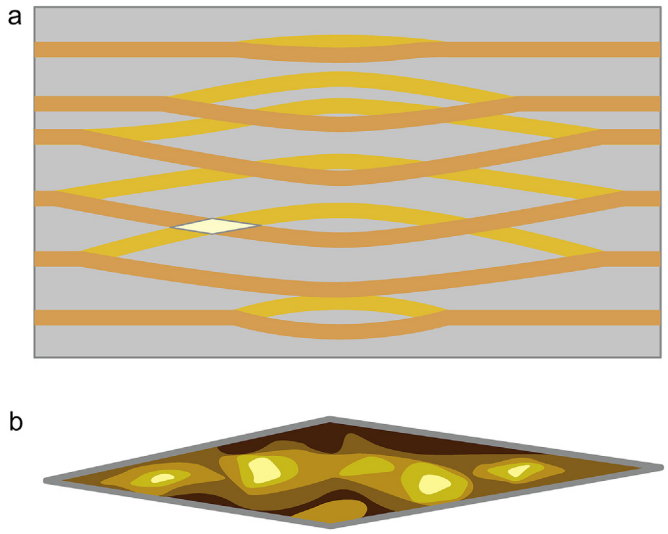


**Fig. 29.** (a) Schematic fault-plane profile or Allan diagram with hanging wall sandstone beds in brown and footwall beds in orange; intervening gray area is shale. Note that only limited portion of fault zone is sandstone–sandstone juxtaposition connections, like beige highlighted one on lower left of profile. (b) Concept of clay smear distribution in juxtaposition window and impact on cross-fault flow. Darkest fringing areas are continuous clay with potential to form capillary seal (no-flow), and lightest area (hole) offers the least resistance to flow (e.g., flow rates = 0.1 rate for sandstone–sandstone connection). As colors become darker, flow rates decrease in order of magnitude steps. Note that in this depiction, although clay smear is present everywhere its contribution to a capillary seal is minimal, and cross-fault flow is restricted to a small area of fault with highest cross-fault fluxes.

under-appreciated in the literature and thus we infer only a small contribution of capillary seal from clay smear (Fig. 29). This distinction is important because it bears on the consideration of 'calibration' studies, although Dee et al. (2007) have shown that it is possible to tune analyses to yield similar results by both approaches.

Fig. 29 also illustrates how a juxtaposition area beyond the fraction covered by a capillary clay smear gouge, clay smear has a variable and irregular distribution of flow properties. It is within this conceptual framework of uneven effects of clay smear developed in a fault zone that we approach the Field Studies section.

### 3.3.2. Field studies outline

Field studies incorporate the full spectrum of flow from static, no-flow conditions where clay smear acts as a capillary seal, to full 3D flow studies where clay smear restricts cross-fault flow of oil, gas, and water fluids that is focused along stratigraphic beds (Fig. 28). For capillary seal studies the inference of clay smear products is derived from a stratigraphic model of the distribution of sandstone and shale lithologies and a structural model that defines the position and offset of normal faults that displace the stratigraphic section (Table 4). Measured subsurface data used to infer the effectiveness of the clay-smear capillary-seal include oil and gas column heights, wireline saturations of oil and gas from well logs that define the spatial distribution of fluid types in the subsurface, and wireline pressure data used to define fluid pressure with depth in respective fluid types (Table 4). Sometimes core materials are available with faults in them, and the flow properties of the sampled faults are analyzed in the laboratory (Table 4).

Flow studies that include cross-fault flow provide information on the aggregate permeability of a fault zone for Darcy flow (Fig. 28), a potentially valuable addition to the information provided through the capillary seal analysis. However, flow solutions are non-unique (e.g., Jolley et al., 2007), and it is difficult to find well-conceived cross-fault flow experiments that reduce the non-uniqueness of the solution. Although studies that incorporate cross-fault flow add further useful data (e.g., single and multi-well tests and downhole pressure records; Table 4), the resulting clay smear inferences are also dependent on the analytical methods used to analyze the data, ranging from analytical models used to interpret individual well tests to box-based mass-balance calculations to full 3D flow simulations (Table 4).

In this section we use the framework of observations and analyses defined in Table 4 to evaluate the literature devoted to field studies, and in particular clay smear calibrations based on this literature. An important perspective to maintain through this section is the sometimes competing interests and demands of commercial application of the clay smear concept and the scientific prerequisites that give us deeper insight into fault processes.

### 3.3.3. Clay smear interpreted as a capillary seal

Clay smear was originally applied to problems of capillary or membrane seals in which a continuous veneer of gouge maintains oil or gas saturation below a critical saturation threshold that is necessary for percolation (Fig. 28). Oil and gas on either side of a fault exist at different pressures at the same elevation, and if water is in pressure communication across the fault, contacts between different fluid phases will form at different elevations. This was the primary application considered by Weber et al. (1978) for trap considerations in the Niger Delta and Smith (1980) in the U. S. Gulf Coast. We infer that in both of these studies the stratigraphic framework applied at the analyzed faults was based on 1D models derived from well logs and that the fault framework was based on 2D seismic data of unknown spacing combined with fault interpretations based on missing section in wells (Table 4). An important component of these early studies is that they relied to a large extent on fluid contacts logged by petrophysical measurements because this was the most ubiquitous data type available. The value of pressure data was likely well appreciated but limited to rare drill-stem and production tests; no pressure data are reported in the early works.

Bouvier et al. (1989) offered the next advancement in the application of clay smear to subsurface field studies by introducing 3D seismic data into the analysis. Using newly developed interpretation and visualization techniques, the critical issue of fault continuity and cross-fault reservoir connectivity emerged, at least as expressed in seismic time slices. Fault juxtaposition diagrams were constructed using seismic sections extracted in the fault footwall and tied to well-log stratigraphic profiles. The effects of clay smear were overlain on this geometric representation by lumping calculated CSP values into high, medium, and low categories. Interestingly, higher CSP values are calculated where the proportion of shales in the stratigraphic section increases, and as the authors admit the chance for reservoir juxtaposition against shale increases (Bouvier et al., 1989). This is a conundrum that occurs in many, if not most, clay smear field studies.

Berg and Avery (1995) presented an interesting additional perspective in their discussion of complex fluid contact relations in the U. S. Gulf Coast. They used dip-meter data to document significant dip deviations in shale in fault zones. Although they describe this behavior as clay smear, the consistency of dips within limited intervals suggests tilted but coherent intervals of shale (lithology based on SP and resistivity curves). In a current context it might be more appropriate to

**Table 4**
Summary of subsurface field studies and data types applied.

| Reference | 1D strat model[a] | 3D strat model[b] | 3D seismic data[c] | Oil & gas column heights[d] | Wireline saturations[e] | Wireline pressures[f] | Fault core & characterization[g] | Single well tests[h] | Well interference tests[i] | Downhole pressure history[j] | Well rate history[k] | Mass balance calculation[l] |
|---|---|---|---|---|---|---|---|---|---|---|---|---|
| Bentley and Barry, 1991* | Y | *y* | Y | | Y | ? | ? | ? | ? | | *y* | Y |
| Berg and Avery, 1995 | Y | | | Y | Y | | Y | | | | | |
| Bouvier et al., 1989 | Y | | Y | | Y | | | | | | | |
| Childs et al., 2002 | Y | | Y | | Y | Y | | | | | | *y* |
| Childs et al., 2009b | Y | Y | Y | | *y* | *y* | | | | | | |
| Davies et al., 2003 | Y | | Y | Y | Y | | | | | Y | | |
| Ottesen Ellevset et al., 1998 | Y | | Y | Y | Y | | Y | | | | | |
| Fristad et al., 1997 | Y | | Y | | Y | Y | Y | | | | | |
| Gibson, 1994 | Y | | Y | Y | Y | | Y | | | | | |
| Gibson and Bentham, 2003 | Y | | Y | Y | Y | Y | | | | | | |
| Harris et al., 2002 | Y | | Y | | Y | Y | | | | | | |
| Jev et al., 1993 | Y | | Y | | Y | Y | | | | | | |
| Jolley et al., 2007* | Y | *y* | Y | | Y | | | | | Y | Y | Y |
| Knai and Knipe, 1998* | Y | | Y | | | | Y | | | Y | *y* | Y |
| Koledoye et al., 2003 | Y | | Y | | | Y | | | | | | |
| Myers et al., 2007* | Y | *y* | Y | | Y | *y* | | | | Y | Y | Y |
| Nybakken, 1991* | *y* | | *y* | | *y* | Y | | | | | | |
| Sassi et al., 1992* | Y | *y* | | | Y | | Y | *y* | | | | |
| Smith, 1980 | Y | | | | Y | | | | | Y | | |
| Speksnijder, 1987 | | | Y | | | | | | | | | |
| Sverdrup et al., 2003* | Y | | Y | | | Y | Y | | *y* | | *y* | *y* |
| Weber et al., 1978 | *y* | | | | Y | | | | | | | |
| Wehr et al., 2000 | Y | *y* | Y | | *y* | | Y | | | | *y* | Y |
| Welbon et al., 1997 | *y* | | *y* | | *y* | *y* | | | | | | |

*In these papers the '*y*' designation indicates that this data type likely exists based on figures presented (e.g, a cross-section suggests that 3D seismic data may have been available), but those original data remain unverified in the publication (i.e. unable to independently reproduce the result).

[a] Stratigraphic model derived from petrophysical data and cores collected in a vertical borehole.

[b] Stratigraphic model based on petrophysical data and seismic attributes, for example, used to condition interpretations away from wellbores.

[c] Primary issue is data resolution, which depends on rock physics, data acquisition parameters, and data processing steps; latter two improve with time.

[d] Height between crest of column and fluid contact; depth uncertainties usually unspecified, and fluid types sometimes unrecorded.

[e] Petrophysical data necessary to define gas, oil, and water saturations at all available well depths; fluid contacts included if encountered in well.

[f] Down-hole pressure profiles defined in newly drilled well; critical issues is vintage of gauge, which affects pressure precision and accuracy.

[g] In best case includes cores of small-scale and large-scale (seismically imaged) faults; complementary wellbore dipmeter and image logs.

[h] For example, Drill Stem Test (DST) in which pressure recovery is evaluated in same wellbore as flow has occurred (extraction or injection).

[i] Requires two wells, preferably located nearby across fault; one well monitors pressure while other well produces or injects fluid.

[j] In best case pressure gauges installed near reservoir interval monitor pressure (Flowing Bottom-Hole Pressure) during production and injection, especially when wells shut-in (Shut-in Pressure); otherwise derived from well-head pressures.

[k] Record of volumes of fluid produced from or injected into a well (daily basis); in best case well section open to flow is limited; may include 4D seismic results of changing sub-surface saturations or well tracer studies.

[l] Model used to evaluate effects of produced or injected volumes on resulting pressure history; models can be simple box-models or 3D simulations.

think of these tilted, shale-dominated intervals as fault relays or lenses (e.g., Childs et al., 1997), a particular component of clay smear products.

Gibson (1994) used core, outcrop, and fluid contact data (defined as column heights) to infer clay smear processes for a number of gas and oil accumulations in the Columbus Basin of Trinidad. This paper is a good example of the part of the literature that seeks to apply clay smear models in order to reduce

oil and gas exploration risk, but the insights it adds to clay smear processes are limited. Notwithstanding these comments, Gibson (1994) contributed to and further supported the idea that clay smear continuity is the single most critical aspect when applying a clay smear model. Moreover, Gibson's contribution is unique in that it introduced the idea of clay smear variability in a fault zone and explored that variability in the context of explaining traps that contain both oil and gas. Gibson (1994) realized that in order to trap both oil and gas in a fault-bounded trap, gas fill must be limited by capillary leak at the highest elevation of the fault-dependent trap component, precisely defining a critical pore throat diameter to limit the amount of gas trapped, while oil spills across the fault at the oil-water contact where capillary resistance is negligible. It is interesting that this insight appears to have been largely overlooked in subsequent field studies.

Similarly, Ottesen Ellevset et al. (1998) made inferences about fault properties based on core observations and offset gas-water contacts in the Sleipner Vest Field, Norway. Without incorporating pressure data to evaluate whether different contacts were the result of fluid segregation in the gas or water phases, these authors deduced fault compartmentalization in the gas column and inferred capillary fault properties, including clay smear, based on this assumption. However, in this field it is also plausible to interpret the offset contacts as a result of disconnected water bodies (Paul Hicks, personal communication to P. Vrolijk, 1997), an interpretation that alters the inferences of fault rock properties and continuity.

*3.3.3.1. Clay smear interpretations including pressure data.* In the 1990's the more common availability of wireline pressure data found its way into clay smear interpretations for subsurface studies. As described above, this development was important for helping to uniquely establish which fluid phases are connected and which are segmented across a fault. For example, Nybakken (1991) identified pressure differences in the Tampen Spur area of the North Sea, which he attributed to clay smear and injection as the most effective processes that create those pressure differences. However, Nybakken (1991) only inferred the effects of clay smearing in a qualitative sense; there is no attempt in this paper to select a clay smear model, apply it to all faults, and check for the internal consistency of all resulting interpretations (i.e. are capillary leaks and seals interpreted for the same value of clay smear quantity, like SGR?).

Welbon et al. (1997) combine the effects of shale smear with other deformation mechanisms like cataclasis and a generalized reservoir connectivity probability based on a paper by Knott (1993) into a 'Fault Seal Probability' product. Although the appeal for combining the results of so many complex processes into a single probability parameter is apparent, it also makes it difficult to isolate which processes are most important along any particular fault segment. Welbon et al. (1997) attempt to overcome this limitation by independently producing a shale smear map for one fault in their study. In constructing this map they appear to use a limiting SSF of 7 as defined by Lindsay et al. (1993) but for which other authors at this point had begun to suggest that this critical value is actually much lower (e.g., Gibson, 1994).

Pressure data were first used in a systematic way to evaluate cross-fault pressure differences by Fristad et al. (1997) and Yielding et al. (1997). In this approach wireline pressure data are used to define pressures in permeable sandstone intervals on both sides of a fault (in the context of a defined fluid phase), and those pressure differences compared with a spectrum of SGR values calculated on the entire fault surface (Fig. 30). Note that this approach relies on the definition of fluid pressure models that may be either loosely constrained with a single pressure measurement and an independent definition of fluid density (i.e. $\Delta p/\Delta z$), or well constrained with many pressure measurements. The resulting

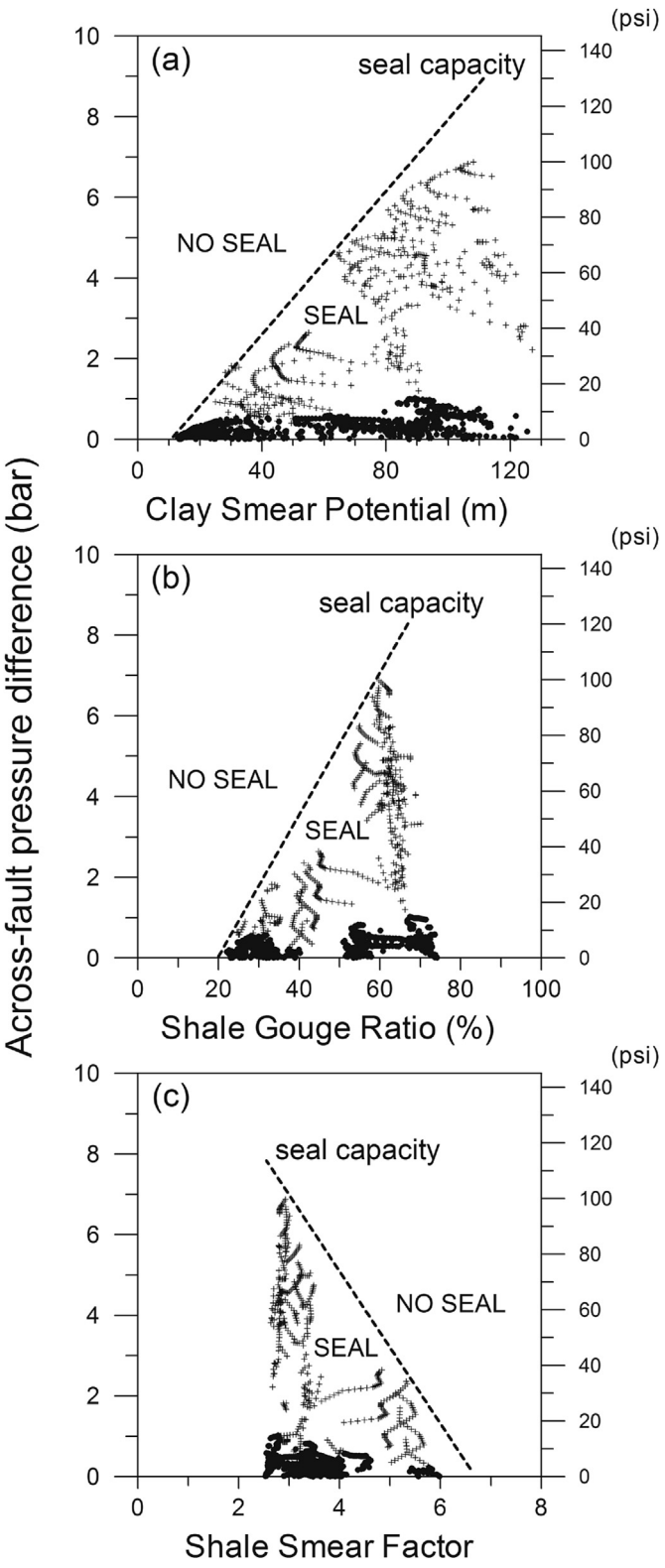


**Fig. 30.** Calculated cross-fault fluid pressure differences for various representations of clay smear, including (a) CSP, (b) SGR, and (c) SSF. Plots developed to provide empirical definition of fault capillary seal for modeled clay-smear parameters. Reproduced *with permission* from Yielding et al. (1997).

cross-plots of SGR versus pressure difference (Fig. 30) is then used to infer a capillary leak point and its capillary properties. A bounding envelop, typically drawn as a straight line in SGR-pressure difference space, defines a calibrated leak envelope. In both of these publications, this approach was initially applied to the complexly faulted Oseberg Syd field in the Norwegian North Sea, and Yielding et al. (1997) extended the analysis to the Nigerian Nun River field (Bouvier et al., 1989) and accumulations in Trinidad described by Gibson (1994).

While this approach appears attractive in that it attempts to incorporate information across an entire fault zone, several questions arise. First, there is no *a priori* reason why entry pressure should increase with increasing SGR given experimental (Crawford et al., 2002) and theoretical information (Revil and Cathles, 1999), both of which achieve the greatest permeability reduction with incorporation of up to 30–40% clay and little or no further permeability reduction with additional clay. Indeed, debate on whether this effect exists is ongoing (e.g., Childs et al., 2009b; Davies et al., 2003). Second, threshold SGR values (i.e. the lowest SGR values that support a cross-fault pressure difference) tend to occur at small pressure differences, as it does in Yielding et al. (1997). Small pressure differences are difficult to evaluate out of context, especially in light of the evolution of pressure gauge precision and accuracy that occurred over the period of these studies. Remarkably, the issue of accuracy continues today even with high precision and accuracy pressure gauges when considering pressure differences of 1–20 kPa because depth uncertainty yields that much error (e.g., an apparent 10 kPa pressure difference results from a 10 m depth error applied to a water gradient of 10 kPa/m). Caution is warranted when seeking significance of SGR points defined for small pressure differences (Fig. 30). Fewer data define the bounding envelope at higher SGR values, and it is valid to ask whether alternative geologic interpretations might account for the highest values (e.g., juxtaposition seal), thereby shifting the bounding curve to higher SGR values.

The development of this technique by Fristad et al. (1997) and Yielding et al. (1997) remains a significant contribution to the application of clay smear effects in the subsurface, and in spite of the reservations expressed above, this comprehensive approach of mapping SGR and pressure difference values across an entire fault zone succeeds in testing the logical, internal self-consistency of the interpretation – there can be only be one unique leak point for each hydrocarbon phase trapped – a check that other studies have failed to complete. This fault mapping approach is a step in the right direction toward building an internally consistent interpretation, but it should be expanded to the entire field using a compartment approach like that described by Vrolijk et al. (2005a) in which the fate of any oil or gas that leaks out of any single compartment must be traced to the next downstream compartment until it exits the field completely. Does the calibration of SGR on one fault and applied to another fault in the field cause the trapped oil to back up and fail to reach the field spill point? Sometimes the interpretation of leakage is as critical as the interpretation of a capillary seal.

This discussion helps illustrate the point made at the outset of this section that in the absence of comprehensive field studies, there are always questions that arise that limit the value of a calibration formed on a subset of the field data. Critical questions invariably arise about the input data for the analysis that render at least parts of that analysis irreproducible.

### 3.3.4. Clay smear defined by core analyses

While broad-scale field studies were being undertaken in the 1980's and '90's, another line of investigation opened up based on the examination of faults encountered in cores (e.g., Knipe, 1992). The basic methodology and resulting fault classification scheme was defined early on (Fisher and Knipe, 1998) so there is a reasonable uniformity found in the literature. Although it is difficult to discern from individual papers, it is likely that most faults encountered in core were sampled accidently rather than planned in the context of a scientific experiment (i.e. a specific, testable hypothesis identified before drilling and tested by the sampled core), and Hesthammer and Fossen (2000) discuss potential sampling biases encountered in a detailed study of the Gullfaks Field.

The analysis of various fault samples from core has resulted in vast databases of fault properties and characterization data, most of which are proprietary and unavailable to the scientific community. However, this characterization effort also brought an additional graphical tool for evaluating clay smear among other fault rock types: the triangle diagram of Knipe (1997) that evolved from Bentley and Barry (1991). This type of display attempts to allow consideration of a much richer geologic description of offset lithologies and resulting fault rocks than the simple, binary seal/non-seal classification. In particular, this approach defines a possible hybrid clay smear in a phyllosilicate framework fault rock (PFFR; Gibson, 1994; Knipe, 1992), a rock type containing abundant sand grains but which may reflect the flow properties of a clay-dominated clay smear (Knipe, 1997). Although the PFFR type is conventionally interpreted as a product of faulting clay-bearing sandstones (Gibson, 1994; Knipe, 1992), we think the experimental evidence of sand-clay mixing (Schmatz et al., 2010a, b) offers an additional mechanism to achieve the same product, especially if sand has deformed by independent particulate flow, an issue broached by Freeman et al. (1998). Note that the limit of 40% clay used to define the PFFR type is at the boundary where the addition of more clay yields little or no additional permeability decrease (Crawford et al., 2002).

While the triangle diagram approach defines juxtaposition windows and gouge types across all possible fault offsets, the analysis relies on a deterministic stratigraphic section, often defined at an existing wellbore whose location was likely chosen for reasons other than its utility for defining a stratigraphic section for fault-seal analysis.

There are two principle limitations in the application of core sample results to the problem of cross-fault flow influenced by clay smear:

1. Core samples offer little insight into the critical aspect of clay smear – clay smear continuity. Although it is possible to measure in the laboratory the capillary and permeability properties across a clay smear, extrapolation of those properties away from the core requires a model that core observations lack the ability to test comprehensively.
2. Core samples come from proprietary cores, and results are reported in the literature as either 'typical' results without attribution to a specific fault or location in the Earth, or they are amalgamated into large databases of fault rock properties. Even when sample analyses are reported in the context of a field study (e.g., Ottesen Ellevset et al., 1998), the results are presented lacking the context of the fault from which the samples were derived. Gibson (1998) sought to overcome this issue by presenting data tables that report results on an individual sample basis.

The primary contribution of core studies to the clay smear problem is to define a trend of decreasing permeability with increasing clay content in the fault (e.g., Gibson, 1998; Manzocchi

et al., 1999; Fisher and Knipe, 2001; Sperrevik et al., 2002). While the issue of clay smear continuity is recognized in these studies (e.g., Fisher and Knipe, 2001), there are no unique observations made from core samples to address this issue.

*3.3.5. Modern clay smear field studies – the rise of uncertainty*

Since the late 1990's, the data types with which modern subsurface studies are performed became routine – 3D seismic data; abundant accurate and precise wireline pressure data; complete wireline log characterization (including gamma ray, neutron porosity, bulk density, resistivity, and corresponding derivative Vshale, saturation, and porosity curves); and a myriad of tools for the evaluation and integration of diverse data types. Complete integration of these diverse data in order to achieve a logical, comprehensive interpretation of multiple oil and gas columns in a complexly faulted stratigraphic section can prove daunting. In an example from the Exmouth basin of Australia, Bailey et al. (2006) consider clay smear (high SGR) in the context of other trap leak controls and attribute a spectrum of mechanisms for the observed fluid type and pressure distributions.

A pair of studies by Childs et al. (2002) and Davies et al. (2003) consider a similar case of gas and water at the same elevation across a fault combined with a large difference in water pressure across the fault. In the Tune Field (Norway) example discussed by Childs et al. (2002), gas occurs in the hanging wall and is connected to an aquifer with a much higher pressure than the aquifer in the footwall. In contrast, Davies et al. (2003) discuss a Gulf of Mexico example in which the higher aquifer pressure is observed in the footwall while gas is trapped in the lower pressure hanging wall. In both of these studies, however, an attempt is made to account for the gas distribution and water pressure offset across the fault by interpreting a cross-fault water flux. Childs et al. (2002) model the relative permeability of water through the gas cap where the water saturation is above the irreducible water saturation value. Davies et al. (2003) interpret water flow in the opposite direction (i.e. from the higher pressure, water-saturated footwall into the gas column in the hanging wall) but without the corresponding calculations to illustrate the feasibility of this interpretation. And although Davies et al. (2003) acknowledge data uncertainty in their analysis, they dismiss the impact of that uncertainty on their conclusions without reporting the work done to reach that conclusion.

This interpretation of faults that form a capillary seal while allowing the flux of water through the gas column is interesting in that it has potentially significant implications for pressure histories during production. For example, the Tune Field example by Childs et al. (2002) suggests that pressure depletion during gas production will be offset to some degree by aquifer support, an interpretation that should be apparent in plots of pressure normalized for gas compressibility (P/z) as a function of time and through the early occurrence of water break-through. Moreover, as contacts rise, water saturations and the relative permeability of water will also increase, resulting in an increasing flux of water across the fault and a rapid pressure decline that offsets the aquifer support.

Other authors more directly addressed two types of uncertainties in predicting subsurface clay smear development: (1) log definition of the clay fraction in a faulted stratigraphic section (e.g., Bretan et al., 2003) and the resulting threshold value of a clay smear parameter like SGR that results in a capillary seal; and (2) detailed fault zone definition using core data and high resolution seismic reflection data (e.g., Childs et al., 1997; Faerseth et al., 2007; Hesthammer and Fossen, 2000; Koledoye et al., 2003). In certain settings challenges arise in defining the stratigraphic section. For example, Bretan et al. (2003) claim that: 'Different vintages of $V_{shale}$ analysis of the same well by different petrophysicists working in the same company can be alarmingly different.' Bretan et al. (2003) then go on to apply a revised method for determining the input $V_{shale}$ value (with respect to the original work reported by Fristad et al., 1997), derive different SGR values from a $V_{shale}$ curve that includes 'mica and kaolin' (Bretan et al., 2003), and define a higher SGR value necessary to achieve a capillary seal. Childs et al. (1997) illustrate how various natural fault zone complexities, including multiple slip surfaces that define fault relays and lenses, result in different interpretations of cross-fault connectivity, the fundamental basis necessary for considering the effects of clay smear. Hesthammer and Fossen (2000) discuss additional detailed fault complexities that affect cross-fault connectivity based on core description studies in the Gullfaks Field, and Koledoye et al. (2003) document how paired slip surfaces identified in high resolution seismic data from Nigeria promote the incorporation of shale in the fault zone, perhaps in the manner of fault-bounded, coherent shale lenses in the context of Berg and Avery (1995). These ideas are further developed by Faerseth et al. (2007) in which they attempt to define a methodology for accounting for these uncertainties within a risk framework.

The problem with recognizing these uncertainties is that solutions for addressing them are complex. Attempts to generalize complexity (e.g., Knott, 1993) lack the necessary detail for addressing questions related to individual faults. Specifically, Childs et al. (1997) suggest that: 'The distribution of fault rocks cannot be characterized from well data, raising the question of whether purely deterministic methods for fault seal prediction can ever be successful.' This kind of doubt ultimately led to efforts to systematically explore likely uncertainties (e.g., Childs et al., 2009b; Manzocchi et al., 2008a,b,c).

On the one hand this emerging realization of the impact and importance of uncertainty in the input parameters and its impact on the resulting clay smear calculations presents a sobering picture. On the other hand this period is also marked by studies attempting to 'calibrate' clay smear calculations against subsurface observations using the methods of Yielding et al. (1997). From papers like Bretan et al. (2003), Bretan and Yielding (2005), Harris et al. (2002), and Yielding (2002) there arises a definition of SGR values above 15–20% necessary to create a capillary seal. Specifically, there are examples of low SGR where there is little evidence of a capillary seal and others with high SGR values that are associated with a capillary seal. This conclusion is further supported by the uncertainty study undertaken by Childs et al. (2009b). The transition region around an SGR value of 20% remains problematic, however. Does the resulting threshold entry pressure increase with increasing SGR? Over what range of SGR values does this transition occur? While exploring some uncertainty parameters (i.e. it remains challenging to incorporate alternative fault geometry interpretations), Childs et al. (2009b) conclude the following: 'The data also demonstrate that the level of fill in individual traps can be extremely sensitive to minor variations in the seal capacity envelope.'

Further complicating matters, Dee et al. (2007) used a clay smear approach to evaluate a field study described by James et al. (2004) in which a stochastic approach to evaluating juxtaposition geometries was employed. Dee et al. (2007) produced a similar gas column distribution to the one originally described by James

et al. (2004). A logical conclusion from this result is that both approaches are an imperfect description of subsurface geology and that both predict faults that form capillary seals when shale is relatively abundant in the faulted stratigraphic section and the absence of seals in shale-poor sections. Indeed, when more comprehensive analyses of stratigraphic uncertainty are undertaken (e.g., Clarke et al., 2006; Hovadik and Larue, 2010), it seems likely that at least some documented examples of capillary seal from clay smear might better be attributed to uninterpreted stratigraphic complexities. Consequently, it is difficult to glean deep physical insights into clay smear processes from the existing field studies literature that considers clay smear as a capillary seal.

#### 3.3.6. Clay smear under transient, production-scale flow conditions

An alternative application of clay smear predictions is for the interpretation of cross-fault flow during the hours to years timescales common to fluid production or injection. In these studies the effects of pressure transients introduced into the subsurface by wells producing or injecting gas, oil, or water fluids is monitored and the results interpreted in terms of aggregate permeability properties of intervening faults. With the increased number of parameters needed to define such a system (Fig. 28), an additional strategy is required to model the effects of faults in flow simulations (e.g., Manzocchi et al., 2002). As Manzocchi et al. (2010) point out, evaluation of the flow effects of clay smear are complementary to those of capillary membrane seals because: 'fault seal capacity relies on outliers of fault property distributions (the sealing capacity of a fault is controlled by the weakest point) while across-fault Darcy flow is controlled by average properties.' Interestingly, this facet of the literature is dominated by field studies from Mesozoic reservoirs in the North Sea with a minor, secondary contribution of older literature from the Niger Delta.

Speksnijder (1987) commented for the first time on the effectiveness of clay smear for cross-fault flow in the Cormorant Field of the North Sea. Speksnijder (1987) focused on the complex fault interpretation revealed by new 3D seismic data, and the impact of that interpretation on cross-fault flow is only briefly defined in the conclusion of the paper for CSP values that are apparently associated with production performance data, none of which is presented.

Fault patterns in the Cormorant Block IV field were evaluated by Sassi et al. (1992) in order to define the impact of various size groups of normal faults (defined in terms of throw) on flow within the Brent Group. Note that in their interpretation, cross-fault flow restriction only becomes important on medium-scale faults (throw 10–50 ft; 3–15 m), and only in the thin-bedded Ness Formation where the effects of juxtaposition seal and clay smear are hard to differentiate.

In a detailed study of a trap-bounding fault in the Niger Delta, Jev et al. (1993) reported multiple independent oil columns accumulated in a stacked deltaic reservoir sequence. In the younger, more shale-prone interval of the stratigraphic section, higher CSP values are calculated than in the deeper, older, more sandstone-rich part of the section. Based on this geologic description, Jev et al. (1993) were able to rationalize a capillary seal for the oil accumulations in the upper intervals while attributing water flow across the fault in the deeper sections resulting from oil production and pressure depletion in the neighboring Cawthorne Channel Field; water flows from deeper unproduced intervals (Akaso G reservoirs) across the fault to replenish the fluid withdrawn by production (Cawthorne Channel E reservoirs). Jev et al. (1993) also recognize the value of detailed reservoir simulation studies for unraveling the details of this kind of fluid pressure depletion response but show the value of initial geologically comprehensive analytical evaluations.

While the pressure history that arises from production fluid extraction yields additional insight into the permeability properties of a fault zone, those properties can only be inferred with additional information about production rates, connected pore volumes, the properties of the fluids contained within those pores (e.g., compressibility), the timing and history of all wells either producing or injecting fluid, and additional case-specific parameters. The calculated pressure histories introduced by Fulljames et al. (1997) begin to illustrate the complexity of even a simple pressure response. Rivenaes and Dart (2002) suggest that capillary effects maintaining higher water saturation in fault zones further reduce the relative permeability of a fault, adding another dimension to the problem. Fisher and Jolley (2007) further developed the idea of relative permeability in a fault zone. Ultimately the use of a geocellular reservoir simulation model was introduced to help keep track of these various parameters and dependencies.

Bentley and Barry (1991) provide the first application of a reservoir simulation study of a faulted reservoir, also basing their work on Cormorant Block IV. They describe different intervals of CSP into clay smear 'type panels,' which they used to classify different types of cross-fault flow. Interestingly, they comment that 'the complexity of the structural pattern and production history from Block IV rule out the option of simple calibration using production data' (Bentley and Barry, 1991), although they did iterate on leak paths within the model in the context of a well history match to define a threshold CSP = 5 for fault 'sealing' (which is interpreted to be negligible cross-fault flow rather than no-flow). Subsequent work by Wehr et al. (2000) on the same field investigated the flow effects of various fault gouge scenarios, including clay smear (CSP), on reservoir flow simulation models compared against water-cut data from production wells. Wehr et al. (2000) advanced the simulation approach toward the current practice of applying different fault transmissibility values to different parts of a fault guided by an independent geologic interpretation and illustrated the efficiencies gained in the reservoir simulation and history-matching process given *a priori* definition of fault gouge properties and distribution.

As reservoir simulations improved through evolution of raw computing power, it ultimately became possible to treat and evaluate a full continuum of fault properties in a comprehensive reservoir simulation. Jolley et al. (2007) provided one of the first examples in an evaluation of the Brent Group fields in the North Sea. They recognized how hard it is to construct the faulted reservoir framework needed to evaluate the flow effects of fault gouge, including clay smear, and identified the definition of the fault framework as a 1$^{st}$-order sensitivity for the modeling process. Jolley et al. (2007) also describe the application of fault properties via the assignment of transmissibility multipliers; the methodologies for defining transmissibility multipliers are described in other literature (e.g., Fisher and Jolley, 2007; Manzocchi et al., 1999). An important outcome of this study is the conclusion that with the time and care invested in constructing a viable reservoir framework and the systematic application of transmissibility multipliers based on geologic principles and clay smear models, the path to achieving an acceptable history match is far more efficient.

Many similar conclusions were reached by Myers et al. (2007) in a reservoir simulation study of the Ringhorne Field, Norway: the fundamental necessity of accurately constructing the faulted reservoir framework in the simulation model and the vast advantage in the history-matching exercise of starting with an array of geologically-defined fault transmissibilities that reflect

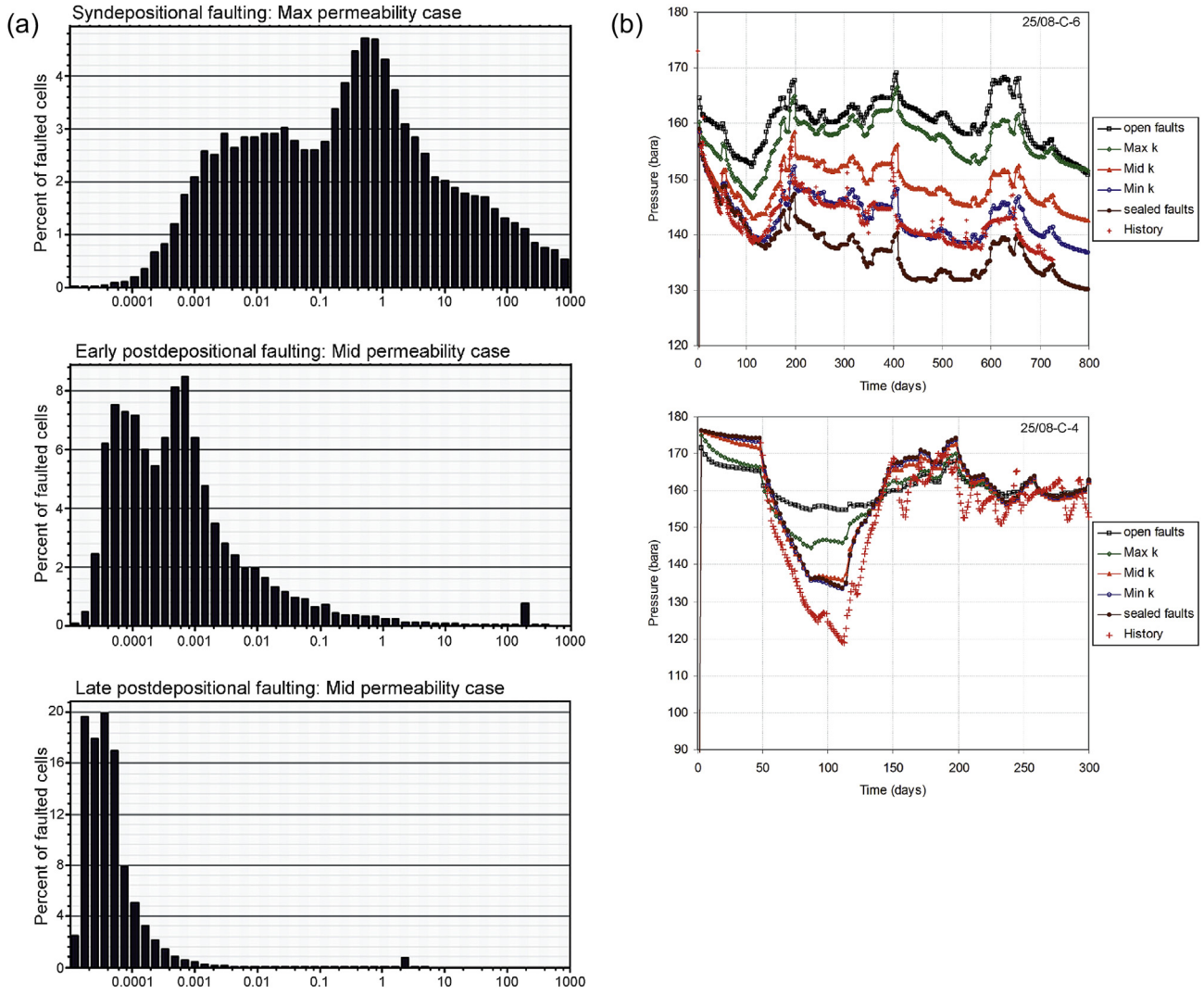


**Fig. 31.** Illustration of how modeled effects of different failure modes, expressed here as burial depth of faulting, result in variable fault permeabilities and resulting producing well pressure histories. Note that history match was only possible after various other geologic problems in model were identified and rectified. (a) Histogram of fault permeabilities (milliDarcies) applied across entire model for three faulting scenarios: syndepositional, early post-depositional (shallow), and late post-depositional (deep) faulting. (b) Flowing bottom-hole pressure records for two producing oil wells in model compared against calculated pressures for three fault histories described in (a) as well as fault-open and fault-closed end-member scenarios. Reproduced *with permission* from Myers et al. (2007).

clay smear properties. An important distinction in the approach used by Jolley et al. (2007) and Myers et al. (2007) is the way in which the clay smear product (e.g., SGR) is transformed to permeability. Jolley et al. (2007) used an empirical transform that relates fault permeability to shale fraction as expressed by SGR. In contrast, Myers et al. (2007) implemented a permeability calculation based on the geometry of the clay component in an aggregate fault zone consisting of multiple gouge types. Myers et al. (2007) also used this approach to explore alternative fault permeability scenarios for different material property definitions arising from different burial and faulting histories (Fig. 31). This approach represents a significant development in that it for the first time attempts to link a fault-process model with a resulting cross-fault flow calculation. Further information about how these two approaches (empirical permeability definition versus process-based evaluation) relate to the flow problem is outlined in the text inset.

Even when reservoir simulation is used to test models of fault properties, the results are non-unique given the large number of degrees of freedom that remain in the model (i.e. multiple combinations of parameters consistent with measured data produce the same fluid pressure and rate histories). One way to further reduce the degrees of freedom in a model is with an independent data type, and Sverdrup et al. (2003) have shown how the application of 4D (time-lapse) seismic data are used to track the spatial movement of gas and water fluids and the corresponding pressure changes between repeat surveys. In particular, the amplitude difference map in Sverdrup et al. (2003; their Fig. 11) is a beautiful illustration of gas pooling against a fault and begs the questions of whether a sandstone connection exists at that location to support potential gas leakage across the fault, and if so, whether the gas is pooling in a small attic above the juxtaposition connection. If both of those geometric criteria are met, then cross-fault flow is restricted by fault gouge, possibly a clay smear.

Clay smear algorithms have the following units basis:

$$\cdot \quad SGR = \frac{\sum Vcl \times \Delta z}{throw} * 100\% \quad dimensionless \;\; length \tag{2}$$

$$\cdot \quad CSP = \sum \frac{thickness^2}{distance} \quad length \tag{3}$$

$$\cdot \quad SSF = \frac{throw}{thickness} \quad dimensionless \; length \tag{4}$$

Insofar as these parameters are used to evaluate cross-fault flow, we compare them via Darcy's Law to properties that resist flow (permeability or hydraulic conductivity) which have units of $L^2$ and L/t, respectively. In this context it is possible to see SGR and SSF as proportionality constants that could be applied to the permeability definition (Hubbert, 1940):

$$k = Cd^2 \tag{5}$$

where $C$ is the proportionality constant that further modifies *SGR* or *SSF* parameters ($d$ is the diameter of uniform glass bead particles in Hubbert's formulation); both define properties of the medium through which flow occurs. *CSP* values with a length dimension may require additional information from the taper geometry to become dimensionless.

Attempts to relate some measure of clay smear to flow have used *SGR* as a non-linear proportionality constant in a permeability definition:

$$\log k_f = 0.4 - 4SGR - 0.25 \log(D) * (1 - SGR)^5 \tag{6}$$

$$k_f = a * SGR^{-b} \tag{7}$$

$$k_f = \left(F_{vsh} * k_{sh}^{(1-2Cf)} + (1 - F_{vsh}) * (k_{ss} * k_{cat})^{(1-2Cf)}\right)^{-(1-2Cf)} \tag{8}$$

In all cases $k_f$ = fault permeability. Equation (6) is from Manzocchi et al. (1999; arithmetic average permeability); $D$ = fault throw (m). Equation (7) is from Jolley et al. (2007) where a and b are constants from $k_f$ −clay % transforms. Equation (8) comes from Myers et al. (2014), and $F_{vsh}$ = volume fraction of shale in the fault, $k_{sh}$ and $k_{ss}$ represent shale and sandstone permeabilities, respectively, and Cf represents a clay smear continuity factor.

Notwithstanding the success of these history-matching exercises, the issues of geologic uncertainty are still prominent for reservoir simulation problems, not least for models constructed to predict reservoir performance before production wells are drilled. In particular, some of the geometric uncertainties explored by Manzocchi et al. (2010) warrant careful thought when considering cross-fault flow.

*3.3.6.1. Aquifer flow studies.* Additional information about cross-fault flow is available from aquifer studies. Darcy flow is simpler in aquifer studies with a single fluid phase in the fully saturated zone (Fig. 28). However, the subsurface geologic structure, which may be constrained by surface outcrop exposures, is often less well defined in the absence of seismic reflection data that prove so useful in petroleum field studies. For example, Bense et al. (2003) offer detailed descriptions of faults and clay smear in shallow, unlithified sediments studied in trenches in the Netherlands with detail well beyond what is possible in petroleum field studies. They infer flow restriction across the fault based on an observed 5 m difference in the phreatic surface over a 25 m distance.

In a more comprehensive study in the Lower Rhine Embayment, Bense and Van Balen (2004) document differences in hydraulic head between different fault blocks. The area studied encompasses the lignite mines reported by Weber et al. (1978) where the original detailed observations of clay smear were made. The geologic and fault framework is derived from exposures in the open pit mines and numerous wellbores used to define coal distribution so some level of detail in the fault structure is expected to be missing from this extrapolation. In spite of this limitation, hydraulic head differences >100 m are interpreted across faults near open-pit mines where wells locally drop the local groundwater level in order to keep the mines dry. In some areas, though, the effects of the prominent clay smear are defeated by unbreached fault relays that enable fault-unhindered groundwater flow between fault blocks, albeit through a more restricted cross-section.

Results from the Bense and Van Balen (2004) work illustrate one difficulty in deducing fault flow properties from subsurface flow studies. In that work, they plot SGR-value against aquifer potential difference, from which they infer that SGR is related to fault permeability. However, this approach assumes that there are no holes in the clay gouge whose presence would dominate flow. If holes were present, the same pattern of hydraulic potential contours could be possible, even for the case of limited cross-fault flux (Fig. 32); in this example, fault flow (i.e. SGR) properties are constant, and the range in hydraulic potential difference is large.

In subsequent work in the Lower Rhine Embayment, Bense et al. (2008) document thermal anomalies, which they ascribe to vertical water flux. Spiller et al. (2004) similarly address vertical aquifer flux in the open-pit mines in the area and interpret a deep aquifer source based on temperature and water chemistry results. Although the geologic cross-section presented by Spiller et al. (2004) indicates potential flow paths back-and-forth across faults through juxtaposed permeable intervals, this kind of pathway is probably inadequate for producing thermal anomalies. Bense et al. (2008) appeal to high permeability along the fault dip, possibly resulting from sand lenses entrained within the fault zone. However, Spiller et al. (2004) infer erosion processes along the fault that create high permeability conduits, erosion that may be specific to the local environment of unlithified sediments and low stresses.

Ironically then, in the area where the clay smear process was first identified and documented, groundwater flow is influenced by an array of geologic processes and conditions, including fault relays and groundwater-induced erosion processes. These examples illustrate the difficulty in inverting flow responses for clay-smear properties alone without considering the potential impact of other processes that may also affect cross-fault flow. However, combining fluid potential data with independent temperature (Bense et al., 2008) and chemical tracer (Cilona et al., 2015) data help reduce the number of degrees of freedom in solutions, much as 4D seismic images help define the distribution and movement of

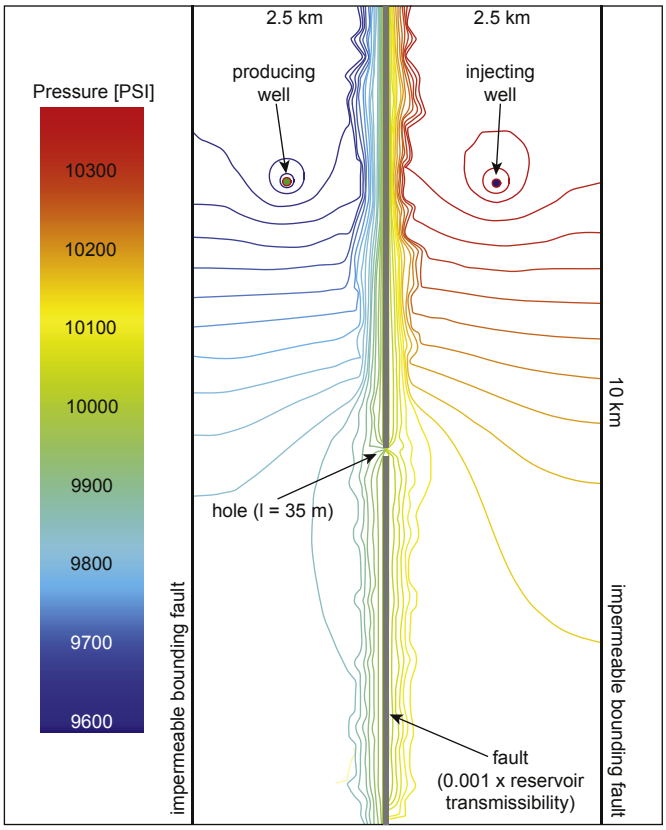


**Fig. 32.** Cross-fault flow simulation to illustrate complexities in deducing fault properties from general hydraulic data. Model includes closed, limited area (area of figure), bounding faults (vertical black lines extending vertically across figure representing no-flow boundaries), middle fault (middle line) with constant, limited transmissibility (0.001 × reservoir transmissibility) and 35 m long hole in middle of model, uniform reservoir properties (1000 mD and 0.79 m thick), producing well (left fault block) and injecting well (right fault block) maintaining mass balance (5000 bbl/day; 795 $m^3$/day). Resulting steady-state flow defined after 1 year of flow, and pressure contours (20 psi contour interval; 138 kPa interval). Small flux across fault results in tight clustering of contours along fault, but majority of flow along fault block and through hole in middle. Note that biggest pressure difference across fault defined between wells, and smallest pressure difference immediately adjacent hole, even though gouge permeability is constant.

different fluid types during gas, oil, and water production and injection.

### 3.3.7. Clay smear dilemma in subsurface studies

The problem with subsurface studies is that evidence of the presence of clay smear fails to establish that clay smear has a material impact on subsurface fluid flow; the observation of clay smear provides necessary but not sufficient information to reach this conclusion. Moreover, the failure to account for subsurface fluid distributions with simple juxtapositions (i.e. offsets along a single fault surface) is insufficient to deduce the presence and effect of clay smear. To illustrate this point further by specific example, two fault interpretation examples are presented from the Hibernia Field, Canada.

*3.3.7.1. Hibernia background.* The Hibernia Field is a large oil and gas field on the Grand Banks offshore Eastern Canada (Mackay and Tankard, 1990). It is well suited for evaluating problems of cross-fault fluid flow because the field is heavily faulted (two near-orthogonal fault strike orientations interpreted to have formed in the Cretaceous; Sinclair et al., 1999), and the Cretaceous braided fluvial reservoir varies on a scale that is much larger than a fault block (i.e. local fault problems are evaluated with high confidence in the stratigraphic distribution because of the interpreted stratigraphic continuity). Faults with offsets larger than the reservoir thickness result in separation of gas, oil, and water fluids, and faults with smaller offsets result in fluid continuity across the fault. Even though the reservoir is heavily faulted, gas, oil, and water fluids communicate where the geometric juxtaposition of permeable reservoir intervals permit that communication. Faults between permeable intervals rarely prevent cross-fault flow but rather serve to hinder or re-direct it.

Cross-fault fluid continuity is defined as the same original, pre-production fluid pressure in the same fluid type at the same depth on either side of a fault (i.e. no capillary membrane seal), even though that connectivity may be established via a long meandering pathway through multiple fault blocks. For fault blocks sharing the same initial conditions, the question becomes whether those juxtaposition connections are sufficient for allowing pressure communication during production (i.e. are rates of cross-fault flow significant?). There is substantial evidence for cross-fault fluid connectivity during production in Hibernia based on: (1) deviations of fluid pressure from original pressure conditions in undeveloped fault blocks as a result of production or injection of fluids in adjacent fault blocks; and (2) interpretation of cross-fault fluid flux necessary to account for mass balance constraints invoked in reservoir simulation. The production data suggest that where porous and permeable reservoir sandstones exist, cross-fault flow is common.

However, two significant exceptions to these generalizations are known, and they are instructive for considering the uniqueness of geologic interpretations for clay smear calibrations. Here we can address the following questions: Does clay smear form in these locations? Is it continuous? Are there other mechanisms for separating permeable sandstones?

*3.3.7.2. Oil column separation – clay-smear or complex faulting?.* In 2011 a well was drilled into an untested fault block in the southern part of the field. This fault block is at the junction of two independent oil columns (i.e. oil columns with different original pressures at the same elevation) – a higher pressure oil column documented to the east, and a lower pressure oil column to the west (Fig. 33). The question was which oil column defined the pressures in the untested fault block, and what geologic interpretation would yield a successful prediction? A range of pre-drill scenarios were defined that separated the oils along a fault on the western side and eastern side of the fault block to be drilled, but here we focus on the interpretations on the W-bounding fault.

Seismic profiles across down-dip portions of the W-bounding fault suggest there should be a geometric connection between permeable intervals in this reservoir section that should allow the western, lower pressure oil to communicate across this fault (Fig. 34). The sandstone-rich nature of the faulted section results in low SGR values for all plausible offsets up to full reservoir separation (Fig. 35) with calculated SGR values < 0.2. Such low SGR values occur elsewhere in the field for the same Layer 3 juxtapositions and are associated with cross-fault flow during production, so it is unlikely that a similar SGR value should produce a capillary seal here (Table 5).

Further complicating matters is the observation along the updip section of the W-bounding fault where reservoir separation is interpreted by a complex intersection fault geometry imaged in the seismic data (Fig. 36). In these sections a W-dipping fault is cut by the primary E-dipping fault with the result that the apparent offset across the entire fault zone appears minimal while in fact the offset on the E-dipping fault creates a juxtaposition seal with younger

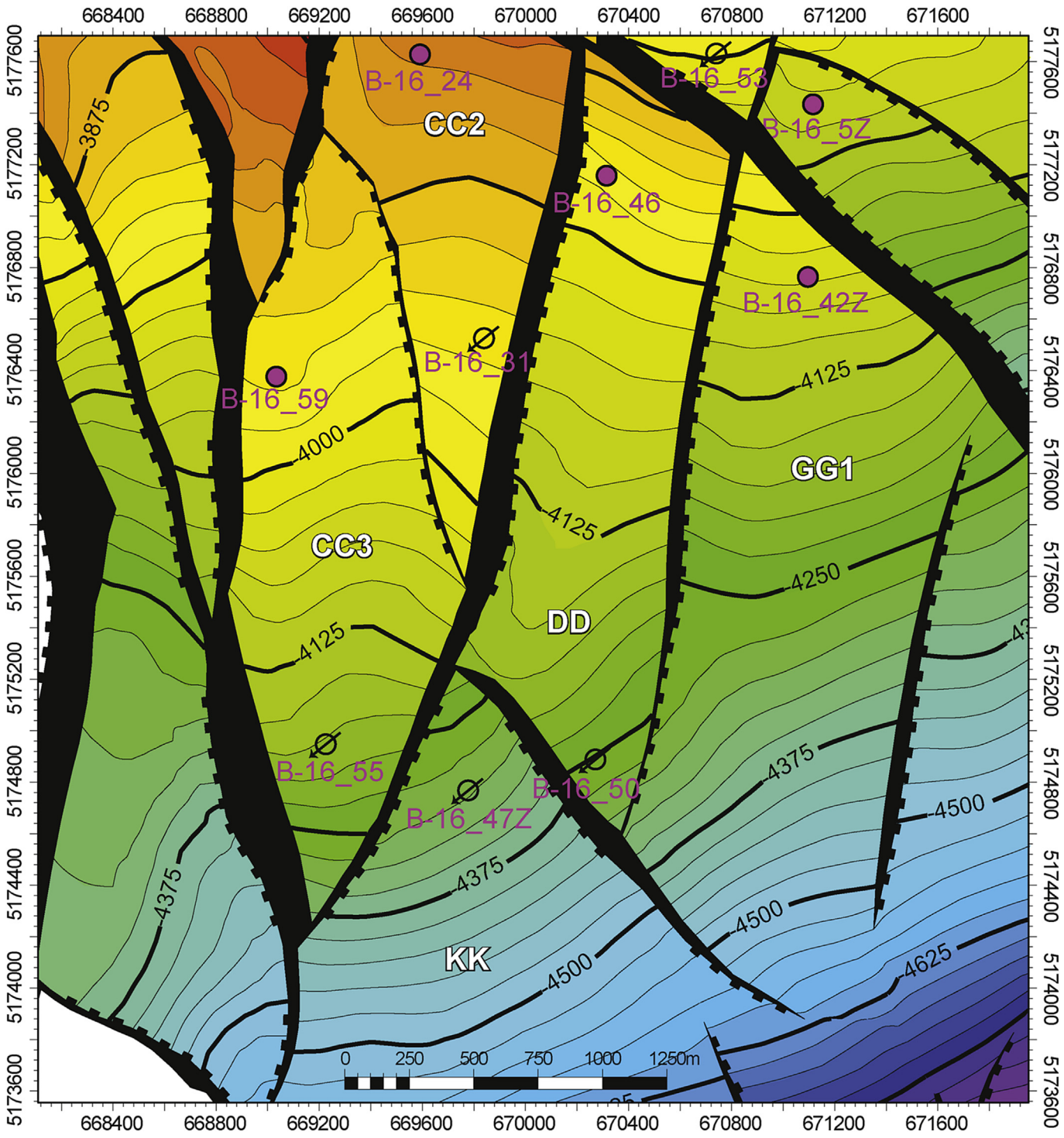


**Fig. 33.** Depth-structure map of southern portion of Hibernia Field, offshore Eastern Canada. Map shows fault blocks on west (CC 2 & CC3) that define lower pressure oil column (at specified depth) than fault blocks further to east (DD). Geologic problem involves accounting for oil pressure properties observed by drilling into KK-fault block. Note that hanging wall (downthrown) block on each fault depicted by fault-teeth symbols. Warm colors are shallower than cool colors, and contour labels in meters below sea level; filled circles are oil producing wells, and open circles with arrows are water injection wells.

shales. The offset on the E-dipping fault is compensated by the older W-dipping fault with the result that an additional juxtaposition seal is created by insertion of an older shale interval.

In down-dip sections only the E-dipping fault is recognizable in the seismic data, and the apparent offset remains minimal. However, given the complexity of the geology and the seismic resolution available at a depth >4500 m, an additional plausible interpretation involves maintaining the W-dipping fault geometry observed up-dip, even though the seismic data fail to require that interpretation, with the result that same top- and base-seal juxtapositions are maintained (Fig. 36). Note that the interpretation presented in Fig. 36b is non-unique, which it must be for an interpretation under-constrained by data. Indeed the seismic data also allow a more complicated interpretation than the one shown, especially for

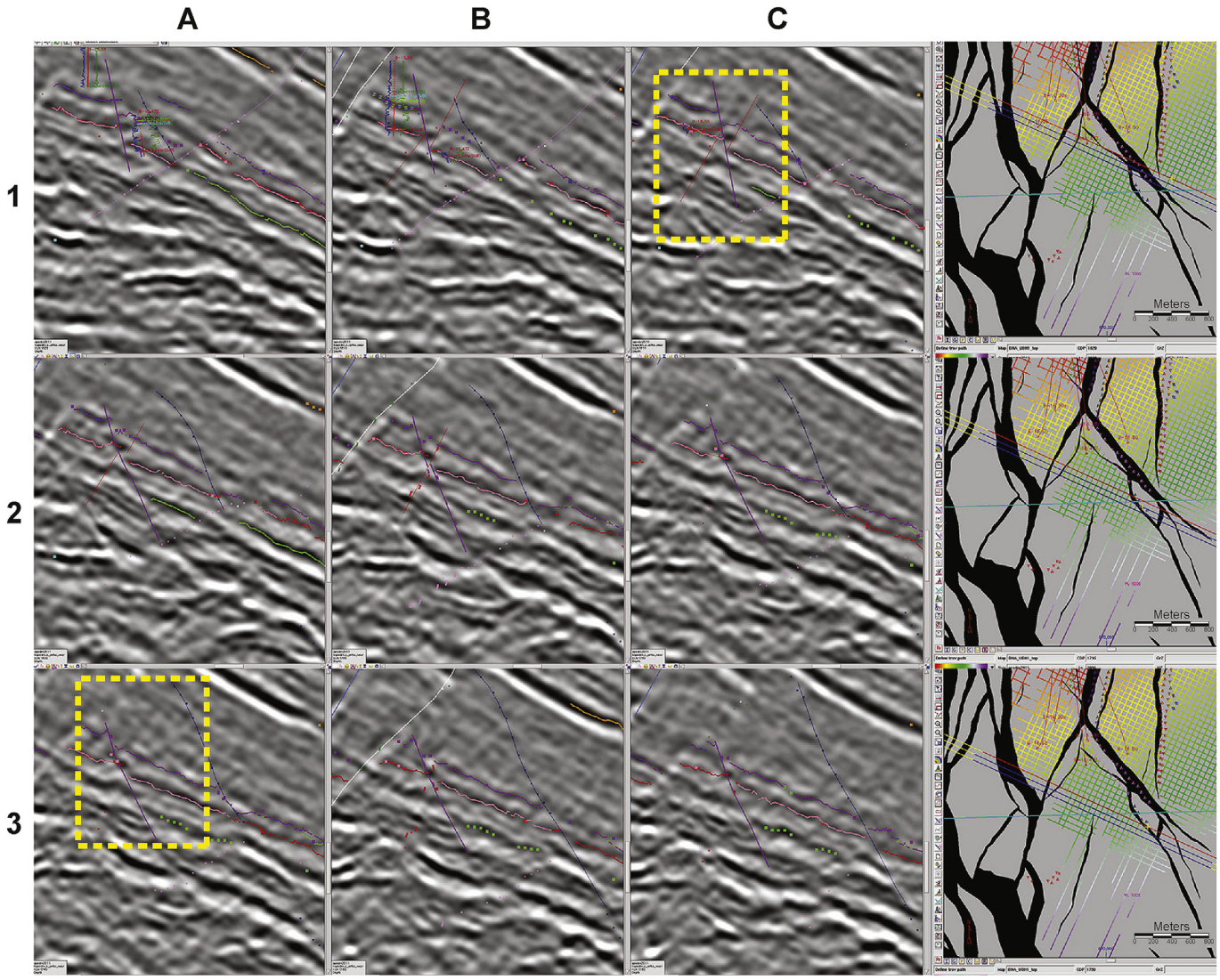


**Fig. 34.** Serial seismic profiles across fault that separates CC3 and KK fault blocks. Seismic profiles progress from north (upper left corner: A1) to south (lower right corner: C3). Each row of 3 profiles correspond to blue and red lines (oriented WNW-ESE) in map at end of row (A to C = N to S). Note how E-dipping purple fault has little displacement, especially in the last row of profiles where imaging is compromised, in part, by fault shadowing effects beneath white fault. Reservoir interval contained between purple and red/pink horizons. Seismic data outlined in yellow boxes shown in Fig. 36.

faults that are closer to being synchronous (e.g., mutually offsetting synthetic and anthithetic faults).

Oil pressures measured in the drilled well were the same as those in fault blocks to the east, indicating that the W-bounding fault was responsible for separating oil columns. In this example we conclude that the observed oil separation is unlikely for juxtaposition seal on a simple fault surface, unlikely for a capillary clay smear, and thus more likely for the complex cross-cutting fault pattern observed updip in the seismic data. Note that if we had failed to observe this fault complexity, we might have been tempted to interpret a clay smear capillary-seal at an anomalously low SGR value.

*3.3.7.3. Water trapped above oil – fault lens-enclosed shale?.* In our clay smear definition, we include both the high shear-strain clay that accommodates significant fault offset and stratigraphically coherent lenses of shale that exist as part of the clay smear fault structure. This example further develops the idea that shale lenses may contribute to capillary seals in the sense of Berg and Avery (1995).

In 2011 another well was drilled into the Hibernia reservoir and encountered water in the midst of a thick oil column; the well documented an oil-water contact, and another well structurally down-dip in the next fault block previously documented oil (Fig. 37). Both oil occurrences are interpreted to be parts of the same continuous oil column in original pressure communication (pressures in the 2011 well were perturbed by production, which is why this is an interpretation rather than an observation), and the seismic data (Fig. 38) indicate a Layer 2–3 juxtaposition connection for a simple fault surface interpretation with no evidence for a complex antithetic fault as in the previous example (notwithstanding the fact that an antithetic fault would like be unable to create a juxtaposition seal in this part of the stratigraphic section). As in the previous example, the reservoir Layer 2–3 fault juxtaposition connection that traps water in the up-dip fault block (Fig. 38) is similarly associated with extensive pressure and fluid communication elsewhere in the field (Table 6), and so the automatic deduction of a clay smear capillary seal is difficult based on conflicting evidence.

Although faulting of the Medial Shale unit, a continuous marine

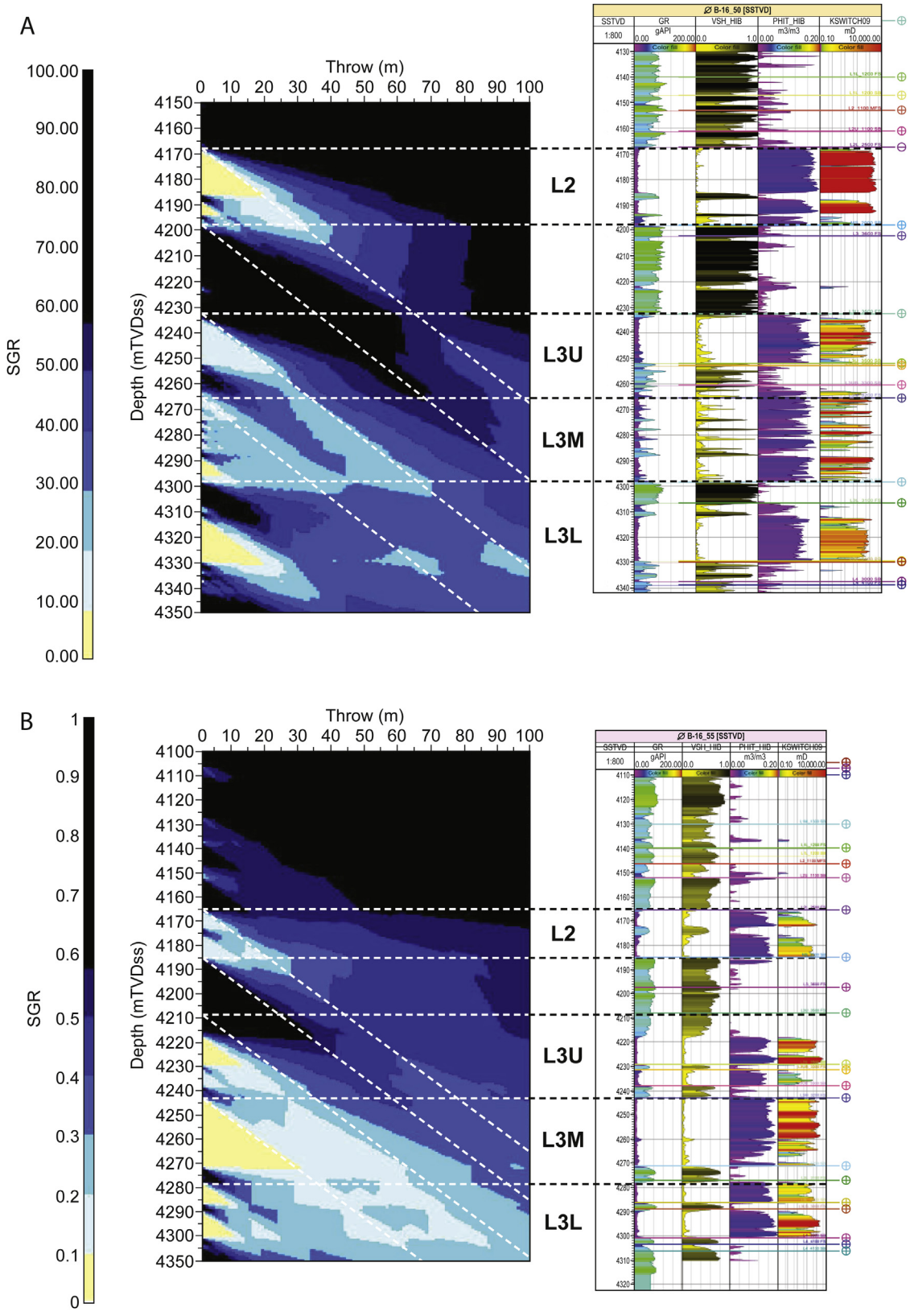


**Fig. 35.** Well log representation of offset reservoir stratigraphy, including calculated SGR values for fault throws up to full reservoir offset. Note that sandstone-rich nature of Layer 3 limits value of SGR calculated, resulting in inference of SGR value no greater than 0.35–0.38 in (A) and <0.2 for the same L3U/L3L juxtapositions in (B); L2 = Layer 2, L3U = Layer 3 Upper, L3M = Layer 3 Middle, L3L = Layer 3 Lower. Although these wells are bound and are separated by <500 m from fault of interest (Fig. 33), subtle differences in stratigraphy yield some fairly significant differences in SGR calculation and resulting inference of capillary-sealing versus leaking for same critical SGR value (e.g., 0.2) depending upon precise stratigraphic development of L3M.

**Table 5**
Summary of layer 3 juxtaposition properties.

| Layer 3 reservoir connections | Pre-production pressure connection | Neighboring pressure disturbance | Significant mass flow to neighbor |
|---|---|---|---|
| KK-CC blocks | No | No | No |
| Rest of field | Yes | Yes | Yes |

shale interval that separates the Layer 2 and 3 reservoirs, results in higher calculated SGR values than in the Layer 3 self-juxtaposition example above (Fig. 39), most other Layer 2–3 juxtapositions allow production time-scale pressure communication. However, the Medial Shale unit is comparable in thickness to the Layer 2 reservoir interval, and it is feasible to interpret a fault lens containing the Medial Shale between the Layer 2 and 3 reservoirs as a juxtaposition seal based on incorporation of a structurally coherent shale lens in the fault zone (Fig. 38), but a shale lens incorporated as part of clay smear processes.

How does a fault lens component of a clay smear interpretation satisfy the argument of conflicting observations for the same SGR? For this we assert that SGR is a poor predictor of the development of fault lenses (Noorsalehi-Garakani et al., 2013). Next, we conclude that fault lenses have limited lateral extent (e.g., Noorsalehi-Garakani et al., 2013). Then we observe that the fault separating water and oil is among the shortest fault-block segments in the field and deduce that all other fault segments are longer than any similar fault lenses that may be developed on those faults. Accepting that this interpretation is correct because alternative interpretations are excluded based on lack of evidence or conflicting observations, we then find evidence that the mechanics of clay smear processes are critical for predicting when shale-filled lenses will form. It also becomes crucial to know how long lenses can be because this defines which fault segments are candidates for this prediction.

These two examples illustrate the fact that complex fault geometries are a third alternative to simple juxtaposition and SGR-based clay smear predictions. Any clay smear calibration studies that have been undertaken without considering the potential for complex fault geometries to contribute to cross-fault flow must be viewed with caution. The clay-smear, fault-lens interpretation is a strong motivator for including a clay-smear mechanics component in prediction models.

### 3.3.8. *Summary of subsurface field studies*

Clay smear is interpreted to hinder cross-fault flow in many different field studies. Although clay smear was originally conceived of as a capillary, membrane seal, its impact on throttling the flux of fluids across faults in the presence of a fluid potential

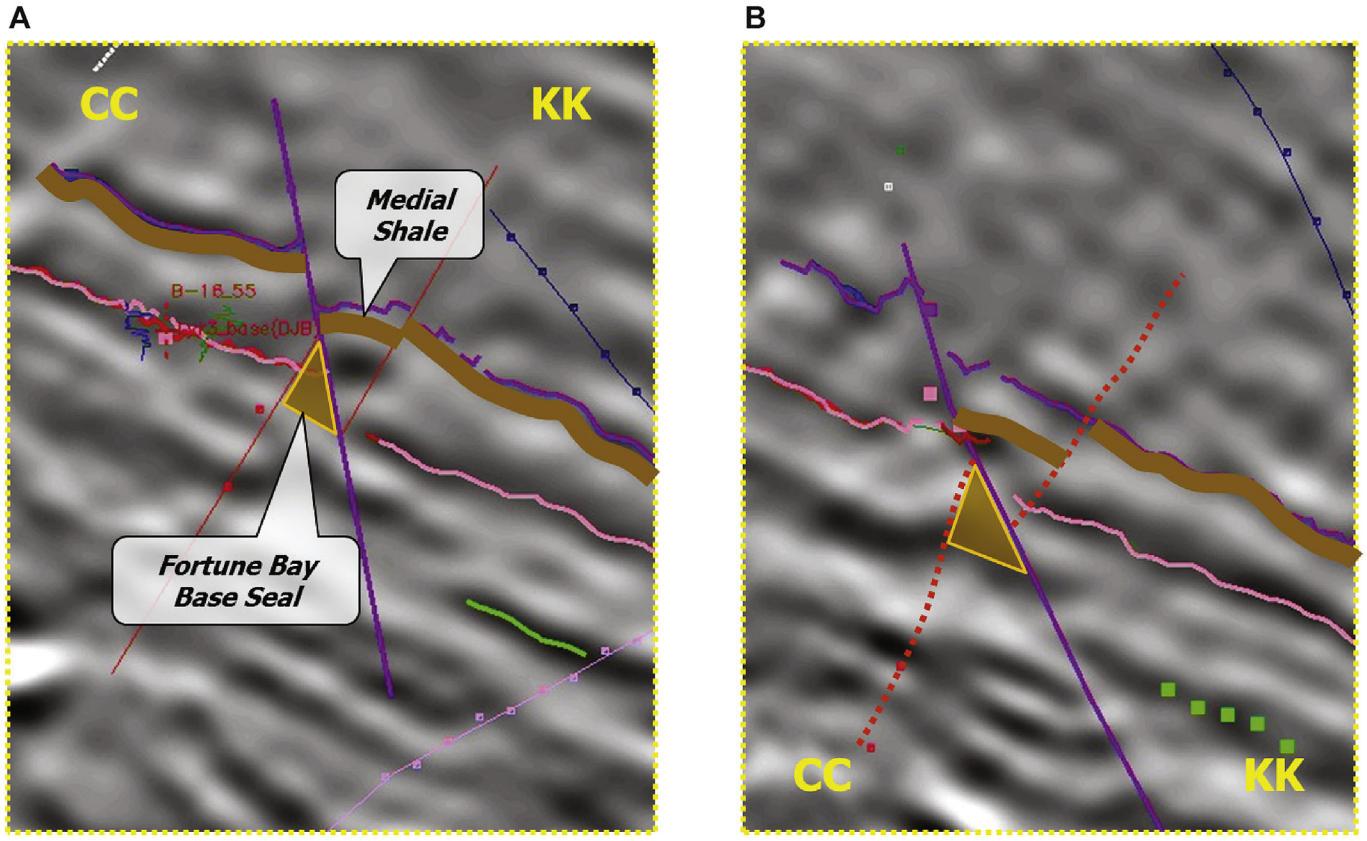


**Fig. 36.** Close-up views of up-dip and down-dip seismic profiles highlighted in yellow boxes in Fig. 34 (width of view approximately 1 km). In up-dip profile (A), W-dipping fault intersects E-dipping fault within reservoir sequence and creates downward displacement of top-seal wedge and upward displacement of base-seal wedge relative to reservoir interval on both sides of fault system, which appears to have minimal offset across this system, although fault throw on each segment is significant. In down-dip section (B), W-dipping fault is no longer evident in seismic data even though horizon offset across entire fault system is minimal. Speculative extrapolation of W-dipping fault is shown with dotted fault interpretation and maintains juxtaposition seal geometries interpreted in up-dip profile. Medial shale is marine shale associated with Maximum Flooding Surface below Layer 2 and above thick shale-rich interval at top of Layer 3U (Fig. 35). Fortune Bay Base Seal is shale interval below oldest reservoir interval that supports large pressure difference with underlying Jeanne d'Arc units.

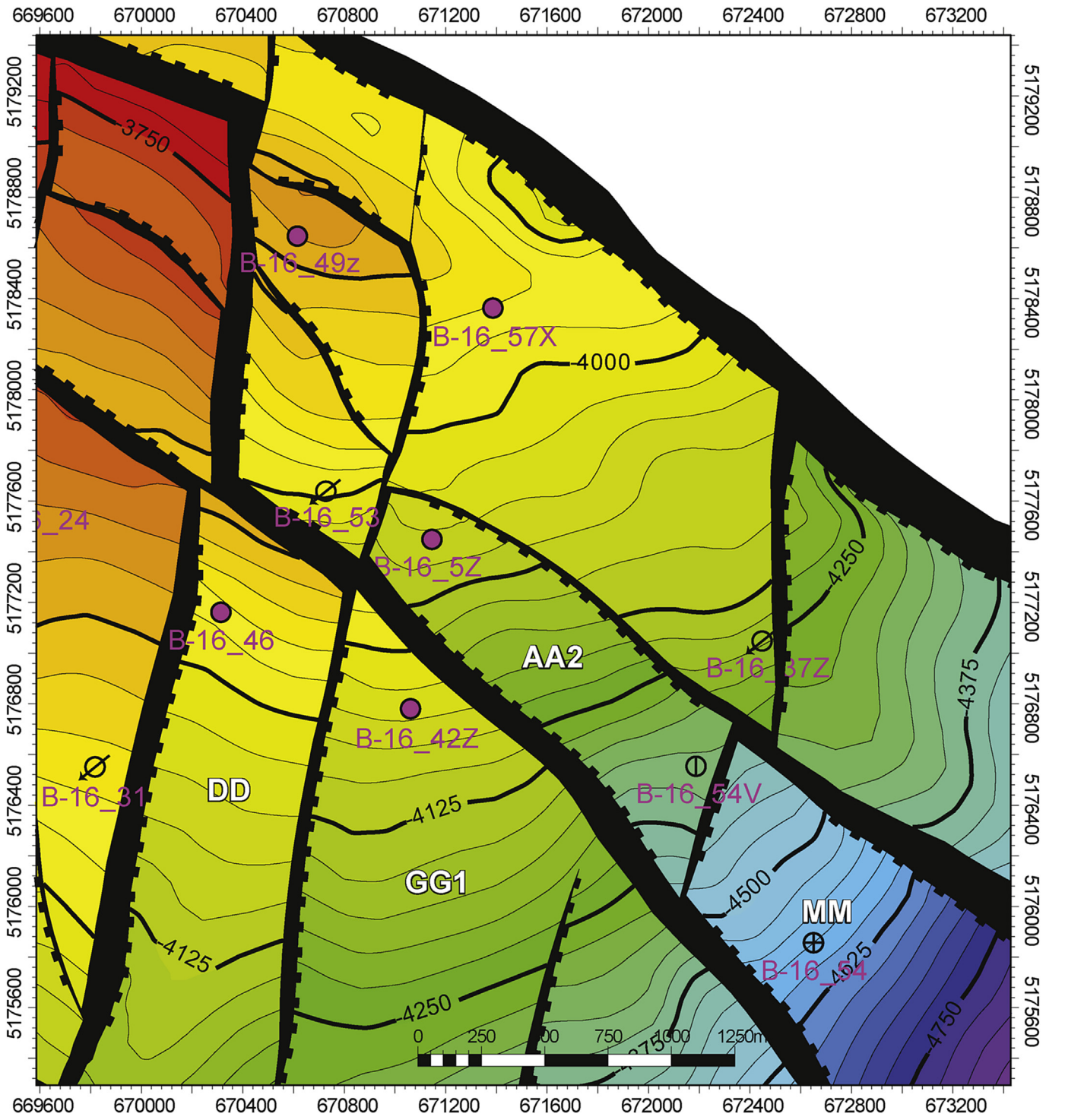


**Fig. 37.** Depth-structure map of southern portion of Hibernia Field, offshore Eastern Canada. Map shows up-dip fault block (AA2) that contains thick interval of water above oil observed down-dip in MM fault block (interpreted original pressure communication). Fault offset with GG1-block is enough to create full separation of reservoir intervals, but AA2-MM fault offset is too small.

difference (i.e. production flow) was also appreciated early on. Much of the literature on the application of clay smear processes is derived from Tertiary deltaic sedimentary systems where rocks are often underconsolidated and the stratigraphic continuity of intervals up to faults where fault juxtaposition diagrams are created may be open to alternative interpretations. Moreover, although disturbed juxtaposition relations that arise from non-planar fault structures have been recognized, there is no coherent strategy for accounting for this complexity.

We think it is hard to gain meaningful insights into clay smear processes based on the types of field studies to date (Table 7). Although there is a considerable literature that addresses clay smear as a capillary seal, the interpretation of a continuous clay smear without the sparse holes described by Wehr et al. (2000),

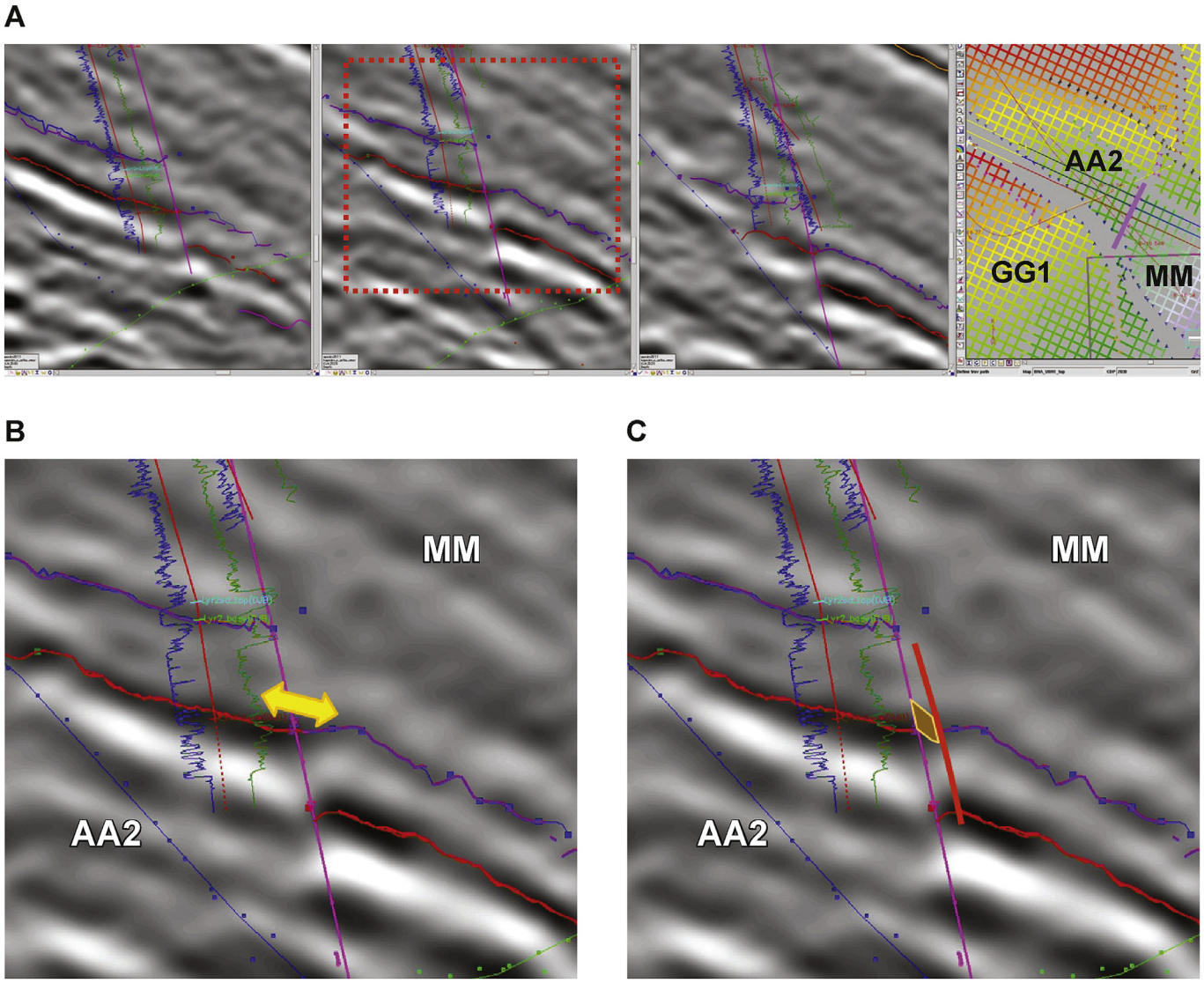


**Fig. 38.** (A) Series of 3 seismic profiles crossing fault separating AA2 (up-dip) and MM (down-dip) fault blocks. Position of lines shown on map at end of row with profiles progressing from N (left) to S (right). Width of profiles approximately 2.4 km; no vertical exaggeration. (B) Blow-up of middle profile (inside dotted red box). Red curve that parallels pink fault interpretation is path of well bore in down-dip portion of AA2 fault block. Adjacent blue curve is gamma-ray curve taken in well; shale intervals identified by parts of curve closest to wellbore curve, and sandstone intervals by those farthest from wellbore curve. Green curve on right side of wellbore is resistivity curve; in sandstone intervals high resistivity (green curve farthest from wellbore curve) intervals represent oil and low resistivity (green curve close to wellbore curve) represents water. Note that for thick section of sandstone (blue curve) between purple and red horizons, resistivity indicates water with minor interpretations that a bit of oil exists at top but much of interval contains water in spite of Layer 2–3 juxtaposition (yellow arrow). Layer 2 reservoir interval lies above purple horizon interpretation. (C) Speculative fault relay or lens introduces wedge of Medial Shale (brown polygon outlined in yellow) displaced short distance from hanging wall but enough to occlude Layer 2–3 juxtaposition.

especially in light of data and interpretation uncertainties, seems difficult to achieve. Although there are no doubt examples in nature where clay smear has created a capillary seal to oil and gas, it is difficult to specify which faults achieve a continuous clay smear from the perspective of reproducibility embodied in the scientific method.

Most studies remain under-constrained (Table 4), but the integrated simulation studies (Jolley et al., 2007; Myers et al., 2007) begin to define more detailed information about fault zone properties (Table 4), especially when constructed from first-principles geologic models (i.e. models in which various fault geometries and properties are defined as an input). The logical continuation of this approach is to make specific geologic and flow predictions and then drill wells, collect and analyze samples, and perform specific flow experiments to test those models. Aquifer studies (Table 7) offer additional insights on cross-fault flow if only because nearby

**Table 6**
Summary of layer 2–3 juxtaposition properties.

| Layer 2–3 reservoir connections | Pre-production pressure connection | Neighboring pressure disturbance | Significant mass flow to neighbor |
|---|---|---|---|
| AA2-MM blocks | No – water[a] | Unknown | No – water[a] |
| Rest of field | Yes | Yes | Yes |

[a] Can only be established for water phase encountered in well; no compelling evidence to conclude that original oil pressure communication or subsequent oil flux occurs along upper part of fault where oil is found on both sides of fault or via some alternative path of fault connections.

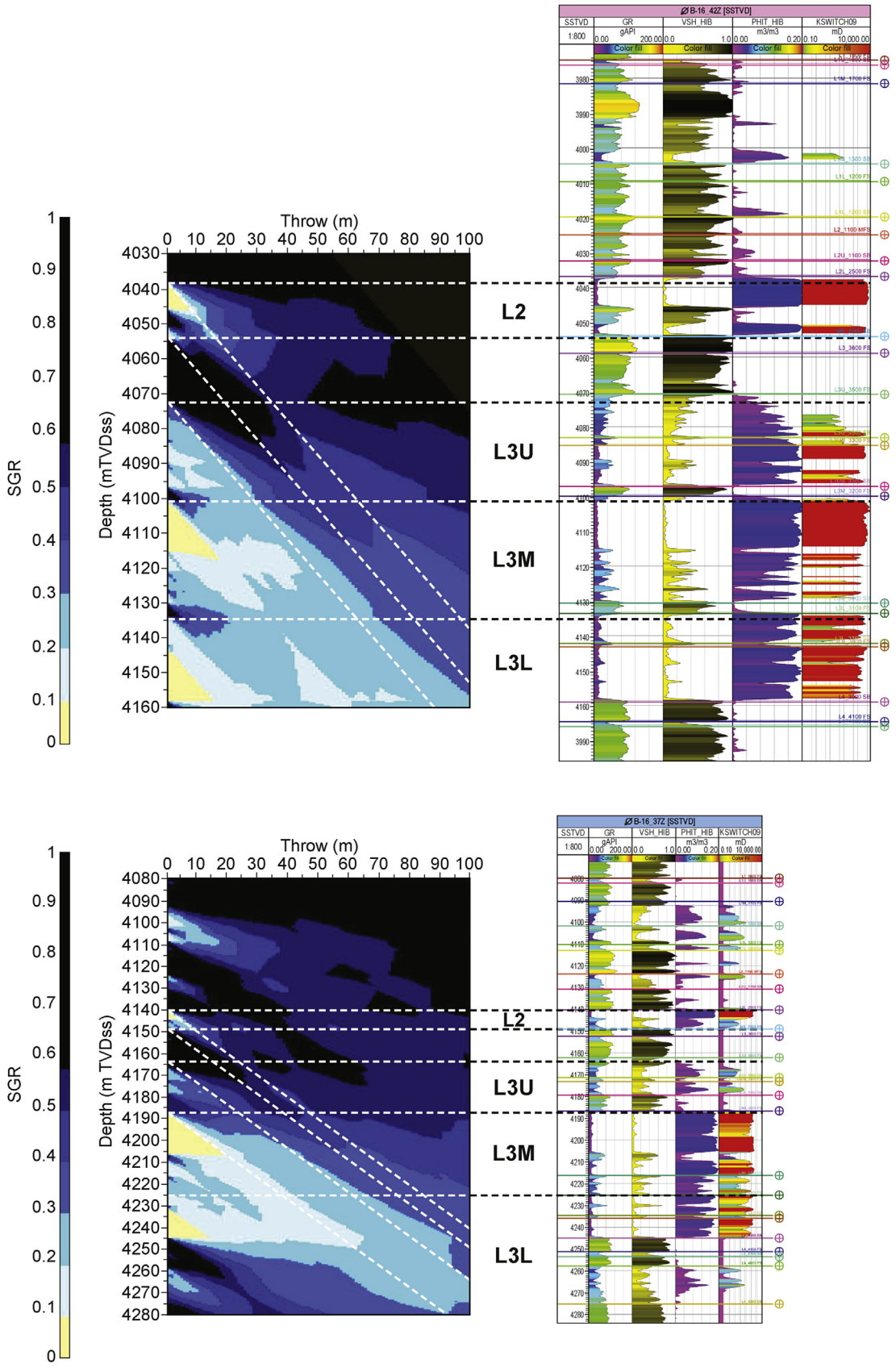


**Fig. 39.** Well log representation of offset reservoir stratigraphy, including calculated SGR values for fault throws up to full reservoir offset. Note that SGR values increase as L2 is increasingly offset to progressively juxtapose L3U, L3M, and L3L, with SGR values decreasing from 0.55 to 0.36; L2 = Layer 2, L3U = Layer 3 Upper, L3M = Layer 3 Middle, L3L = Layer 3 Lower. In this instance there is little difference between SGR values calculated for two closest wells; both well results are dominated by relatively shaley development of L3U interval. Note that for capillary seal required by seismic data in Fig. 38, SGR values are lowest. Applying 'typical' threshold SGR value of 0.2 for creation of capillary seal, though, contradicts observations of production-scale pressure depletion elsewhere in field across same kind of juxtaposition connection and for similar stratigraphic development (NB both cross-fault pressure depletion and build-up above original pressure observed for pressure-maintained oil production via both gas and water injection).

**Table 7**
Rating summary of subsurface studies and clay smear.

| Contribution | Understanding | Comments |
|---|---|---|
| Capillary seal | ✪✪✪✪✪ | Although claimed in the literature, uncertainty evaluation and consideration of alternative interpretations left largely under-explored; interpretation reproducibility limited; presence of clay smear largely untested by independent core samples |
| Permeability reduction in oil & gas flow | ✪✪✪✪✪ | Same limitations as for capillary seal; production data used in history-match analysis offers more definitive but non-unique data constraints; tested in full 3D models that help enforce internal interpretation consistency |
| Permeability reduction – aquifer flow | ✪✪✪✪✪ | Same limitations as for capillary seal; less sub-surface definition than for oil & gas flow and more restricted data constraints (changes in potential surface); better integration of surface outcrop data possible |
| Fault mechanisms responsible | ✪✪✪✪✪ | Subsurface studies focus on the flow effects of clay smear and offer few insights into the processes that generate clay smear; effects of geometric ambiguities recognized, but data resolution often prevents independent evaluation of those geometries |

Note: Star rating reflects score (red stars) out of maximum potential score (blue stars).

outcrops offer relevant information about aquifer properties in the sub-surface. However, the subsurface aquifer definition is poorer than in oil and gas fields, and the history-matching approach seems less well developed. The aquifer environment offers the opportunity for inexpensive diagnostic cross-fault flow tests because well costs are comparatively cheap.

Subsurface field studies offer little about the mechanics of the clay smear process – how clays are incorporated into a fault zone, how they are deformed once between the shear zone boundaries, and how clay smears develop holes. Core analyses in subsurface studies offer confirmation for the existence of clay smear but the scale of these samples hinders further interpretation. In the end subsurface studies are essential for testing clay smear models developed elsewhere, but to do so requires public disclosure of a comprehensive dataset, including all raw data to insure interpretation reproducibility, and the application of well-conceived cross-fault flow tests designed to test and differentiate clay smear models. There is no more effective means to interrogate the geometry and continuity of clay smear products in a fault zone than with subsurface flow studies, and current approaches can be useful for addressing questions of reservoir compartmentalization, but advances in understanding will require more definitive subsurface tests.

### 3.4. Discussion and synthesis from laboratory to subsurface

We have shown in this review that clay smear is much more than the weighted average of a faulted lithologic section. Rather, it is the ensemble of fault structures that develop during fault evolution. That ensemble is the result of the deformation regime during faulting, the mechanical properties of the faulted rocks, the effective stress, the geometric evolution of the fault network, and the lithology of the faulted section. In addition, mineral reaction and recrystallization processes are possible but have remained outside the clay smear context. When considering the effects of clay smear on subsurface flow problems, the single most important fault structures are the holes in the gouge. Therefore, even if all other aspects of the clay smear process are fully understood, predicted flow properties will remain uncertain if our understanding of how holes form remains incomplete.

Although we consider faults in this review that rarely have offsets greater than a hundred meters, the complexity is already enormous and diverse. Thus research into the clay smear problem for the purpose of improving subsurface flow predictions has also yielded important insights into fault localization phenomena. Exchange with other applications like earthquake studies is seen as promising, but those associations have yet to be fully developed.

In this section we synthesize insights across the three areas we developed in this paper: Outcrop Studies, Laboratory and Numerical Modeling Studies, and Subsurface Studies. We seek to better define what 'clay smear' is, trying to remain faithful to the history of the subject, providing a terminology framework useful for future studies, and thereby reducing potential confusion. We then step back and evaluate how deep we think our understanding has reached into the various processes that create clay smear. In a complementary evaluation, we summarize our knowledge of how clay smear has affected subsurface fluid flow, leading to the question of how effective current predictive models are. On the basis of these evaluations, we then conclude with a section that describes how we think future advancements will arise.

#### 3.4.1. What is clay smear?

'Clay smear is a loosely defined term born in hydrocarbon geology; its usage differs between publications, and the definition of processes operating is often unclear. In the most general meaning, the term includes all processes, which somehow transform clay in the wall rock into clay that is part of the fault zone' (van der Zee et al., 2003). More than a decade after this perspective was given, we think this assessment is still correct.

Therefore clay smear, although sometimes referred to as a process, is better considered encompassing a multitude of fault processes that combine and interact in various fashions to create a myriad of fault structures, some of which collectively define a clay smear. Clay smear is an umbrella term for a series of fault processes, and similarly a term that includes many different fault structures. Thus we use the term 'clay smear' when it is efficient for referring to a collection of processes and structures but then rely upon the more detailed and explicit terms (e.g., abrasion, shear, and layered gouge) included beneath the umbrella term to achieve better insight into the problem.

Processes associated with clay smear reflect the evolution of a fault propagating through a mechanically heterogeneous sedimentary section. There are many different paths available for this evolution, resulting in the rich diversity of structures described in the literature. At its root, incipient clay smear is a fault localization phenomenon combined with reworking in high shear strain in the fault zone.

Lastly, although there is a temptation to focus the attention of the clay smear processes onto the high shear strain component of the fault zone, the available outcrop and experimental observations illustrate the crucial importance and ephemeral nature of structurally coherent lenses of sandstone, limestone, and in particular shale for the overall fault zone structure. The creation of shale-rich fault lenses is an integral part of the clay smear process, especially for considering the cross-fault flow problem and as a source of clay-rich material available to promote localization with increasing fault offset.

In the final analysis, clay smear is a special case of multiple fault processes and structures that arise when a faulted section contains mudstones and shales. It encompasses the presence and distribution, geometry and continuity of the deformed and faulted

lithologies. In outcrop studies without mudstones or shales similar fault structures are found, and in the experimental section arguments were developed to build a clay smear process model based on localization models developed in pure sand systems.

*3.4.2. How deep is our understanding of fault processes that result in clay smear?*

From our review of available outcrop studies and complementary laboratory and numerical experiments, we conclude that the development of clay smear depends on three components:

1) how much clay exists in the faulted section
2) the geomechanical properties of the faulted lithologies defined in relation to:
   a) in-situ effective stress (i.e. brittleness)
   b) geometric evolution of fault system

These components have many complicated feedbacks, and different domains of processes arise out of these interactions.

The results of experimental and numerical simulations of fault processes, outcrop observations, and subsurface studies are very different windows into the clay smear phenomenon, and we face hurdles in relating the results from one area of investigation to another. For example, in the experimental section we discussed the limitations of grain size in experiments and grid size in simulations and the issues associated with scaling processes to natural dimensions. The boundary conditions in existing experimental and numerical simulations of clay smear processes are strongly influenced by the need to produce a large shear in a small model. Many boundary conditions in nature are unattainable in simulation. Conversely, outcrops lack the height and width needed to completely examine a faulted layer and the incremental strain history necessary to relate a series of final structures to the initial boundary conditions and subsequent fault evolution; process is an interpretation rather than an observation in this environment. And subsurface studies, which through the fluid flow problem allow us to interrogate complete fault zones, lack the detailed resolution necessary to observe the critical fault structures.

We find it useful to think of the deformation domains defined in experimental studies because they provide the means to relate a group of distinguishing processes in a domain to a series of diagnostic fault structures (Fig. 27). What makes this approach appealing is that the deformation behavior of sand and shale components is a consequence of material properties, stress conditions during faulting, and the previous stress history of the materials. In other words, weak clay deformed at low stress can deform by the same processes and result in the same diagnostic structures as stronger clay deformed at higher effective stresses. We arrive at this understanding as a result of observing clay fragments formed by extensional fractures at a propagating fault tip and then 'flowing' in the fault zone as a result of that same clay deforming in critical state (degree of softening depending on initial cementation). Although these deformation domains provide a highly simplified framework, it is nonetheless useful as a starting point for incorporating the mechanics of deformation into clay smear predictions, which currently lack any input from this perspective.

Fault geometric evolution plays a crucial role in early fault zone development and is as important a consideration for clay smear evolution as the geomechanical aspects described above. In outcrops and experiments we observe fault zones with clay smear associated with multiple slip surfaces (zones of localization), and laboratory and numerical experiments demonstrate both a discontinuous (or continuous) migration of localized shearing through the material and simultaneous displacement on multiple localizations. Moreover, the evolution of fault relays and lenses has a profound effect on how clay is incorporated into the fault zone and how it deforms once it is within the fault zone (e.g., reworking of coherent fragments in fault lenses). Fundamental questions like what controls the migration of deformation into the footwall versus hanging wall as the fault zone evolves and what determines the total number of slip surfaces (deformation bands) that develop have an important effect on the final clay smear structure.

Unfortunately, our understanding of the geometry of early localization is limited. Some insights are provided by models of a basement fault that propagates into a sedimentary section (Nollet et al., 2012), and outcrop observations show fault relay and lens structures resulting from different stratigraphic stacking patterns (Vrolijk et al., 2005b). Moreover, there is information about geometric processes like tipline bifurcation (e.g., Childs et al., 2007) at our disposal, but the means to know when to consider these geometric processes is lacking. There is a consensus in the literature that large contrasts in strength between adjacent intervals lead to wider and more complex fault zones, especially when one of the layers fails in extension. But understanding how a fault zone propagates in 3D through a mechanically layered package is still limited, even though this insight is required for understanding how clay smear develops in this fault.

Interestingly, perhaps our greatest deficiency in understanding clay smear processes is in the one aspect most important for evaluating subsurface flow problems – the creation of holes in the clay smear structure. Holes are made sometimes in experiments, but we rarely observe how they emerge. They are rarely described in outcrop, and when they are the structures associated with them are poorly described. Underlying this quandary is the model proposed by Weber et al. (1978) that holes form as the result of attenuation and only once the clay smear has been offset significantly from its source bed. However, we now recognize that holes form at the source clay bed if the clay is incorporated via a brittle fragmentation process (shear or tensile failure). This process is reflected in no current shale smear algorithm other than the probabilistic shale smear methods, but this realization introduces a whole new perspective on the flow problem – clay smears can improve with displacement if an initial shale fragment associated with a continuous sand pathway across the fault becomes reworked into a clay smear.

With existing observations and incorporation of geomechanical principles, there are some generalizations that help guide us to the conditions that favor hole formation. For example, a wider fault zone (for the same throw) has a higher chance for continuous clay gouge, (once the sand layers are disrupted by boudinage processes), especially in the low mechanical contrast case (failure of both lithologies in shear). Alternatively in the strong contrast case (i.e. clay failing in extension and sand in shear), a wider fault zone may cause the clay continuity to decrease because the ability of a clay fragment to become reworked in a critical state may be reduced in a wider fault zone.

The role of secondary fault structures like Riedel shears has also been associated with the potential for holes, and this effect is likely enhanced when the clay smear is thin relative to the shear zone thickness and Riedels are formed at high angles to the smear. Are there conditions that favor the development of Riedels, and if so, at what orientation? An interesting and consistent observation is the absence of taper in clay gouge away from the source layer, both in outcrops and in models. Rather, the persistence of clay smear thickness is associated with erosion of the clay source bed and continuous addition of clay.

It is also worth remembering that although clay and other mineral reactions are important in other fault settings, they are typically excluded from consideration in clay smear studies. Pressure solution of quartz, feldspar, and carbonate grains and

clay recrystallization are common in some of the systems considered in this paper and are manifested by enhanced softening of fault zone materials. Moreover, these chemical and mineralogical processes can influence the amount of clay found in a fault zone.

Moreover, we think our understanding could benefit from greater collaboration with related fields. For example, there are opportunities for cross fertilization between clay smear research and the part of the rock mechanics community concerned with containment assurance and fault reactivation prediction. Brittleness, dilatancy, and resealing by reworking in faults has been recognized and is becoming more important in many different rock mechanics applications – a few examples of relevant papers are Olgaard et al. (1997), Ingram and Urai (1999), Ishii et al. (2011), Schulz et al. (2014), and Bourne et al. (2014). There is a potential for incorporating better predictors for shale strength and brittleness that have been developed in recent years into improved mechanical clay smear calculations (e.g., van der Zee and Urai, 2005; Kleine Vennekate, 2013). On the other hand, containment and reactivation studies often use highly simplified models of the fault zones under consideration, and the concepts reviewed in this paper can provide improved fault zone models for these calculations.

Perhaps even more surprising is the potential for cross fertilization between the clay smear community and those concerned with studies of fault gouge interpreted to have formed by seismic faulting using observations from outcrop, underground observatories and from laboratory tests. Perhaps the best attempt to bridge these disciplines was accomplished by Faulkner et al. (2010) in which a clear and concise section on clay smear and fault sealing is presented. Bullock et al. (2015) recognize how modest amounts of clay, perhaps introduced by clay smear mechanisms, can alter the seismic behavior of a carbonate system, by evaluating the effects of clay on velocity weakening, dilatancy, permeability evolution, and other effects of earthquake faulting. Earthquake processes are related in complicated couplings, for example flash heating (Platt et al., 2015), pressure solution (Gratier, 2011), and mechanical effects of fabric evolution. Here we ask the question: did the clay smears discussed in our paper form as a result of seismic slip? The clay smear literature never approaches this question, although most papers seem to imply that faulting is aseismic. There have been no studies of velocity weakening in clay smears, and usually the faults for which clay smear is important have formed at effective stresses and areas which are too low to generate significant seismic moment. Perhaps one way to form clay smears by seismic slip is when the seismic event is triggered in asperities in hard layers above or below the zone with clay smear, and propagates into the clay smear. Alternatively, clay smear in a normal fault above basement could lead to a larger fault rupture area for an earthquake initiated in the basement. On the other hand, clay smear research has provided interesting data on 3D geometry of fault structures, and these have received little attention in the quake-related studies. Insights gained from how clay is incorporated into a fault zone and subsequently evolves provide input for the geometries in models of seismic faulting.

In summary, our physical understanding of clay smear processes is incomplete. Overall we might grade our knowledge with a C with some components like the geomechanical effects somewhat better understood and others like the processes that result in holes somewhat worse. In our opinion there is substantial opportunity for improving physical understanding through better interactions with complementary rock mechanics research, and in particular certain aspects of earthquake research. We now ask, however, whether and how this current, albeit incomplete understanding is currently used in subsurface flow evaluations.

#### 3.4.3. How does clay smear affect subsurface fluid flow?

There is no question that clay smear has the ability to impede subsurface fluid flow, and each of the components of clay smear from the high shear strain, localized, clay-rich fault zone to the coherent, undeformed block of shale caught in a fault lens has the ability to contribute to that impediment. Perhaps what is more uncertain is the extent to which each of these components contributes to reduced flow in any particular fault and for all faults in general. Moreover, in the little bit of work that has been done to evaluate processes that create gouge holes, it appears that they might develop quite readily, although more easily in some environments than others. So holes are an integral part of the ensemble of clay smear structures for the subsurface flow problem, even though they may only occupy a small fraction of the fault zone and be of far lesser consequence for its mechanics.

Therefore, for a larger fault area, the probability of finding a hole somewhere on this fault is greater than on a small fault area. Based on the arguments above, we propose that fully continuous clay smear on large faults is rare, and therefore the creation of a capillary seal by clay smear on a large fault surface is rare. Wehr et al. (2000) illustrated the consequences of introducing a small fraction of holes in a fault zone, consequences that may well be realized through the application of probabilistic clay smear calculations (e.g., Childs et al., 2007; Yielding, 2012). Returning to the contrast between multi-fault geometric analyses (James et al., 2004) and clay smear calculations (Dee et al., 2007), it seems reasonable to conclude that a large part of the cross-fault capillary seal problem is dictated by the geometry of fault juxtapositions that form by faulting but that the development of clay smear distributed within the fault zone has the potential to modify that juxtaposition window. The question then becomes: is that contribution significant or negligible in the context of the geometric uncertainties arising from the fault juxtaposition evaluation?

The second example of the Hibernia field study in which a small perched water accumulation is trapped in a geometric configuration that requires a downdip barrier that prevents the draining of water, is intended to illustrate this conundrum. In this instance, the calculation of a clay smear parameter (SGR) yields a value that must be compatible with cross-fault oil flow and pressure depletion during production. For this reason, we explored the possible interpretation of a largely undeformed shale lens in the fault zone as the clay smear structure that could cause the trapping of water. Moreover, we identified this example as one occurring on a fault segment with limited extent, thereby acknowledging the idea that a larger fault would increase the chance of a hole developing at a depth that would have allowed more water to drain from the fault trap. This line of reasoning leads us to speculate on the characteristic length scales of fault lens and relay structures and whether these scales have an influence on the area of a fault where clay smear processes may supplement traps created by fault juxtaposition.

For the more general case of cross-fault water, oil, and gas flow, the effects of clay smear are more compelling. The evidence from comprehensive subsurface oil and gas field studies (e.g., Jolley et al., 2007; Myers et al., 2007) and aquifer studies (e.g., Bense and Van Balen, 2004) show clear evidence of the effects of fault gouge, including and especially clay smear, on flow patterns resulting from fluid production. However, our understanding is plagued by similar issues to the capillary seal problem, including:

- How are the proportion and distribution of high shear strain clay found in the principle fault slip zones and less deformed shale lenses between those shear zones determined?
- What is the distribution and size of holes that form in the clay smear?
- How is flow (e.g., water) distributed between small, high permeability holes and large areas of thin, low permeability clay smear?

The effects of clay smear are present in subsurface flow problems, but the questions are how well the flow properties of clay smear are deduced from subsurface measurements, and how good the prediction of those effects can be. We pose these questions in the full knowledge that the fidelity of the answer often depends on the question posed. Although we strive to achieve a deep, simple, generalized understanding like Byerlee's Law and seek to define the means to know when we have found that insight, we recognize that there is utility in practical applications of less complete understanding.

In summary, improved understanding of clay smear processes and their effect on cross-fault fluid flow will only come about with more comprehensive, detailed, and reproducible experiments and analyses of subsurface data. In addition, improved understanding of clay smear processes will result in better predictions of deformation regimes where clay smear has more or less influence on cross-fault flow.

*3.4.4. How effective are predictive models of clay smear?*

Clay smear predictive algorithms (Eqs. (2)–(4)) are incomplete because they only account for the amount of clay or shale in a stratigraphic section in the context of the fault throw and make no accommodation for the large variety of fault processes and structures that create that lithologic offset. CSP is the only model with a mechanical basis, but it is defined in terms of only one facet of the mechanical problem (i.e. the clay incorporation process).

Thus attempts to 'calibrate' or 'validate' must be viewed with suspicion. Are calibration datasets drawn from faults in the same deformation regime? We know of no fully convincing demonstration of subsurface fault seal (capillary membrane seal) by clay smear, although we accept that such cases may exist. These are strong, provocative statements intended to address the terms 'calibrate' and 'validate' used in the literature, which we also find to be strong claims. We think these terms can only be applied when studies incorporate the most rigorous standards of experimental testing which we think are largely lacking. Scientifically rigorous experiments are difficult to conduct because most subsurface tests are designed for other purposes. However, it is possible to design subsurface experiments to appropriately test clay smear models in the context of specific, testable hypotheses.

We accept that clay smear affects subsurface fluid flow, and we accept that current clay smear models and algorithmic approaches can prove useful in some cases to estimate the nature of those effects. Keeping in mind the four main parameters that control clay smear, it is difficult to accept that only one of these can be used to predict. However, the current state makes it difficult to understand when those models may be misleading or when they might be right for the wrong reasons. For example, could the development of a shale lens predictor be more useful than a clay smear predictive model?

So when we claim that we know of no fully convincing demonstration of subsurface fault seal by clay smear, we mean this in the context of the data used in the subsurface evaluation. Too many data interpretations are non-unique, fraught with undefined spatial uncertainty, or limited by unresolved geometric complexities. We find the balance of evidence brought forward in subsurface field studies to be insufficient to convict. However, we also acknowledge that application of the existing imperfect models has proved useful in contributing to practical subsurface applications when the geologic setting has had some resiliency and flexibility for imperfect models.

*3.4.5. Ways forward*

There are excellent opportunities for the advancement of clay smear research that will improve our understanding of fault processes in sedimentary rocks and the effects of the resulting fault structures on subsurface fluid flow. Those advancements will be realized via the development of advanced predictive models that will entail a forward deformation model based on an input stratigraphic section, effective stress conditions, and mechanical property characterizations for each faulted lithology. The resulting geometric description of faulted and deformed lithologies within a fault zone will then be used with a geologic model of the subsurface to better evaluate and predict cross-fault flow and for earthquake studies to predict whether any fault geometry prediction is more or less susceptible to seismicity for an imposed stress field.

We will achieve an advanced understanding of clay smear processes necessary for a predictive forward model by advancements in each of the contributing areas that have led to our current state of knowledge. In outcrop studies future work should identify which aspects of the clay smear evolution the observations relate to (shale incorporation, fault zone evolution, and clay smear disruption) with special attention dedicated to observations of clay smear disruption; this will likely involve a greater emphasis on outcrop observations in 3D. In addition, all relevant geometric aspects of the faulted outcrop should be recorded and documented to better inform numerical and laboratory modeling studies; a goal of outcrop studies should be a 3D retro-deformable fault interpretation. Lastly, outcrops need to be documented in a way that allows the faulted stratigraphy to be evaluated with current and future clay smear models and ultimately fault-deformation forward models.

Laboratory studies will help elucidate complex, nonlinear fault processes for given initial and boundary conditions. However, each contribution needs to be documented and qualified for the limitations imposed by the experimental design; we need to know which observations are independent of design attributes and which may be influenced by those conditions. Experimental material characterization must be documented in relation to mechanical standards like the Benchmark experiments in order to insure reproducibility. And like outcrop studies a geometric characterization of the resulting fault structure is required to compare against observations in nature.

Numerical models require many of the same qualifications as laboratory studies, including explicit statements about the limitations of the applied modeling approach, application of benchmarked, standard material properties, and geometric characterization of resulting fault structures. In our opinion this domain of research has been plagued by the lack of reproduced results and benchmarks. The path toward a fault-deformation forward model likely begins with models that reproduce laboratory experiments where initial and boundary conditions are known, expanding to models that reproduce complete outcrop observations (ideally a fault described tip-to-tip), and ultimately to prediction of fault structures where only the initial and boundary conditions are given. The ultimate fault forward-model may be a numerical simulation or it may be a simpler model based on numerical simulations. The most significant advancements, however, will come from research dedicated to defining processes that

create holes in clay smear and that allows us to better evaluate the relative importance of holes compared with all other clay smear structures.

The single most important requirement of subsurface field studies is to conduct subsurface flow tests that interrogate limited areas of faults for which cross-fault flow predictions exist. In this instance and all other field evaluations that involve faults, all necessary information must be documented to allow others to reproduce the experiment and reach the same conclusion. Subsurface flow predictions must entail measurable quantities, like a prediction of fluid type, fluid pressure, and fluid contacts (Vrolijk et al., 2005) in untested fault blocks. With these more rigorous analytical requirements, field studies of fluid flow can interrogate large fault areas, searching for the weak link that is difficult to find in outcrops, for example. Lastly, predictive models of fluid flow need to incorporate aspects of the mechanics of deformation to improve their accuracy.

We think that the existing research has laid a foundation for a more complete model of clay smear development in normal faults in clastic sedimentary sections. That model may build upon the model presented in Fig. 27 that emphasizes the geometric components of the resulting fault structures and lithologies contained within those structures. The resulting predictive model of fault deformation will nevertheless provide geometric attributes of clay smear components that will be used in an advanced clay smear flow predictive model, perhaps along the lines of Equations (6)–(8) that involve existing fault zone predictions (e.g., SGR) and supplement them with geometric constraints (especially Eq. (8)).

The path to applying the results of a clay-smear predictive model for earthquake studies is more speculative, but *a priori* knowledge of heterogeneous fault structure may influence those who consider the effects of such heterogeneous structure on earthquakes. In addition, it is conceivable that different faults with different structure (e.g., amount and continuity of a clay component) may be more or less susceptible to induced seismicity caused by changes in stress state in an area.

## 4. Summary

Significant advancements in understanding normal fault processes in clastic sedimentary sequences and the effects of those processes on cross-fault gas, oil, and water flow have come about as a result of clay smear studies over the past four decades. From the initial conception of clay distributed along the dip of a normal fault using a process model developed from outcrop observations, laboratory experiments, and geomechanical principles, our understanding has advanced from additional research in all these areas and from subsurface flow studies. An important part of this evolution includes technological advancements, which have resulted in better numerical simulation methods, better subsurface data characterization, and new laboratory capabilities.

Although current clay smear prediction algorithms are based on simple stratigraphic and fault offset parameters, our review of the work committed to exploring fault processes in outcrop and in laboratory and numerical models suggests that we stand on the precipice of a new type of model that incorporates the manner in which rocks deform during faulting taken in concert with models of fault geometric evolution. The evidence supporting the idea that these factors play a fundamental role in fault processes is unequivocal. We think our understanding of potential fault deformation regimes is sufficient to apply today, even though that understanding remains incomplete. However, better predictive capabilities for fault network evolution require additional work to be similarly useful.

Interestingly, although the importance of holes in clay smear was recognized at the beginning as a crucial part of the clay smear problem, and this realization has resurfaced repeatedly over the years, there has been surprisingly little work until recently to investigate the processes that create holes and the conditions that favor those processes. Ongoing work will continue to develop this understanding, and we think that this is one of the most exciting areas of current research in this area.

## Acknowledgments

The ideas in this paper have evolved for over twenty years and we would like to express our gratitude to the many colleagues who shared their ideas, helped with experiments, supported field work or discussed complex subsurface problems.

PJV wishes to thank a whole host of people who have influenced my thinking over the years, some of whom I acknowledge by citing their work in this review, but others who have worked on this problem without fully publishing their results, and others still who have participated in the publication process but gifted me their insights in informal discussions and debates. In particular, I acknowledge the contributions of Rod Myers, Brooks Clark, Bill Shea, Lee Fairchild, Bill James, Ellen Meurer, Michael Tsenn, Paul Hicks, Gretchen Nakayama, Martha Gerdes, B J McPherson, Dave Stern, Dave Chorneyko, Dave Braisted, Joyce Schmatz, Sohrab Noorsalehi-Garakani, Sofie Nollet, Gisa Kleine Vennekate, Conrad Childs, Tom Manzocchi, Martin Schoepfer, John Walsh, and Graham Yielding. Dana Butters helped me with the Hibernia Field example by making his seismic interpretation available to me. Lastly, I wish to thank Chuck Tautfest, who supported me in what would have been one of the most comprehensive and definitive cross-fault flow experiments had it not been for a critical mechanical failure.

JLU wishes to thank Georg Mandl and Florian Lehner, for initial inspiration, and Yves Leroy, Pascal Richard, John Walsh, Pieter Vermeer, Wouter van der Zee, Robrecht Schmitz, Joyce Schmatz, Heijn van Gent, Marc Holland, Steffen Abe, Sohrab Noorsalehi-Garakani, Alexander Raith, Martin Ziegler, Gisa Kleine Vennekate, Steffen Giese, and Werner Kraus for sharing their ideas and for important lessons learned in a wide variety of fields.

MK and JLU thank Sven Asmus, Peter Lokay and Ulrich Krüger from RWE Power AG for providing the possibility to investigate faults in the Hambach lignite mine and all students who helped in the field.

Thoughtful reviews by Brandon Dugan and Conrad Childs, both of whom demonstrated perseverance in their tasks, is gratefully acknowledged.

Finally, JLU and MK acknowledge financial support by the German Science Foundation (Projects UR 64-2, ZI 714/4-1 and UR 64/10-1); and by ExxonMobil Upstream Research Company.

## Appendix A. Supplementary data

Supplementary data related to this article can be found at http://dx.doi.org/10.1016/j.jsg.2015.09.006.

## References

Abe, S., Latham, S., Mora, P., 2006. Dynamic rupture in a 3-D particle-based simulation of a rough planar fault. Pure Appl. Geophys. 163, 1881–1892.

Allan, U.S., 1989. Model for hydrocarbon migration and entrapment within faulted structures. AAPG Bull. 73, 803–811.

Aydin, A., Eyal, Y., 2002. Anatomy of a normal fault with shale smear; implications for fault seal. AAPG Bull. 86, 1367–1381.

Bailey, W.R., Underschultz, J., Dewhurst, D.N., Kovack, G., Mildren, S., Raven, M.,

2006. Multi-disciplinary approach to fault and top seal appraisal; Pyrenees-Macedon oil and gas fields, Exmouth Sub-basin, Australian Northwest Shelf. Mar. Pet. Geol. 23, 241–259.
Balthasar, K., Gudehus, G., Kulzer, M., Bertini, A., 2006. Thin layer shearing of a highly plastic clay. Nonlinear Process. Geophys. 13, 671–680.
Belytschko, T., Chian, H.-Y., Plaskacz, E., 1994. High resolution two-dimensional shear band computations: imperfections and mesh dependence. Comput. Methods Appl. Mech. Eng. 119, 1–15.
Bense, V.F., Person, M.A., Chaudhary, K., You, Y., Cremer, N., Simon, S., 2008. Thermal anomalies indicate preferential flow along faults in unconsolidated sedimentary aquifers. Geophys. Res. Lett. 35, L24406.
Bense, V.F., Van Balen, R., 2004. The effect of fault relay and clay smearing on groundwater flow patterns in the Lower Rhine Embayment. Basin Res. 16, 397–411.
Bense, V.F., Van den Berg, E.H., Van Balen, R.T., 2003. Deformation mechanisms and hydraulic properties of fault zones in unconsolidated sediments; the Roer Valley Rift System, The Netherlands. Hydrogeol. J. 11, 319–332.
Bentley, M.R., Barry, J.J., 1991. Representation of fault sealing in a reservoir simulation: Cormorant Block IV, UK North Sea. In: SPE Annual Technical Conference and Exhibition, 6–9 October, Dallas, Texas.
Berg, R.R., Avery, A.H., 1995. Sealing properties of tertiary growth faults, Texas Gulf Coast. AAPG Bull. 79, 375–393.
Bourne, S.J., Oates, S.J., van Elk, J., Doornhof, D., 2014. A seismological model for earthquakes induced by fluid extraction from a subsurface reservoir. J. Geophys. Res. Solid Earth 119, 8991–9015.
Bouvier, J.D., Kaars-Sijpesteijn, C.H., Kluesner, D.F., Onyejekwe, C.C., van der Pal, R.C., 1989. Three-dimensional seismic interpretation and fault sealing investigations, Nun River Field, Nigeria. AAPG Bull. 73, 1397–1414.
Bretan, P., Yielding, G., 2005. Using buoyancy pressure profiles to assess uncertainty in fault seal calibration. In: Boult, P., Kaldi, J. (Eds.), Evaluating Fault and Cap Rock Seals. The American Association of Petroleum Geologists, pp. 151–162.
Bretan, P., Yielding, G., Jones, H., 2003. Using calibrated shale gouge ratio to estimate hydrocarbon column heights. AAPG Bull. 87, 397–413.
Buiter, S., Babeyko, A., Ellis, S., Gerya, T., Kaus, B., Kellner, A., Schreurs, G., Yamada, Y., 2006. The numerical sandbox: comparison of model results for a shortening and an extension experiment. Analog. Numer. Model. Crustal-Scale Process. 253, 29–64.
Bullock, R.J., De Paola, N., Holdsworth, R.E., 2015. An experimental investigation into the role of phyllosilicate content on earthquake propagation during seismic slip in carbonate faults. J. Geophys. Res. Solid Earth 120, 3187–3207.
Burhannudinnur, M., Morley, C.K., 1997. Anatomy of growth fault zones in poorly lithified sandstones and shales: implications for reservoir studies and seismic interpretation: part 1, outcrop study. Pet. Geosci. 3, 211–224.
Byerlee, J., 1978. Friction of rocks. Pure Appl. Geophys. 116, 615–626.
Caine, J.S., Evans, J.P., Forster, C.B., 1996. Fault zone architecture and permeability structure. Geology 24, 1025–1028.
Caine, J.S., Minor, S.A., 2009. Structural and geochemical characteristics of faulted sediments and inferences on the role of water in deformation, Rio Grande Rift, New Mexico. Geol. Soc. Am. Bull. 121, 1325–1340.
Childs, C., Manzocchi, T., Walsh, J.J., Bonson, C.G., Nicol, A., Schöpfer, M.P.J., 2009a. A geometric model of fault zone and fault rock thickness variations. J. Struct. Geol. 31, 117–127.
Childs, C., Sylta, Ø., Moriya, S., 2002. A method for including the capillary properties of faults in hydrocarbon migration models. Nor. Pet. Soc. 11, 127–139.
Childs, C., Sylta, O., Moriya, S., Morewood, N., Manzocchi, T., Walsh, J.J., Hermanssen, D., 2009b. Calibrating fault seal using a hydrocarbon migration model of the Oseberg Syd area, Viking Graben. Mar. Pet. Geol. 26, 764–774.
Childs, C., Walsh, J.J., Manzocchi, T., Strand, J., Nicol, A., Tomasso, M., Schopfer, M.P.J., Aplin, A.C., 2007. Definition of a Fault Permeability Predictor from Outcrop Studies of a Faulted Turbidite Sequence, Taranaki, New Zealand, Structurally Complex Reservoirs. Geological Society of London, London, pp. 235–258.
Childs, C., Walsh, J.J., Watterson, J., 1997. Complexity in fault zone structure and implications for fault seal prediction. In: Møller-Pedersen, P., Koestler, A.G. (Eds.), Hydrocarbon Seals: Importance for Exploration and Production. Norwegian Petroleum Society, Trondheim, Norway, pp. 61–72.
Ciftçi, N.B., Giger, S.B., Clennell, M.B., 2012. Testing fault seal prediction algorithms using geomodels of experimentally produced fault zones. In: Fault and Top Seals 2012, Montpellier, France, pp. 1–3.
Çiftçi, N.B., Giger, S.B., Clennell, M.B., 2013. Three-dimensional structure of experimentally produced clay smears: implications for fault seal analysis. AAPG Bull. 97, 733–757.
Cilona, A., Aydin, A., Johnson, N., 2015. Permeability of a fault zone crosscutting a sequence of sandstones and shales and its influence on hydraulic head distribution in the Chatsworth Formation, California, USA. Hydrogeol. J. 23, 405–419.
Clarke, S.M., Littler, M., Burley, S.D., Williams, G.D., Hughes, D., Coogan, S., 2006. Modelling the effects of stratigraphical uncertainty on fault seal and trap-fill in faulted structures. Pet. Geosci. 12, 143–156.
Clausen, J.A., Gabrielsen, R.H., 2002. Parameters that control the development of clay smear at low stress states: an experimental study using ring-shear apparatus. J. Struct. Geol. 24, 1569–1586.
Clausen, J.A., Gabrielsen, R.H., Johnsen, E., Korstgård, J.A., 2003. Fault architecture and clay smear distribution. Examples from field studies and drained ring-shear experiments. Norw. J. Geol. 83, 131–146.
Cosserat, E., Cosserat, F., 1909. Theorie des corps deformables. A. Hermann et fils, Paris.
Crawford, B.R., Faulkner, D.R., Rutter, E.H., 2008. Strength, porosity, and permeability development during hydrostatic and shear loading of synthetic quartz-clay fault gouge. J. Geophys. Res. 113, B03207.
Crawford, B.R., Myers, R.D., Woronow, A., Faulkner, D.R., Rutter, E.H., 2002. Porosity-permeability relationships in clay-bearing fault gouge. In: SPE/ISRM Rock Mechanics Conference, 20–23 October. Society of Petroleum Engineers, Irving, Texas.
Crook, A.J.L., Willson, S.M., Yu, J.G., Owen, D.R.J., 2006. Predictive modelling of structure evolution in sandbox experiments. J. Struct. Geol. 28, 729–744.
Cuisiat, F., Skurtveit, E., 2010. An experimental investigation of the development and permeability of clay smears along faults in uncemented sediments. J. Struct. Geol. 32, 1850–1863.
Cundall, P.A., Drescher, A., Strack, O.D.L., 1982. Numerical experiments on granular assemblies; measurements and observations. In: Vermeer, P.A., Luger, H.J. (Eds.), IUTAM Conference on Deformation End Failure of Granular Materials. Delft, Balkema, Rotterdam, pp. 553–568.
Cundall, P.A., Strack, O.D.L., 1979. A discrete numerical model for granular assemblies. Géotechnique 29, 47–65.
Davatzes, N.C., Aydin, A., 2005. Distribution and nature of fault architecture in a layered sandstone and shale sequence; an example from the Moab Fault, Utah. AAPG Mem. 85, 153–180.
Davies, R.K., An, L., Jones, P., Mathis, A., Cornette, C., 2003. Fault-seal analysis south Marsh Island 36 field, Gulf of Mexico. AAPG Bull. 87, 479–491.
Dee, S.J., Yielding, G., Freeman, B., Bretan, P., 2007. A Comparison between Deterministic and Stochastic Fault Seal Techniques. In: Geological Society, London, Special Publications, vol. 292, pp. 259–270.
Doughty, P.T., 2003. Clay smear seals and fault sealing potential of an exhumed growth fault, Rio Grande rift, New Mexico. AAPG Bull. 87, 427–444.
Egholm, D.L., 2007. A new strategy for discrete element numerical models; 1, Theory. J. Geophys. Res. 112, B05203.
Egholm, D.L., Sandiford, M., Clausen, O.R., Nielsen, S.B., 2007. A new strategy for discrete element numerical models; 2, Sandbox applications. J. Geophys. Res. 112, B05204.
Egholm, D.L., Clausen, O.R., Sandiford, M., Kristensen, M.B., Korstgard, J.A., 2008. The mechanics of clay smearing along faults. Geology 36, 787–790.
Eichhubl, P., D'Onfro, P.S., Aydin, A., Waters, J., McCarty, D.K., 2005. Structure, petrophysics, and diagenesis of shale entrained along a normal fault at Black Diamond Mines, California—implications for fault seal. AAPG Bull. 89, 1113–1137.
Faerseth, R.B., 2006. Shale smear along large faults; continuity of smear and the fault seal capacity. J. Geol. Soc. Lond. 163, 741–751.
Faerseth, R.B., Johnsen, E., Sperrevik, S., 2007. Methodology for risking fault seal capacity; implications of fault zone architecture. AAPG Bull. 91, 1231–1246.
Faulkner, D.R., Jackson, C.A.L., Lunn, R.J., Schlische, R.W., Shipton, Z.K., Wibberley, C.A.J., Withjack, M.O., 2010. A review of recent developments concerning the structure, mechanics and fluid flow properties of fault zones. J. Struct. Geol. 32, 1557–1575.
Finch, E., Hardy, S., Gawthorpe, R., 2004. Discrete-element modelling of extensional fault-propagation folding above rigid basement fault blocks. Basin Res. 16, 489–506.
Fisher, Q.J., Jolley, S.J., 2007. Treatment of Faults in Production Simulation Models. In: Geological Society, London, Special Publications, vol. 292, pp. 219–233.
Fisher, Q.J., Knipe, R.J., 1998. Fault sealing processes in siliciclastic sediments. In: Jones, G., Fisher, Q.J., Knipe, R.J. (Eds.), Faulting, Fault Sealing and Fluid Flow in Hydrocarbon Reservoirs. Geological Society of London, London, pp. 117–134.
Fisher, Q.J., Knipe, R.J., 2001. The permeability of faults within siliciclastic petroleum reservoirs of the North Sea and Norwegian Continental Shelf. Mar. Pet. Geol. 18, 1063–1081.
Foxford, K.A., Walsh, J.J., Watterson, J., Garden, I.R., Guscott, S.C., Burley, S.D., 1998. Structure and content of the Moab Fault Zone, Utah, USA, and its implications for fault seal prediction. In: Jones, G., Fisher, Q.J., Knipe, R.J. (Eds.), Faulting, Fault Sealing and Fluid Flow in Hydrocarbon Reservoirs. Geological Society London, London, pp. 87–103.
Freeman, B., Yielding, G., Needham, D.T., Badley, M.E., 1998. Fault seal prediction: the gouge ratio method. In: Coward, M.P., Daltaban, T.S., Johnson, H. (Eds.), Structural Geology in Reservoir Characterization. Geological Society London, London, pp. 19–25.
Fristad, T., Groth, A., Yielding, G., Freeman, B., 1997. Quantitative fault seal prediction: a case study from Oseberg Syd. In: Møller-Pedersen, P., Koestler, A.G. (Eds.), Hydrocarbon Seals: Importance for Exploration and Production. Norwegian Petroleum Society, Trondheim, Norway, pp. 107–124.
Fulljames, J.R., Zijerveld, L.J.J., Franssen, R.C.M.W., 1997. Fault seal processes: systematic analysis of fault seals over geological and production time scales. In: Møller-Pedersen, P., Koestler, A.G. (Eds.), Hydrocarbon Seals: Importance for Exploration and Production. Norwegian Petroleum Society, pp. 51–59.
Gibson, R.G., 1994. Fault-zone seals in siliciclastic Strata of the Columbus Basin, Offshore Trinidad. AAPG Bull. 78, 1372–1385.
Gibson, R.G., 1998. Physical character and fluid-flow properties of sandstone-derived fault zones. In: Coward, M.P., Daltaban, T.S., Johnson, H. (Eds.), Structural Geology in Reservoir Characterization. Geological Society London, London, pp. 83–97.
Gibson, R.G., Bentham, P.A., 2003. Use of fault-seal analysis in understanding petroleum migration in a complexly faulted anticlinal trap, Columbus Basin, offshore Trinidad. AAPG Bull. 87, 465–478.
Giger, S.B., Clennell, M.B., Ciftci, N.B., Harbers, C., Clark, P., Ricchetti, M., 2013. Fault

transmissibility in clastic-argillaceous sequences controlled by clay smear evolution. AAPG Bull. 97, 705–731.
Giger, S.B., Clennell, M.B., Harbers, C., Clark, P., Ricchetti, M., Ter Heege, J.H., Wassing, B.B.T., Orlic, B., 2011. Design, operation and validation of a new fluid-sealed direct shear apparatus capable of monitoring fault-related fluid flow to large displacements. Int. J. Rock Mech. Min. Sci. 48, 1160–1172.
Gratier, J.P., 2011. Fault permeability and strength evolution related to fracturing and healing episodic processes (years to millennia): the role of pressure solution. Oil Gas Sci. Technol. Rev. IFP Energies Nouv. 66, 491–506.
Gudehus, G., Karcher, C., 2007. Hypoplastic simulation of normal faults without and with clay smears. J. Struct. Geol. 29, 530–540.
Gudehus, G., Nubel, K., 2004. Evolution of shear bands in sand. Geotechnique 54, 187–201.
Haines, S.H., Kaproth, B., Marone, C., Saffer, D., van der Pluijm, B., 2013. Shear zones in clay-rich fault gouge: a laboratory study of fabric development and evolution. J. Struct. Geol. 51, 206–225.
Hall, S., Bornert, M., Desrues, J., Pannier, Y., Lenoir, N., Viggiani, G., Besuelle, P., 2010. Discrete and continuum analysis of localised deformation in sand using X-ray μCT and volumetric digital image correlation. Geotechnique 60, 315–322.
Hardy, S., Finch, E., 2005. Discrete-element modelling of detachment folding. Basin Res. 17, 507–520.
Hardy, S., Finch, E., 2006. Discrete element modelling of the influence of cover strength on basement-involved fault-propagation folding. Tectonophysics 415, 225–238.
Harris, D., Yielding, G., Levine, P., Maxwell, G., Rose, P.T., Nell, P., 2002. Using Shale Gouge Ratio (SGR) to model faults as transmissibility barriers in reservoirs; an example from the Strathspey Field, North Sea. Pet. Geosci. 8, 167–176.
Herle, I., Feda, J., 2001. Interaction of spread footings with sandy subsoil. Eng. Mech. 8, 1–12.
Herle, I., Feda, J., 2002. Interaction of spread footings with sandy subsoil. Part 2: plane strain FE modelling. Eng. Mech. 9, 259–272.
Hesthammer, J., Fossen, H., 2000. Uncertainties associated with fault sealing analysis. Pet. Geosci. 6, 37–45.
Heynekamp, M.R., Goodwin, L.B., Mozley, P.S., Haneberg, W.C., 1999. Controls on fault-zone architecture in poorly lithified sediments, Rio Grande Rift, New Mexico: implications for fault-zone permeability and fluid flow. In: Haneberg, W.C., Mozley, P.S., Moore, J.C., Goodwin, L.B. (Eds.), Faults and Subsurface Fluid Flow in the Shallow Crust. American Geophysical Union, Washington D.C, pp. 27–49.
Holland, M., Urai, J.L., van der Zee, W., Stanjek, H., Konstanty, J., 2006. Fault gouge evolution in highly overconsolidated claystones. J. Struct. Geol. 28, 323–332.
Hovadik, J.M., Larue, D.K., 2010. Stratigraphic and Structural Connectivity. In: Geological Society, London, Special Publications, vol. 347, pp. 219–242.
Hubbert, M.K., 1940. The theory of ground-water motion. J. Geol. 785–944.
Hügel, H.M., 1995. Prognose von Bodenverformungen, Institut für Bodenmechanik und Felsmechanik. Fridericiana Universität, Karlsruhe.
Ingram, G.M., Urai, J.L., 1999. Top-seal Leakage through Faults and Fractures: the Role of Mudrock Properties. In: Geological Society, London, Special Publications, vol. 158, pp. 125–135.
Ishii, E., Sanada, H., Funaki, H., Sugita, Y., Kurikami, H., 2011. The relationships among brittleness, deformation behavior, and transport properties in mudstones: an example from the Horonobe Underground Research Laboratory, Japan. J. Geophys. Res. Solid Earth 116.
James, W.R., Fairchild, L.H., Nakayama, G.P., Hippler, S.J., Vrolijk, P.J., 2004. Fault-seal analysis using a stochastic multifault approach. AAPG Bull. 88, 885–904.
Jev, B.I., Kaarssijpesteijn, C.H., Peters, M., Watts, N.L., Wilkie, J.T., 1993. Akaso field, Nigeria – use of integrated 3-D seismic, fault slicing, clay smearing, and RFT pressure data on fault trapping and dynamic leakage. AAPG Bull. 77, 1389–1404.
Jolley, S.J., Dijk, H., Lamens, J.H., Fisher, Q.J., Manzocchi, T., Eikmans, H., Huang, Y., 2007. Faulting and fault sealing in production simulation models: Brent Province, northern North Sea. Pet. Geosci. 13, 321–340.
Karakouzian, M., Hudyma, N., 2002. A new apparatus for analog modeling of clay smears. J. Struct. Geol. 24, 905–912.
Kettermann, M., Urai, J.L., 2015. Changes in structural style of normal faults due to failure mode transition: first results from excavated scale models. J. Struct. Geol. 74, 105–116.
Kleine-Vennekate, G., 2013. Numerische Simulationen zur Scherfugenentwicklung in Sand-Ton-Wechselfolgen/Numerical Simulations of Shear Zones in Layered Sand-clay Sequences, Fakultät für Bauingenieurwesen (PhD thesis). RWTH Aachen University, Aachen.
Kleine-Vennekate, G., Noorsalehi-Garakani, S., Urai, J.L., Ziegler, M., 2014. Numerische simulationen des clay-smear-prozesses in sandboxversuchen. Geotechnik 37, 83–95.
Knai, T.A., Knipe, R.J., 1998. The Impact of Faults on Fluid Flow in the Heidrun Field. In: Geological Society, London, Special Publications, vol. 147, pp. 269–282.
Knipe, R.J., 1992. Faulting processes and fault seal. In: Larsen, R.M., Brekke, H., Larsen, B.T., Talleraas, E. (Eds.), Structural and Tectonic Modelling and its Application to Petroleum Geology, NPF Special Publication, vol. 1. Elsevier, Amsterdam, pp. 325–342.
Knipe, R.J., 1997. Juxtaposition and seal diagrams to help analyze fault seals in hydrocarbon reservoirs. AAPG Bull. 81, 187–195.
Knott, S.D., 1993. Fault seal analysis in the North Sea. AAPG Bull. 77, 778–792.
Koledoye, B.A., Aydin, A., May, E., 2003. A new process-based methodology for analysis of shale smear along normal faults in the Niger Delta. AAPG Bull. 87, 445–463.
Kolymbas, D., 1988. Eine konstitutive Theorie für Böden und andere körnige Stoffe. Institut für Bodenmechanik und Felsmechanik der Universität Fridericiana, Karlsruhe.
Kristensen, M.B., Childs, C., Olesen, N.O., Korstgard, J.A., 2013. The microstructure and internal architecture of shear bands in sand-clay sequences. J. Struct. Geol. 46, 129–141.
Latham, S., Abe, S., Mora, P., 2006. Parallel 3-D simulation of a fault gouge using the lattice solid model. Pure Appl. Geophys. 163, 1949–1964.
Lehner, F.K., Pilaar, W.F., 1997. The emplacement of clay smears in synsedimentary normal faults: inferences from field observations near Frechen, Germany. In: Møller-Pedersen, P., Koestler, A.G. (Eds.), Norwegian Petroleum Society Special Publications: Hydrocarbon Seals: Importance for Exploration and Production. Elsevier Science, pp. 39–50.
Lewis, G., Knipe, R.J., Li, A., 2002. Fault seal analysis in unconsolidated sediments: a field study from Kentucky, USA. In: Koestler, A.G., Hunsdale, R. (Eds.), Hydrocarbon Seal Quantification, Norwegian Petroleum Society (NPF), Special Publications, vol. 11, pp. 243–253.
Lindsay, N.G., Walsh, J.J., Watterson, J., Murphy, F.C., 1993. Outcrop studies of shale smears on fault surfaces. In: Flint, S.S., Bryant, I.D. (Eds.), The Geological Modelling of Hydrocarbon Reservoirs and Outcrop Analogues. Blackwell Scientific Publications, Inc, Oxford, UK, pp. 113–123.
Loveless, S., Bense, V., Turner, J., 2011. Fault architecture and deformation processes within poorly lithified rift sediments, Central Greece. J. Struct. Geol. 33, 1554–1568.
Luding, S., Hermann, H.J., 2001. Micro-macro transition for cohesive granular media. In: Diebels, S. (Ed.), Zur Beschreibung Komplexen Materialverhaltens. Institut für Mechanik (Bauwesen), Stuttgart.
Lupini, J.F., Skinner, A.E., Vaughan, P.R., 1981. The drained residual strength of cohesive soils. Geotechnique 31, 181–213.
Mackay, A.H., Tankard, A.J., 1990. Hibernia Oil Field Canada, Jeanne D'Arc Basin, Grand Banks, Newfoundland. In: AAPG Treatise of Petroleum Geology, Atlas of Oil and Gas Fields A-019, pp. 145–175.
Maksimovic, M., 1989. Nonlinear failure envelope for soils. J. Geotech. Eng. 115, 581–586.
Mandl, G., 1988. Mechanics of tectonic faulting: models and basic concepts. In: Zwart, H.J. (Ed.), Developments in Structural Geology. Elsevier, Amsterdam.
Mandl, G., Jong, L.N.J., Maltha, A., 1977. Shear zones in granular material. Rock Mech. 9, 95–144.
Manzocchi, T., Carter, J.N., Skorstad, A., Fjellvoll, B., Stephen, K.D., Howell, J.A., Matthews, J.D., Walsh, J.J., Nepveu, M., 2008a. Sensitivity of the impact of geological uncertainty on production from faulted and unfaulted shallow-marine oil reservoirs: objectives and methods. Pet. Geosci. 14, 3–15.
Manzocchi, T., Childs, C., Walsh, J.J., 2010. Faults and fault properties in hydrocarbon flow models. Geofluids 10, 94–113.
Manzocchi, T., Heath, A.E., Palananthakumar, B., Childs, C., Walsh, J.J., 2008b. Faults in conventional flow simulation models: a consideration of representational assumptions and geological uncertainties. Pet. Geosci. 14, 91–110.
Manzocchi, T., Heath, A.E., Walsh, J.J., Childs, C., 2002. The representation of two phase fault-rock properties in flow simulation models. Pet. Geosci. 8, 119–132.
Manzocchi, T., Matthews, J.D., Strand, J.A., Carter, J.N., Skorstad, A., Howell, J.A., Stephen, K.D., Walsh, J.J., 2008c. A study of the structural controls on oil recovery from shallow-marine reservoirs. Pet. Geosci. 14, 55–70.
Manzocchi, T., Walsh, J.J., Nell, P., Yielding, G., 1999. Fault transmissibility multipliers for flow simulation models. Pet. Geosci. 5, 53–63.
Mühlhaus, H.B., 1986. Scherfugenanalyse bei granularem Material im Rahmen der Cosserat-Theorie. Ingenieur-Archiv 56, 389–399.
Myers, R.D., Allgood, A., Hjellbakk, A., Vrolijk, P., Briedis, N., 2007. Testing Fault Transmissibility Predictions in a Structurally Dominated Reservoir; Ringhorne Field, Norway. In: Geological Society Special Publications, vol. 292, pp. 271–294.
Myers, R.D., Vrolijk, P.J., Kiven, C.W., Tsenn, M., 2014. In: Patent, U.S. (Ed.), Method for Predicting Fluid Flow. ExxonMobil Upstream Research Company, Houston, TX, U. S., p. 21
Niemunis, A., 2003. Extended Hypoplastic Models for Soils. Th. Triantafyllidis, Bochum.
Nollet, S., Vennekate, G.J.K., Giese, S., Vrolijk, P., Urai, J.L., Ziegler, M., 2012. Localization patterns in sandbox-scale numerical experiments above a normal fault in basement. J. Struct. Geol. 39, 199–209.
Noorsalehi-Garakani, S., Vennekate, G.J.K., Vrolijk, P., Urai, J.L., 2013. Clay-smear continuity and normal fault zone geometry – first results from excavated sandbox models. J. Struct. Geol. 57, 58–80.
Nübel, K., 2002. Experimental and Numerical Investigation of Shear Localization in Granular Material. Inst. für Bodenmechanik und Felsmechanik. Fridericiana Universität, Karlsruhe.
Nybakken, S., 1991. Sealing fault traps; an exploration concept in a mature petroleum province; Tampen Spur, northern North Sea. First Break 9, 209–222.
Olgaard, D.L., Urai, J.L., Dell'Angelo, L.N., Nüesch, R., Ingram, G., 1997. The influence of swelling clays on the deformation of mudrocks. Proceedings of the 36th U. S. Rock Mechanics Symposium, New York, NY, United States, June 29–July 2. Int. J. Rock Mech. Min. Sci. Geomech. 34 (3–4), 364–374.
Ottesen Ellevset, S., Knipe, R.J., Svava Olsen, T., Fisher, Q.J., 1998. Fault controlled communication in the Sleipner Vest field, Norwegian Continental Shelf; detailed, quantitative input for reservoir simulation and well planning. In: Jones, G., Fisher, Q.J., Knipe, R.J. (Eds.), Structure and Seal Analysis of Hydrocarbon Fields, Geological Society, London, Special Publications, pp. 283–297.

Peacock, D.C.P., Knipe, R.J., Sanderson, D.J., 2000. Glossary of normal faults. J. Struct. Geol. 22, 291–305.
Pevear, D.R., Vrolijk, P.J., Lomgstaffe, F.J., 1997. Timing of Moab Fault displacement and fluid movement integrated with burial history using radiogenic and stable isotopes. In: Carey, H.J., Parnell, J., Ruffell, A., Worden, R. (Eds.), Geofluids II '97: Contributions to the Second International Conference on Fluid Evolution, Migration & Interaction in Sedimentary Basins and Orogenic Belts. The Queen's University of Belfast, Belfast, pp. 42–45.
Platt, J.D., Brantut, N., Rice, J.R., 2015. Strain localization driven by thermal decomposition during seismic shear. J. Geophys. Res. Solid Earth 120, 4405–4433.
Raith, A., 2012. The Evolution of Fault Zones in Brittle Ductile-layered Rocks (MSc thesis). Department of Structural Geology, Tectonics and Geomechanics. RWTH Aachen University, Aachen, p. 76.
Rathbun, A.P., Marone, C., 2010. Effect of strain localization on frictional behavior of sheared granular materials. J. Geophys. Res. Solid Earth 115.
Revil, A., Cathles, L.M., 1999. Permeability of shaly sands. Water Resour. Res. 35, 651–662.
Richard, P.D., Urai, J.L., 2001. In: Nieuwland, D.A., Nijman, M. (Eds.), The Atlas of Structural Geometry: a Digital Collection of 25 Years of Analogue Modelling. Geol. Mijnb./Neth. J. Geosci. 80 (2), 59–60.
Rivenaes, J.C., Dart, C., 2002. Reservoir compartmentalization by water-saturated faults – is evaluation possible with today's tools? In: Koestler, A.G., Hunsdale, R. (Eds.), Hydrocarbon Seal Quantification, Norwegian Petroleum Society (NPF), Special Publications, vol. 11, pp. 173–186.
Rudnicki, J.W., Rice, J.R., 1975. Conditions for the localization of deformation in pressure-sensitive dilatant materials. J. Mech. Phys. Solids 23, 371–394.
Rycroft, C., Wong, Y., Bazant, M., 2010. Fast spot-based multiscale simulations of granular drainage. Powder Technol. 200, 1–11.
Sadrekarimi, A., Olson, S.M., 2010. Shear band formation observed in ring shear tests on sandy soils. J. Geotech. Geoenviron. Eng. 136, 366–375.
Santimano, T., Rosenau, M., Oncken, O., 2015. Intrinsic versus extrinsic variability of analogue sand-box experiments – insights from statistical analysis of repeated accretionary sand wedge experiments. J. Struct. Geol. 75, 80–100.
Sassi, W., Livera, S.E., Caline, B.P.R., 1992. Reservoir compartmentation by faults in Cormorant Block IV, UK Northern North Sea. In: Larsen, R.M., Brekke, H., Larsen, B.T., Talleras, E. (Eds.), Structural and Tectonic Modeling and its Application to Petroleum Geology, NPF Special Publication. Elsevier, Amsterdam.
Savage, J.C., Lockner, D.A., Byerlee, J.D., 1996. Failure in laboratory fault models in triaxial tests. J. Geophys. Res. Solid Earth 101, 22215–22224.
Schmatz, J., Holland, M., Giese, S., van der Zee, W., Urai, J.L., 2010a. Clay smear processes in mechanically layered sequences – results of water-saturated model experiments with free top surface. J. Geol. Soc. India 75, 74–88.
Schmatz, J., Vrolijk, P.J., Urai, J.L., 2010b. Clay smear in normal fault zones – the effect of multilayers and clay cementation in water-saturated model experiments. J. Struct. Geol. 32, 1834–1849.
Schöpfer, M.P.J., Childs, C., Walsh, J.J., 2006. Localisation of normal faults in multilayer sequences. J. Struct. Geol. 28, 816–833.
Schöpfer, M.P.J., Childs, C., Walsh, J.J., 2007a. Two-dimensional distinct element modeling of the structure and growth of normal faults in multilayer sequences: 1. Model calibration, boundary conditions, and selected results. J. Geophys. Res. 112.
Schöpfer, M.P.J., Childs, C., Walsh, J.J., 2007b. Two-dimensional distinct element modeling of the structure and growth of normal faults in multilayer sequences: 2. Impact of confining pressure and strength contrast on fault zone geometry and growth. J. Geophys. Res. 112.
Schultz, R.A., Summers, L.E., Lynch, K.W., Bouchard, A.J., 2014. Subsurface containment assurance program: key element overview and best practice examples. In: Offshore Technology Conference Asia, 25–28 March, Kuala Lumpur, Malaysia, OTC 24851.
Sinclair, I.K., Evand, J.E., Albrechtsons, E.A., Sydora, L.J., 1999. The Hibernia Oilfield – effects of episodic tectonism on structural character and reservoir compartmentalization. In: Fleet, A.J., Boldy, S.A.R. (Eds.), Petroleum Geology of Northwest Europe: Proceedings of the 5th Conference. The Geological Society, London, pp. 517–528.
Smith, D.A., 1966. Theoretical considerations of sealing and non-sealing faults. AAPG Bull. 50, 363–374.
Smith, D.A., 1980. Sealing and nonsealing faults in Louisiana Gulf Coast salt basin. AAPG Bull. 64, 145–172.
Solum, J.G., van der Pluijm, B.A., Peacor, D.R., 2005. Neocrystallization, fabrics and age of clay minerals from an exposure of the Moab Fault, Utah. J. Struct. Geol. 27, 1563–1576.
Speksnijder, A., 1987. The structural configuration of Cormorant Block IV in context of the northern Viking Graben structural framework. Geol. Mijnb. 65, 357–380.
Sperrevik, S., Faerseth, R.B., Gabrielsen, R.H., 2000. Experiments on clay smear formation along faults. Pet. Geosci. 6, 113–123.
Sperrevik, S., Gillespie, P.A., Fisher, Q.J., Knipe, R.J., Halvorsen, T., 2002. Empirical estimation of fault rock properties. In: Koestler, A.G., Hunsdale, R. (Eds.), Hydrocarbon Seal Quantification, Norwegian Petroleum Society (NPF), Special Publications, vol. 11, pp. 109–125.
Spiller, M., Forkel, C., Kongeter, J., 2004. Case study: inflow of groundwater into open-cast mine Hambach, Germany. J. Hydraul. Eng. ASCE 130, 608–615.
Sverdrup, E., Helgesen, J., Vold, J., 2003. Sealing properties of faults and their influence on water-alternating-gas injection efficiency in the Snorre Field, northern North Sea. AAPG Bull. 87, 1437–1458.
Takahashi, M., 2003. Permeability change during experimental fault smearing. J. Geophys. Res. 108.
Tembe, S., Lockner, D.A., Wong, T.F., 2010. Effect of clay content and mineralogy on frictional sliding behavior of simulated gouges: binary and ternary mixtures of quartz, illite, and montmorillonite. J. Geophys. Res. Solid Earth 115.
TerHeege, J.H., Wassing, B.B.T., Orlic, B., Giger, S.B., Clennell, M.B., 2013. Constraints on the sealing capacity of faults with clay smears from discrete element models validated by laboratory experiments. Rock Mech. Rock Eng. 46, 465–478.
Thornton, C., 2000. Numerical simulations of deviatoric shear deformation of granular media. Géotechnique 50, 43–53.
Thornton, C., Zhang, L., 2003. Numerical simulations of the direct shear test. Chem. Eng. Technol. 26, 153–156.
Urai, J.L., Schmitz, R.M., van der Zee, W., Holland, M., Vrolijk, P., 2003. Experimental investigation of clay smear processes in a geotechnical direct shear apparatus, faults and top seals: what do we know and where do we go?. In: EAGE, Montpellier, France, 8–11 September 2003, p. 43.
Urai, J.L., Nover, G., Zwach, C., Ondrak, R., Schöner, R., Kroos, B.M., 2008. Transport processes. In: Littke, R., Bayer, U., Gajewski, D., Nelskamp, S. (Eds.), Dynamics of Complex Intracontinental Basins: the Central European Basin System. Springer-Verlag, Berlin, pp. 367–388.
van der Zee, W., Urai, J.L., 2005. Processes of normal fault evolution in a siliciclastic sequence: a case study from Miri, Sarawak, Malaysia. J. Struct. Geol. 27, 2281–2300.
van der Zee, W., Urai, J.L., Richard, P.D., 2003. Lateral clay injection into normal faults. GeoArabia 8, 501–522.
van Gent, H.W., Holland, M., Urai, J.L., Loosveld, R., 2010. Evolution of fault zones in carbonates with mechanical stratigraphy – insights from scale models using layered cohesive powder. J. Struct. Geol. 32, 1375–1391.
Vardoulakis, I., 1989. Shear-banding and liquefaction in granular materials on the basis of a Cosserat continuum theory. Ing. Arch. 59, 106–113.
Vardoulakis, I., Sulem, J., 1995. Bifurcation Analysis in Geomechanics. Blackie Academic and Professional, London.
Vrolijk, P., James, B., Maynard, J., Sumpter, L., Sweet, M., 2005a. Reservoir connectivity analysis – defining reservoir connections & plumbing. In: SPE Middle East Oil and Gas Show and Conference, 12–15 March. Society of Petroleum Engineers, SPE 93577, Kingdom of Bahrain.
Vrolijk, P., Myers, R., Sweet, M.L., Shipton, Z.K., Dockrill, B., Evans, J.P., Heath, J., Williams, A.P., 2005b. Anatomy of reservoir-scale normal faults in central Utah; stratigraphic controls and implications for fault zone evolution and fluid flow. GSA Field Guide 6, 261–282.
Vrolijk, P., van der Pluijm, B.A., 1999. Clay gouge. J. Struct. Geol. 21, 1039–1048.
Wang, Y., Abe, S., Latham, S., Mora, P., 2006. Implementation of particle-scale rotation in the 3-d Lattice Solid Model. Pure Appl. Geophys. 163, 1769–1785.
Weber, K.J., Mandl, G., Pilaar, W.F., Lehner, F., Precious, R.G., 1978. The role of faults in hydrocarbon migration and trapping in Nigerian growth fault structures. In: Offshore Technology Conference, Dallas, TX, United States, pp. 2643–2653.
Wehr, F.L., Fairchild, L.H., Hudec, M.R., Shafto, R.K., Shea, W.T., White, J.P., 2000. Fault seal; contrasts between the exploration and production problem. AAPG Mem. 73, 121–132.
Welbon, A.I., Beach, A., Brockbank, P.J., 1997. Fault seal analysis in hydrocarbon exploration and appraisal: examples from offshore mid-Norway. Nor. Pet. Soc. Spec. Publ. 7, 125–138.
Welch, M.J., Knipe, R.J., Souque, C., Davies, R.K., 2009. A Quadshear kinematic model for folding and clay smear development in fault zones. Tectonophysics 471, 186–202.
Yielding, G., Freeman, B., Needham, D.T., 1997. Quantitative fault seal prediction. AAPG Bull. 81, 897–917.
Yielding, G., 2002. Shale Gouge Ratio – calibration by geohistory. In: Koestler, A.G., Hunsdale, R. (Eds.), Hydrocarbon Seal Quantification, Norwegian Petroleum Society (NPF), Special Publications, vol. 11, pp. 1–15.
Yielding, G., 2012. Using probabilistic shale smear modelling to relate SGR predictions of column height to fault-zone heterogeneity. Pet. Geosci. 18, 33–42.
Zhao, C., Hobbs, B., Ord, A., Robert, P., Hornby, P., Peng, S., 2007. Phenomenological modelling of crack generation in brittle crustal rocks using the particle simulation method. J. Struct. Geol. 29, 1034–1048.
Zhou, J., Chi, Y., 2002. Shear-band of sand simulated by Particle Flow Code (PFC). In: Konietzky, H. (Ed.), Numerical Modeling in Micromechanics via Particle Methods. Balkema, Rotterdam, Gelsenkirchen, Germany, pp. 205–210.